A BI-LEVEL APPROACH TO FUTURE POWER SYSTEM CO-OPTIMIZATION WITH HIGH PENETRATION OF RENEWABLE ENERGY AND RESPONSIVE DEMAND

A Dissertation

Presented to the Faculty of the Graduate School

of Cornell University

in Partial Fulfillment of the Requirements for the Degree of

Doctor of Philosophy

by

Jialin Liu

August 2019

A BI-LEVEL APPROACH TO FUTURE POWER SYSTEM CO-OPTIMIZATION WITH HIGH PENETRATION OF RENEWABLE ENERGY AND RESPONSIVE DEMAND

Jialin Liu, Ph.D.

Cornell University 2019

Electricity generation accounts for nearly half of the total CO_2 emissions in the United States [1]. For this reason, the development and integration of renewable resources will play an essential role in achieving the societal objective of mitigating climate change through reduction of greenhouse gas emissions. In conjunction with the environmental benefits of renewable energy, the most common renewable sources, such as wind and solar, also increase the uncertainties surrounding generation in power systems, which adds significant challenges to the system operation and planning. The uncertainties and forecasting errors surrounding renewable generation are normally addressed through the use of reserves from traditional generators. At greater levels of renewable penetration, sufficient generator reserves may not be available or economically viable. In contrast, the promise of demand-side resources in this arena lies in the spatially widespread availability, rapid response potential, and lower cost of features that already exist in the system. However, the challenge of responsive demand arises from the need to understand, manage, and incentivize a very large number of resources to participate effectively in efficient operation of the complex power system. Since demand response comes from the distribution system, microgrids as the basic building blocks of future distribution systems will be a critical environment for the study of demand response. To support

integration of microgrids with flexible loads in future power systems, the operational mode of power systems will need to evolve. Therefore, it is going to be critical to have new and efficient co-optimization methods for coordination of the various power market participants and the scheduling of resources in the power systems of the future.

Motivated by the rapid increase in renewable penetration, the need for effective demand response programs, and a changing system structure, this dissertation seeks to define a new strategy that supports co-optimization of various participants in power systems with emphasis on high renewable penetration and demand response. This strategy has three components; 1) an exploration of the capabilities of different types of demand response programs in a microgrid, 2) development and implementation of a bi-level framework for co-optimization of the main grid with high renewable penetration and a microgrid with demand response capabilities, and 3) expansion of the bi-level framework from a microgrid to a general distribution system to explore the advantages of the bi-level co-optimization approach over the traditional optimization approach.

Conclusions of this work illustrate that the stochastic rolling horizon approach could effectively manage the operation of a microgrid with various demand response programs. In addition, the bi-level approach is a promising co-optimization framework for the transmission and distribution levels that could increase system renewable penetration and reduce operation costs. Compared to the traditional framework, the bi-level framework yields more equitable cost sharing patterns among the market participants as well as better support for the power system evolution.

BIOGRAPHICAL SKETCH

Jialin Liu is a 5th year Ph.D. Candidate in the department of Electrical and Computer Engineering department. He was awarded his non-thesis Masters in Auguest 2017 and completed his Bachelor of Science in Electrical and Computer Engineering with a power systems option at the University of British Columbia in 2014. He has had a strong interest in the power industry since his childhood due to family influence. In the past, he interned at the State Grid Corporation of China and New York Independent System Operator, and gained deep knowledge about the power system operation in real world. At Cornell, his research has focused on the optimization of power system operation with an emphasis on renewable penetration, demand response and smart grid technologies. Jialin joined Microsoft Research after graduation.

To my parents Guangzeng Liu and Shuqin Zhang.

ACKNOWLEDGEMENTS

First, I am extremely grateful and fortunate to have had Professor C. Lindsay Anderson as my advisor. Professor Anderson is a very positive, and understanding person who can fill up the air with positive energy. She has consistently been so supportive and encouraging of my research and career decisions. Whenever I ran into problems in the course of my research, she was always there by my, willing to provide help. Her extensive knowledge of power systems and her brilliant mind have greatly enlightened my research and helped me overcome research obstacles over and over again. Besides that, her careful and responsible work attitude, great courage in facing problems and pressure, and masterly way of treating people have served to teach me how to be a better person. I will always feel proud and honored to have been her student.

Second, I want to express my great thanks to my committee members, Professor Carla P. Gomes and Professor David S. Matteson. Professor Gomes has always been so warmhearted and supportive of my work. As the founder of the Institute for Computational Sustainability, her work also greatly inspired my research on integration of renewables in power systems. With her encyclopedic knowledge of optimization, she provided invaluable suggestions for my work and even had her students to assist me with it. I am also very blessed to have had another super benign professor, David S. Matteson, on my committee. I aquired valuable skills and tools from his course in modeling of renewables, which played a vital role in my research. His extensive knowledge of time series and statistics has been a shape weapon for my research problems in this area. I deeply appreciate Professor Matteson's attempt to attend my A-exam, at a time that was not convenient for him, in order to accommodate my need.

Moreover I would like to thank my lab members, Gabriela Martinez, Luckny

Zéphyr, Lingfeng Cheng, Amandeep Gupta, Ge Guo, Zongjie Wang and Mengwei Liu.Gabriela has been a great mentor for me not only for research but also for career advise.Her care and support encouraged me a lot in tough periods.I have really enjoyed working with Luckny on my projects.His meticulous work style and high standards pushed me to be better.Lingfeng has always been so helpful and provided me with great suggestions for career and other things in life.I learned a lot from his super efficient and organized way of work and thinking.Amandeep has been a moral booster and brought so much laughter in the lab.Ge is an extremely friendly person, who has been so supportive for my work.Zongjie and Mengwei though have not been in the lab for long, the interactions and talks with them added great spice to my lab life.

Last but not least, I feel so luckny to have my loving parents, Guangzeng Liu, and Shuqin Zhang, and my lovely sister Wenjun Liu.They are always there to encourage me, accompany me, and share my happiness and sorrow.Their love is unconditional and as deep as ocean.Without them, I would never be able to get this far.

For all the people I mentioned here and so many more who offered me help, I will remember your kindness for a lifetime.In the future, I sincerely hope that I will have opportunities to do something for you in return.I will put my best foot forward in work, and try my best to contribute to the society to live up to your giving.

TABLE OF CONTENTS

LIST OF TABLES

LIST OF FIGURES

CHAPTER 1

INTRODUCTION

A power system consists essentially of three operations: generation, transmission, and distribution. Generation converts mechanical and/or thermal energy to provide power supply. Transmission moves power over larger regions through high voltage networks of transmission lines, from generators to distribution systems at various nodes in the transmission networks. Distribution moves power through a lower voltage system that distribute power to individual loads.

Power system operation can be roughly classified by timescale into long-term planning, day-ahead Unit Commitment (UC), and hour-ahead to real-time operation, In this work, we consider two of the key problems; the day-ahead UC problem, and the hour-head problem. In UC problem, the commitment schedule of the generators must be determined and fixed for the real-time operation to account for startup, shutdown, and run-time constraints of the generators. The generation schedules of the selected generators and the power flow in the transmission network are determined according to the forecasted real-time load. The second key problem is the hour-ahead to real-time economic dispatch (ED) problem, which is often also called a recourse problem. As there are always errors in the forecasted load, the day-ahead generation and power flow decisions need to be adjusted in real-time to compensate for deviations from the load forecasts. The resources used in such generation adjustments are called recourse resources or generation reserves. The day-ahead UC and real-time ED problems are optimized in a way that seeks to minimize the total system operation cost, achieve a balance between system supply and demand, and satisfy

various physical constraints on the system.

1.1 Evolution in Power Systems

There are currently two major changes underway in power system operations. The first is occurring in distribution systems. The popular term "smart grid" is mainly used to describe the evolving distribution systems. Traditional distribution systems are largely passive, with little in the way of active devices such as distributed generation. The network in most traditional distribution systems are radial and limited to uni-directional power flow. As a result, operation of the distribution system is very simple in its current implementation, and the distribution system is normally represented as a single load from the perspective of the transmission system. However, the distribution system of the future is envisioned as a very dynamic and active system with various types of distributed generation (DG) and energy storage devices. In addition, it is possible that the power flow will change from uni-directional to bi-directional. To cater the above changes, the network will transform from a radial network to a meshed network, and the excess generation in the distribution system will be able to be sold back to the transmission system. The current distribution framework will no longer be suitable for accommodating such major changes in power distribution.

To deal with the changing distribution system, the concept of a microgrid (MG) has emerged. MGs are localized grids that can disconnect from the traditional grid and operate autonomously. A comprehensive MG typically includes fossil-fuel based generation, renewable generation, energy storage units, and

flexible loads. During normal operation, most MGs maintains a connection to the main grid, including exchanging energy. In case of a grid disturbance, the MG can disconnect from the grid and operate in an independent "islanded" mode to maintain the supply reliability for the microgrid consumers. In this way, MGs may significantly improve the reliability and security of power systems. In addition, MGs serve as reasonable hosts for DG, as MGs and DG are both intended to meet local power needs and they operate on the same scale. Based on these desirable characteristics, MGs may become the distribution system of the future, as the basic building blocks of the future grid. However, a microgrid is more complex than a traditional distribution system with diverse components and similar functionalities as the main grid, requiring an adequate optimization framework for scheduling of its resources, as well as an ability to cooperate with the main grid.

The second revolution in power systems is the increasing generation of electricity by variable renewable sources of energy such as wind and solar. Currently, 29 of the 50 U.S. states have developed renewable portfolio standards which mandate that a minimum percentage of electricity be generated from renewable sources by some year in the near future [3]. For example, in New York State, the goal is to increase the renewable penetration level from 28% in 2017 to 70% by 2030 [4]. As utilization of renewable resources continues to increase, power systems will require methods for dealing with the uncertainties inherent in the generation of electricity via renewables and methods for leveraging any available flexibility to support operation of the system in an efficient and reliable manner. The current level of generation by renewables in the U.S. power system is low enough that the uncertainties introduced by renewable sources of energy can be managed via ramping and by utilization of reserves provided by

other existing generators within the system. If the penetration by renewables gets significantly higher, these reserves may not be sufficient or could become prohibitively expensive. To address this, the electric power industry is actively investigating alternative strategies to ensure reliability and sustainability. The most daunting challenges in the transformation of power systems arise from the timescale for implementation and the prohibitive cost of solutions such as fast-ramping generation or grid-scale storage.

As renewable generation introduces increased variability in the system, an attractive and sustainable alternative to using fossil-based generation for managing variability is to leverage load flexibility through demand response (DR) programs that adapt the load pattern to accommodate uncertainties and forecasting errors. Responsive loads can be roughly categorized as price-based demand response, in which users respond to price signals, and incentive-based demand response, an approach that's typically managed by aggregators or load-serving entities. Demand response programs are not new; for example, incentive programs designed to reduce load consumption can be traced back to 1970 in the U.S.. Previous research has shown several potential benefits of DR, including peak-load reduction, mitigation of outage risk, market-clearing price reduction, and improvements in social welfare and environmental outcomes [5, 6, 7, 8, 9, 10, 11]. The flexibility provided by DR offers attractive opportunities for dealing with fluctuations in renewable generation. For example, the study presented in [12] shows that price-based DR can mitigate the cost effects of wind generation in UC decision processes, and the simulation analysis performed in [13] illustrates the effects of price-based DR in UC decisions for power systems with wind and solar photovoltaic power. As microgrids will be important building blocks of the power system of the future, it is crucial to examine

the optimal MG framework in the context of assorted DR programs.

Inspired by the aforementioned power system trends and needs, the goal of this dissertation is to develop an appropriate framework for the dynamic distribution system of the future, and a co-optimization framework for the distribution and main grid with sufficient support for high renewable penetration and demand response programs. It is hoped that this work will provide some ideas and insight to support the future smart and sustainable grid.

1.2 Organization of the Dissertation

The rest of this dissertation is organized as follows:

Chapter 2: In this chapter, the potential of DR to reduce system operation cost, while supporting renewable integration is investigated in the context of a microgrid. Three types of DR programs, targeting thermostatically controlled loads (TCL), deferrable loads (DL), and elastic loads (EL), are explored in the context of various system conditions. Since systems with significant renewables and DG are subject to high levels of uncertainty that evolves through time, a stochastic rolling-horizon framework is proposed for optimization of microgrid operation, which incorporates updates of the renewable generation forecast and the energy market real-time prices (RTP).

Chapter 3: Using the proposed optimization method for operation of the microgrid with different DR programs, co-operation of the transmission and microgrid systems is analyzed under a bi-level optimization framework. First, the formulation and solution methodology of this bi-level problem is described, and then its performance on the basis of system performance and renewable in-

tegration is analyzed and compared under various system configurations.

Chapter 4: As a microgrid is a particular form of distribution system, it is important to test the co-optimization strategy presented in the previous chapter on a more general distribution system. This chapter applies bi-level optimization to co-optimize the transmission system and distribution system in a way that meets the needs of the distribution system of the future and takes advantage of DR to address the stochasticity of wind power. The proposed bi-level approach is compared to the traditional centralized optimization approach in terms of the system cost, renewable penetration integration, system expansion, and environmental impact.

Chapter 5: In this chapter, the conclusion of all three studies conducted is presented.

CHAPTER 2

OPTIMAL OPERATION OF MICROGRIDS WITH LOAD-DIFFERENTIATED DEMAND RESPONSE AND RENEWABLE RESOURCES

As the level of renewable and distributed energy resources (DER) increases in power systems, there is a coincident effort to ensure ongoing reliability. The development of microgrids is likely to play a central role in this development globally. However, a counterpoint is the high cost of microgrid operations, and there exists a need to develop efficient tools to operate microgrids optimally and economically. In this chapter, the potential of demand response (DR) to reduce microgrid operation cost while supporting renewable integration, is investigated. Three types of DR, namely thermostatically controlled load (TCL), deferrable load (DL) and elastic load (EL), are explored in the context of various system conditions. Since systems with significant renewables and DER are subject to high levels of uncertainty, the investigation is conducted under a stochastic rolling horizon optimization framework that leverages the update of renewable generation forecast and the energy market real-time prices (RTP). A case study illustrates that certain system conditions, such as price peaks and moderate temperatures, facilitate best demand response performance. Conversely, inaccurate price forecast information can lead to ineffectual operation of microgrids and result in higher cost. The insights provided by the study of various types of DR are helpful for microgrid design with consumers' preferences taken into consideration.

2.1 Introduction

Microgrids, defined by the U.S. Department of Energy as 'localized grids that can disconnect from the traditional grid to operate autonomously' [14], have been receiving increasing attention in recent years. The autonomous operation of microgrids adds the potential to support resilience and reliability of nation's electrical power grid in dealing with disturbances or natural disasters [15]. In addition, microgrids could also alleviate transmission congestion, reduce transmission losses, and provide demand response (DR) capabilities [16]. These characteristics make microgrids a basic building block of a decentralized and robust future grid. The future distribution network could be comprised of many microgrids, which would require the network to operate differently in various ways. One key difference will be the effective and widespread use of DR in response to system signals. Recently, aggregation services that leverage consumers in the distribution network to provide DR to the system have being developed. In the future, the role of DR aggregator could be assumed by microgrids that can provide a range of DR programs for its customers for the purpose of optimizing the microgrid as well as providing services to the broader system.

In pursuit of this future, the optimization of microgrid operations with DR has emerged as an important research area for sustainable power systems. It is generally presumed that a sustainable future grid typically includes renewable generation in conjunction with microgrids, and as a result there is a recent body of work considering the use of microgrid optimization, specifically for the management of renewable uncertainty. These efforts have considered a range of approaches that can be roughly classified as deterministic-equivalent methods or scenario-based stochastic programming. Specifically, authors in [17, 18, 19, 20]

incorporate uncertainty via a deterministic optimization framework with a single *expected* forecast for the uncertain inputs. Subsequently, deterministic rolling horizon approaches have been implemented to take advantage of updated information as the model moves through the operation time-frame, still in a deterministic formulation [21, 22, 23, 24, 25]. However, recent work such as [26, 27, 28, 29], has addressed the issue that a single forecast is unlikely sufficient to characterize the uncertain generation, and develop a stochastic optimization approach. Stochastic programming models use a range of input scenarios that better characterize uncertainty, though none consider the revealing of information over the operating periods. In [30], the authors analyzed the economic and environmental impact of a microgrid with a stochastic model predictive control approach, which makes use of the revealing of information over the operating periods. The approach uses a stochastic programming style formulation that solves for a single policy for all the scenarios and minimizes the expected cost to compensate the deviation between the solution and all the scenarios based on an exogenously defined deviation cost. However, a single policy for all future scenarios put unnecessary restrictions to the flexibility of the solution, and characterize the cost and resource allocation for the future scenarios in a vague way, which might influence the optimality of the current period solution. It is our assertion that since future microgrids will likely incorporate uncertain renewable energy sources, a stochastic optimization approach is suitable to ensure appropriate management of uncertainty. In addition, real-time pricing is a necessary condition for many DR programs and the real-time market clears on a rolling basis, therefore a rolling horizon approach is a natural framework to replicate the constantly updated renewable and pricing information. The combination of these requirements leads naturally to the use of a stochastic rolling

horizon framework to ensure practicality for real microgrid use. The stochastic rolling horizon approach in this paper solves for a solution for each scenario as it evolves through time, which provides a more detailed and accurate picture of cost characterization and resource allocation for each scenario. Only the current period decision, which is the same for all the scenarios, is implemented in each iteration.

DR has been acknowledged as an effective way to reshape the load profile and reduce the system costs [31]. There are two broad classes of DR: price-based DR and incentive-based DR [31]. The former induces DR effect on elastic load under dynamic prices [21, 26, 27, 29, 19, 23], whereas the latter uses structured incentives to achieve the same effect mainly on shiftable loads [21, 22, 28, 25, 32]. Price-based DR has also been applied to the specific case of DR from thermostatically controlled loads in [33, 24]. Despite the recent interest in the impact of DR including on system operations, it seems that none of the previous work has considered the potential of leveraging the three types of DR (i.e., thermostatically controlled load (TCL), deferrable load (DL) and elastic load (EL)) together in a MG. To address this question, the work described here considers three classes of loads within a microgrid, with distinct DR programs for each, as explained in detail in Section 2.2.

To explore the potential of an active microgrid in this context, the system considered here includes a generator, a storage unit, a wind farm, aggregated loads of various types, and the ability to exchange power with the main grid. The aggregated loads provide three types of DR and are based on real load data classifications including thermostatically controlled load, deferrable load and elastic load. Since a microgrid typically covers a small local area with a power

capacity of a few MWs [34] with very limited power in the setting of the market price, it is assumed that the microgrid is a price taker in this context. Under these conditions, a stochastic rolling horizon model is implemented to optimize the operation of the microgrid, including use of the three types of DR available and its interaction with the main network, to lower the microgrid operation cost.

In contrast to previous work, this paper presents a new stochastic rolling horizon approach for the operation of a comprehensive microgrid with renewables, storage, and self-generation. This approach provides an ability to match the characteristics of the real-time market and the uncertain nature of renewable generation. Additionally, this analysis represents realistic DR classes based on accepted classification of real load data to correctly represent flexibility. This modeling framework is implemented in a case study using real historical data from a utility in the United States to accurately reflect system conditions.

2.2 Demand Response

Four types of loads are analyzed in this study, characterized according to the U.S. residential energy use data from Energy Information Administration[35], including thermostatically controlled load (TCL), deferrable load (DL), elastic load (EL) and inelastic load. The load classification is given in Table 2.1. The 'Others' category includes miscellaneous loads such as portable heaters and hair dryers. It is assumed that half of the 'other' group of loads is elastic and half is inelastic. With the exception of the inelastic load, all classes of loads are associated with their own demand response program. In some previous work

relating to load modeling, many classes of load such as DL and TCL are modeled with variations on cross-elastic components. In this work, DL is modeled separately to more accurately characterize this class of load instead of using a cross-elasticity coefficient to represent it. Similarly, TCL is considered as a separate class of loads, and use the more accurate method of representing the aggregated TCLs based on the work of [36]. For the strictly elastic loads, we use an elasticity coefficient based on the reference [37], to characterize their behavior, as modeling them more concretely would not be an easy task.

Category	End Use	Share
TCL	Space cooling	13%
	Space heating	9%
DL	Dishwashers	2%
	Clothes dryers	4%
	Clothes washers	1%
EL	Lighting	11%
	Televisions and related equipment	6%
Inelastic Load	Refrigeration	8%
	Furnace fans and circulation pumps	4%
	Computers and related equipment	1%
	Cooking and water heating	11%
	Freezers	2%
	Others	28%

Table 2.1: Load Classification

2.2.1 Thermostatically Controlled Load

There are many thermostatically controlled loads in homes including; heating, cooling, hot water heaters, and refrigerators. In this work, we consider only heating and air conditioning load to be controllable TCLs, because in the central north region studied in this work, 70% of the heating is by gas according to [38]. In order not to overestimate the contribution of water heating appliances to flexibility, water heaters are excluded. Refrigerators are also excluded, because 1) refrigeration load is much smaller than HVAC, 2) food quality is very sen-

sitive to temperature change, and the temperature inside the refrigerator could change very quickly due to the opening and closing of the doors and/or changes in contents in a small volume, and 3) consumers may not feel comfortable risking food quality for small savings in energy costs. The flexibility of TCL comes from the fact that there is a narrow range of temperature that is considered comfortable [39]. This range (e.g. $21^{\circ}C \sim 23^{\circ}$ C) provides TCL with the flexibility to consume more or less power in response to the changing energy prices to reduce the energy cost. TCL demand response is similar to an energy storage unit in terms of modeling, as they have similar operating characteristics. Specifically, TCL has energy and power bounds due to the comfortable temperature range. The calculations of those bounds and the data for different temperatures are given in [36]. Here it is assumed that the lower bounds of the power capacity and energy capacity are zero. The TCL model is a model of the aggregated power of a population of TCLs, and different TCLs may have different thermal insulation environments, which introduces differences in the TCL characteristics. Therefore, there is some inherent error in this aggregation, as there is in any model. A single TCL model assuming average TCL characteristics is used in this work, which are determined from [36]. The constraints associated with TCL are listed below:

$$0 \leq S_t \leq \bar{S}_t(\mathcal{T}), 0 \leq P_t^c \leq \bar{P}_t^c(\mathcal{T}), \forall t \tag{2.1}$$

$$S_{t+1} = S_t + \delta t(P_t^c - P_t^{cb}(\mathcal{T})), \forall t \tag{2.2}$$

Equation (2.1) restricts the energy and power level of TCL to be within their energy and power bounds respectively. Equation (2.2) is the evolution process of the energy state, wherein the energy state of the TCL in the current period is

the sum of the state in the previous period and any TCL deviation from the TCL baseline in a time step δt for temperature $\mathcal{T}$. The TCL charges when the real power consumption is higher, and vice versa. The power and energy capacity profiles from [40] are used for our study. With bidirectional communication capability between the microgrid control center and the TCL controller, TCL DR is often realized through direct load control [41]. It is assumed that the microgrid controller has the household information and centralized control for this type of resource.

2.2.2 Deferrable Load

The second category of loads are deferrable loads (DL), and are those that can be delayed until later in the day, such as washing machines and dish washers [42]. The timing for serving this type of load has some, though not infinite, flexibility. Dishwasher cycles can be delayed within a few hours to run during lower price periods, for example. However, there may be restrictions on the delay of DL, related to consumer needs or convenience, which necessitates specification of a deadline for completion of the job. Any inconvenience to the user caused by the delay could be specified and penalized in the objective function. For simplicity, the waiting penalty is neglected in this work, though the deferrable loads are constrained to be served within a specified time period. In addition to the energy cost savings, DLs could also benefit from certain incentive programs for load shifting. Specifically, in order to alleviate the stress on the power system during peak hours, some programs are created to encourage load shifting by providing financial incentives to the customers. This is often referred to as the voluntary demand response in industry, such as the Emergency Demand

Response Program (EDRP) in NYISO [43]. Given a baseline consumption for the loads without the DR program, the utility could incent load reduction from that baseline during periods of system stress. For example, EDRP compensates load reduction at the maximum of \$500/MWh or the RTP [44]. In this work, the RTP is used as the load reduction incentive. It is assumed that in future smart homes, the deferrable appliances could be equipped with communication capability that could send information to the microgrid central controller. Given information about the user's preferences and incentives, the microgrid controller schedules the DL in a way that not only satisfies the user's requirements, but also minimizes the cost of DL. The constraints associated with DL are:

$$\sum_{t \in T} L_t^d = \sum_{t \in T} L_t^{db}, \forall s, t \tag{2.3}$$

$$\sum_{t=t_a}^{t_b} L_t^d \leq \sum_{t=t_a}^{t_b} L_t^{db}, \forall t_b \geq t_a \tag{2.4}$$

$$L_t^d \geq 0, \forall t \tag{2.5}$$

Equation (2.3) ensures that the total DL within the operation horizon is the same as the sum of the base DL in the horizon. By requiring the total DL from a starting period t_a to a later period t_b not to be greater than that of the base DL, equation (2.4) ensures that the DL could only be deferred to a later period, rather than moved to an earlier period. The DL constraints apply to the same scenario trajectory across different time periods. This DL model in based on the model in [45]

2.2.3 Elastic Load

In addition to TCL and DL, the last type of responsive load is defined as elastic load, including portable heaters and portable air conditioners, which lack the price responsive controllers to act as TCLs. Entertainment devices, such as televisions are considered price responsive in this case study. The consumption of this type of load is due to the consumer awareness of pricing information and their corresponding actions [46]. If the price for a certain time step is significantly higher than the reference price, the user might use less, which corresponds to a negative price elasticity. Formally, the elasticity of load is defined as the percentage change in load (Δq) due to the percentage change in price (Δp) as shown below [47]:

$$\varepsilon = \frac{\Delta q}{\Delta p}$$

The change in price/load is relative to some reference price/load; the reference price is the fixed electricity price and the reference load is the load under the fixed price. The actual price is the microgrid import cost. The change of load consumption due to the change of price in the same time step is called self-elasticity (ε). The elastic load profile under dynamic prices is as follows:

$$L_t^e = \max\left(L_t^{eb}\left(1 + \varepsilon_t \frac{p_t - p_f}{p_f}\right), 0\right), \forall t \tag{2.6}$$

where L_t^{eb} is the base elastic load in period t, p_t is the real-time price for period t and p_f is the flat-rate price across all periods, which is calculated as the average monthly real-time price. The second term in the parenthesis is the contribution of self-elasticity. Equation (2.6) shows that the elastic load is based on the in-

elastic load plus the contribution of load elasticity, and it is non-negative. This EL model is based on the model in [47].

2.2.4 Inelastic Load

The last category of load is inelastic load which has very limited flexibility and thus does not respond to dynamic prices, and the load profile of this type of load is fixed. Electric cooking load is an example of this type of load, which cannot provide demand response. Similarly computer use is assumed to support work and is not elastic. In the optimization problem, inelastic load is modeled as a fixed load.

2.3 Optimization Model

For clarity, the rolling horizon approach is first described in a deterministic context. The stochastic version used in this work is then described using scenario trees for the uncertain parameters, followed by a summary of the overall implementation of the modeling framework.

2.3.1 Deterministic Rolling Horizon Optimization

A rolling horizon approach is commonly used for the operation planning with constantly updating forecast information in many industries [48]. As illustrated in Fig. 2.1, the main feature of this approach is the incorporation of updated

information, including past decisions, into the optimization model, as they become available. Only the current decisions are implemented, while the future decisions are preliminary and will be updated in future iterations with updated forecasts. This process repeats until all the periods in the planning horizon reach implementable decisions. In this way, all available information is incorporated, and the operation of the current period is scheduled anticipating future system conditions. Please refer to [48] for a detailed treatment of rolling horizon optimization. The objective function of the problem is to minimize the operation

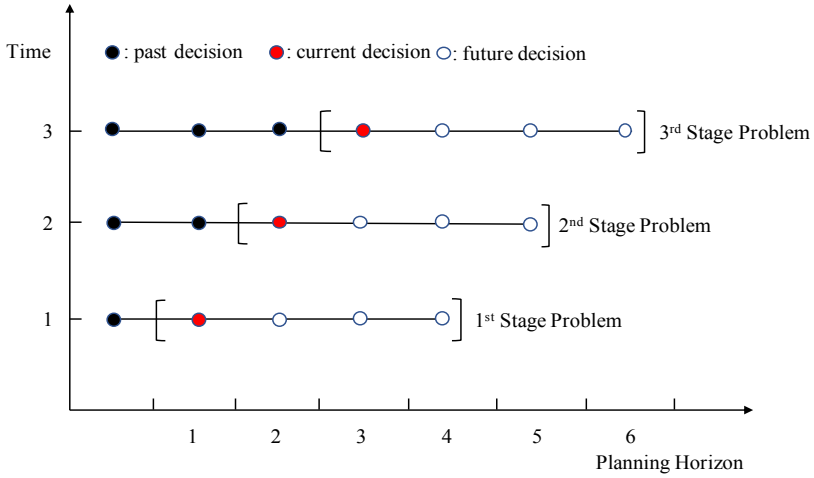

Figure 2.1: Rolling Horizon Framework with Deterministic Forecasts

cost of the microgrid over a planning horizon of T periods starting from period k. The operational cost is associated with the microgrid's generation fuel cost ($P_t^g C^g$), storage cost ($B_t C^b$) for maintaining its energy level, power exchange net cost (i.e., energy import cost ($P_t^{im} C_t^{im}$) - energy export revenue ($P_t^{ex} C_t^{ex}$)) with the main grid, a penalty for deferring DL ($C^{dl}(L_t^d)$) and an incentive for the DL ($(L_t^d - L_t^{db})P_t^{inc}$):

$$obj = \sum_{t=k}^{k+T-1} \left(P_t^g C^g + B_t C^b + P_t^{im} C_t^{im} - P_t^{ex} C_t^{ex} + C^{dl}(L_t^d) - (L_t^d - L_t^{db}) P_t^{inc} \right) \tag{2.7}$$

2.3.2 Stochastic Rolling Horizon Optimization

Though very simple to implement, a deterministic approach may not be realistic in practice, as it does not account for potential deviations from the forecasts. Hence, a stochastic approach is more suitable. Therefore, scenario trees are used to account for different wind scenarios as shown in Fig. 2.2. This structure suggests a stochastic programming approach within the rolling horizon framework. The scenario-based stochastic programming technique presented in [49, 50] has been used in this work. The uncertain parameters in this work are wind gen-

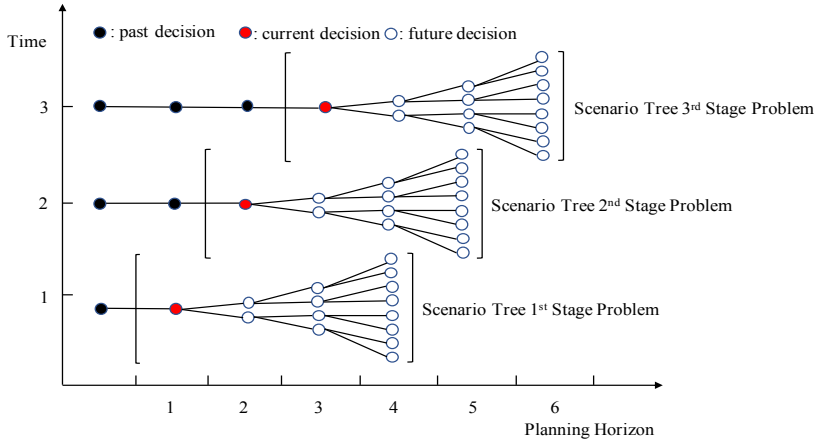

Figure 2.2: Rolling Horizon Framework with Scenarios

eration and the energy price. Realizations of wind generation and prices are rolled out in an hourly fashion. For a modeling timeframe of T periods starting from period k, the wind generation and the microgrid real-time power exchange price are realized for period k. The model uses the realized uncertain variables to reach a single solution for the current period, and future wind scenarios and the day-ahead prices (DAP) to reach a set of solutions for the future. Only the decisions for the current period, which are the same for all the scenarios, are implemented, and the future decision sets are used to guide the decisions tak-

ing into account possible future conditions. This is especially important for the scheduling of the microgrid storage, as optimal charging and discharging decisions are required for the storage using future wind and DAP forecasts.

The optimization model decides the optimal microgrid operation for the following decision variables:

$$x_{t,s} = [P^c_{t,s}, S_{t,s}, B_{t,s}, W^c_{t,s}, P^w_{t,s}, L^d_{t,s}, P^{ex}_{t,s}, P^g_{t,s}, P^{im}_{t,s}, P^b_{t,s}]$$

The interpretation of the cost terms in the multi-scenario objective function is the same as that in the deterministic problem objective function in Eq. 2.7. In contrast to the deterministic framework, now the decision variables are also indexed by a subscript s to account for the variation of the scenarios. The objective function and constraints for the microgrid operation are given below. For the starting period k of T periods, the cardinality of the scenario set S_k is one as the uncertainty is realized for that period.

Multi-scenario Objective function:

$$F(x_{t,s}) = \sum_{t=k}^{k+T-1} \sum_{s \in S_t} \pi_{t,s} \Big(P^g_{t,s} C^g + B_{t,s} C^b + P^{im}_{t,s} C^{im}_t - P^{ex}_{t,s} C^{ex}_t + C^{dl}(L^d_{t,s}) - (L^d_{t,s} - L^{db}_{t,s}) P^{inc}_t \Big)$$

- ***Generation constraints:***

$$R \leq P^g_{t,s} - Pg_{t-1,s} \leq \bar{R}, \forall s \in S_t, t \in k, ..., k+T-1 \tag{2.8}$$

$$P \leq P^g_{t,s} \leq \bar{P}, \forall s, t \tag{2.9}$$

$$P^g_{t,s} \geq 0, \forall s, t \tag{2.10}$$

The generator's ramping constraint is described in Eq. (2.8). Equation (2.9) limits the generator's output to an upper and lower bound.

- ***Storage constraints:***

$$P^b \leq P^b_{t,s} \leq \bar{P}^b, B \leq B_{t,s} \leq \bar{B}, \forall s, t \tag{2.11}$$

$$B_{t,s} = \alpha B_{t-1,s} + \beta P^b_{t-1,s}, \forall s, t \tag{2.12}$$

$$B_{t,s} \geq 0, P^b_{t,s} \in \mathbb{R}, \forall s, t \tag{2.13}$$

Equation (3.23) restrict the storage's output power and the energy state to their upper and lower bounds. Equation (2.12) shows the transition of the storage energy state from one hour to the next considering the energy storage standing loss coefficient α and charging/discharging efficiency β. A positive/negative $P^b_{t,s}$ value corresponds to charging/discharging (note: $\beta P^b_{t-1,s}$ in Eq. (2.12) becomes $\frac{P^b_{t-1,s}}{\beta}$ in the case of discharging). This energy storage model is based on [28].

- ***Point of common coupling constraints:***

$$P^{ex}_{t,s} \leq PCC, P^{im}_{t,s} \leq PCC, \forall s, t \tag{2.14}$$

$$P^{ex}_{t,s}, P^{im}_{t,s} \geq 0, \forall s, t \tag{2.15}$$

At the coupling point of the microgrid with the main network, there is a limit on the amount of power that can be exchanged as characterized by Eq. (2.14).

- ***Wind curtailment constraint:***

$$W^c_{t,s} \leq P^w_{t,s} \leq \overline{P}^w_{t,s}, \forall s, t \tag{2.16}$$

$$P^w_{t,s}, W^c_{t,s} \geq 0, \forall s, t \tag{2.17}$$

Wind curtailment may be necessary if the microgrid cannot absorb all the wind generation, and it is not possible to sell excess power back to the bulk system due to the power limits at the point of common coupling. Equation (2.16) constrains the wind curtailment amount to be less than the total wind generation.

- ***Power balance constraint:***

$$\begin{aligned} &P^g_{t,s} + P^w_{t,s} - P^b_{t,s} - W^c_{t,s} - Li_t - P^c_{t,s}\mathbb{1}_{Pc} - L^e_{t,s}\mathbb{1}_{Le} - L^d_{t,s}\mathbb{1}_{Ld} \\ &= P^{ex}_{t,s} - P^{im}_{t,s}, \forall s, t \end{aligned} \tag{2.18}$$

$$P^c_{t,s}, L^e_{t,s}, L^d_{t,s} \geq 0, \forall s, t \tag{2.19}$$

where $\mathbb{1}_j$ = {1 if the DR type j is enabled, 0 otherwise} is the indicator function for a type of DR. The user could specify what DRs to include in the optimization with the indicator function according to the presence of DRs. Equation (2.18) requires the microgrid load to be met with different power sources.

- ***Demand response constraint:***

The DR constraints in Eqs. (2.1) - (2.6) need to be considered in this problem for each scenario.

Finally, the optimal microgrid dispatch problem reads:

$$\min_{x_{t,s}} \sum_{s\in S_t} \sum_{t=k}^{k+T-1} \pi_{t,s} \left(P^g_{t,s} C^g + B_{t,s} C^b + P^{im}_{t,s} C^{im}_t - P^{ex}_{t,s} C^{ex}_t + C^{dl}(L^d_{t,s}) - (L^d_{t,s} - L^{db}_{t,s}) P^{inc}_t \right) \tag{2.20a}$$

$$\text{s.t.: } S_{t+1} = S_t + \delta t (P^c_t - P^{cb}_t(\mathcal{T})), \forall t \tag{2.20b}$$

$$0 \leq S_t \leq \bar{S}_t(\mathcal{T}) \tag{2.20c}$$

$$0 \leq P^c_t \leq \bar{P}^c_t(\mathcal{T}), \forall t \tag{2.20d}$$

$$\sum_{t\in T} L^d_t = \sum_{t\in T} L^{db}_t, \forall s, t \tag{2.20e}$$

$$\sum_{t=t_a}^{t_b} L^d_t \leq \sum_{t=t_a}^{t_b} L^{db}_t, \forall t_b \geq t_a \tag{2.20f}$$

$$L^d_t \geq 0, \forall t \tag{2.20g}$$

$$L^e_t = \max\left(L^{eb}_t (1 + \varepsilon_t \frac{p_t - p_f}{p_f}), 0\right), \forall t \tag{2.20h}$$

$$R \leq P^g_{t,s} - Pg_{t-1,s} \leq \bar{R}, \forall s \in S_t, t \in k, ..., k+T-1 \tag{2.20i}$$

$$P \leq P^g_{t,s} \leq \bar{P}, \forall s, t \tag{2.20j}$$

$$P^g_{t,s} \geq 0, \forall s, t \tag{2.20k}$$

$$P^b \leq P^b_{t,s} \leq \bar{P^b} \tag{2.20l}$$

$$B \leq B_{t,s} \leq \bar{B}, \forall s, t \tag{2.20m}$$

$$B_{t,s} = \alpha B_{t-1,s} + \beta P^b_{t-1,s}, \forall s, t \tag{2.20n}$$

$$B_{t,s} \geq 0, \forall s, t \tag{2.20o}$$

$$P^{ex}_{t,s} \leq PCC \tag{2.20p}$$

$$P^{im}_{t,s} \leq PCC, \forall s, t \tag{2.20q}$$

$$P^{ex}_{t,s}, P^{im}_{t,s} \geq 0, \forall s, t \tag{2.20r}$$

$$W^c_{t,s} \leq P^w_{t,s}, \forall s, t \tag{2.20s}$$

$$P^w_{t,s}, W^c_{t,s} \geq 0, \forall s, t \tag{2.20t}$$

$$P^g_{t,s} + P^w_{t,s} - P^b_{t,s} - W^c_{t,s} - Li_t - P^c_{t,s} \mathbb{1}_{Pc} - L^e_{t,s} \mathbb{1}_{Le} - L^d_{t,s} \mathbb{1}_{Ld} = P^{ex}_{t,s} - P^{im}_{t,s}, \forall s, t \tag{2.20u}$$

$$P^c_{t,s}, L^e_{t,s}, L^d_{t,s} \geq 0, \forall s, t \tag{2.20v}$$

The above stochastic program, written in extensive form, is linear since the objective function and the constraints are linear functions of the decision variables. Therefore, the problem has a global optimal solution. In addition, the problem is of modest size, as a result, it can be solved easily with any commercial linear programming (LP) solver such as CPLEX, Gurobi and MOSEK, or open-source LP software such as COIN-OR Linear Programming (CL), GNU Linear Programming Kit (GLPK) and Modular In-core Nonlinear Optimization System (MINOS), using using widely accepted algorithms such as interior point method. Fig. 2.3 provides a typical solution procedure for the problem.

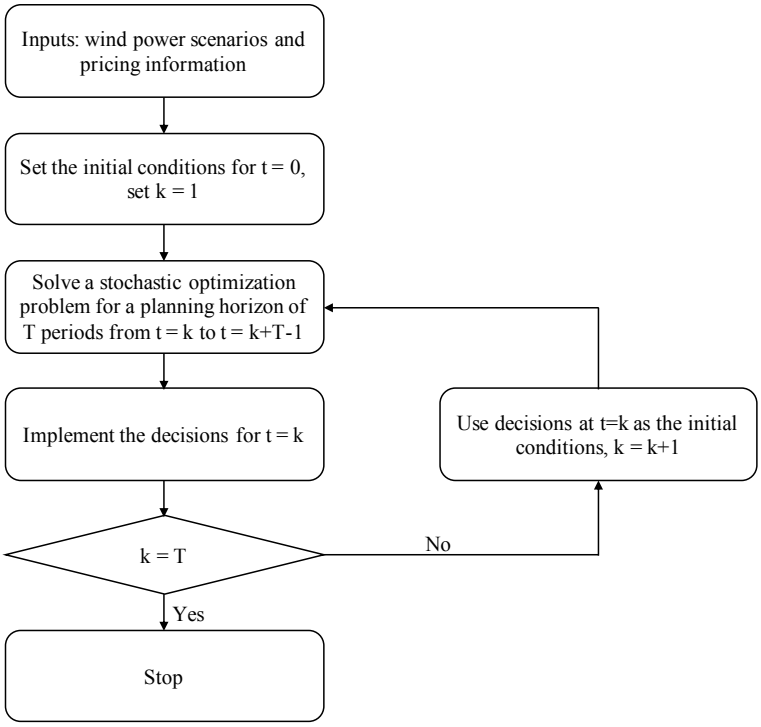

Figure 2.3: Flowchart of Stochastic Rolling Horizon Optimization Algorithm

2.4 Wind Scenario Generation and Reduction

The uncertainty associated with the power generated from wind resources is a critical aspect of this model, and is represented by wind speed scenarios, which are then converted to wind power scenarios through the use of a piece-wise linear power curve, as described in [50]. In the literature, ARMA class models are popular choices for wind speed scenario generation [50, 49]. In this work, an autoregressive model is applied on wind speed time series data to generate scenarios. The detailed steps are given in Algorithm 1:

Algorithm 1: Wind Scenario Generation

1: Create a stationary wind speed w_t^s time series by subtracting the original wind speed time series w_t by the daily wind speed mean μ_t and divide by the daily wind speed standard deviation σ_t.

$$w_t^s = \frac{w_t - \mu_t}{\sigma_t}$$

2: Fit the stationary wind speed data to an empirical distribution function F_e.

$$W_t^s = F_e(w_t^s)$$

3: Do an inverse normal distribution cumulative distribution function (CDF) N^{-1} on the empirical CDF W_t^s to get a Gaussian stationary time series w^{ns}.

$$w_t^{ns} = N^{-1}(W_t^s)$$

4: Estimate the AR model parameters including the autoregressive coefficient ϕ_i and the noise term ϵ_t using the Yule-Walker equations.

$$w_{t+1}^{ns} = \sum_{i=1}^{p} \phi_i w_t^{ns} + \epsilon_t$$

5: Sample error terms from a Gaussian distribution in each period to create multiple scenarios.
6: Do the inverse process of step (3)-(1) to get untransformed wind speed scenarios.
7: Map the wind speed scenarios into wind power scenarios using the wind power-speed curve.

The wind power scenario generation step results in a large set of scenarios, which are then reduced by k-means clustering to determine a representative set. This is necessary to reduce the computational burden inherent to solving

the stochastic problem. Since wind scenario generation and reduction is not the focus of this work, interested readers are referred to [50] for details.

2.5 Numerical Results

The case study considered here uses historical hourly data from the ComED historical database. Load data is the scaled aggregated load in the ComEd service region[51]. The disaggregation of the ComEd load is assumed to have the same profile as that of the national load shown in Table 2.1. The day-ahead price and real-time price (RTP) data for the corresponding load are also from ComEd[52], and cannot be influenced by the microgrid. In addition, the temperature and wind speed data are measured at Chicago O'Hare airport within the ComEd region[53]. The microgrid used in the case study has a capacity of 15 MW. It is assumed that there are 300 households and TCLs in this microgrid. The cost parameters are based on references [54, 55]. Other parameters used in the study are given in Table 2.2. For each test case, simulations are run in Matlab and solved by Gurobi as they are linear programs for a winter month (February, 2016), a summer month (August, 2016) and a mid-year month (May, 2016) for different system conditions. The operational principles of the DRs are invariant with seasons, but the summer season provides the most varied system conditions for the model to navigate. Therefore results from summer season are provided as illustration of the proposed framework.

Parameters	C^b	C^g	$\overline{R}$	$\underline{R}$	PCC	$\underline{P}^b$	$\overline{P}^b$	$\overline{P}$
Values	\$1/MWh	\$30/MWh	1.5 MW	-1.5 MW	15 MW	-7.5 MW	7.5MW	5 MW

Parameters	$\underline{P}$	C^w	$\underline{B}$	$\overline{B}$	T	α	β	Load	$\overline{P}^w_{t,s}$
Values	0 MW	\$500/MWh	0 MWh	15 MWh	24	0.99	0.99	2.5-8 MW	1.5 MW

Table 2.2: MG parameter values

First, the results when the three types of DRs are in effect are presented. Then for each type of DR, the daily operation cost of the microgrid is first compared to a base case without DR. Subsequently, typical days are presented to illustrate the various conditions, and the resulting performance of DR resources under each. The results are presented below, for each of the DR types.

2.5.1 Conjunction of All Types of Demand Response

The first result considered for this case study is the cost savings impact of implementing all three DR programs simultaneously; TCL, DL and EL. The cost saving of the microgrid with all three types of DR compared to the microgrid without DR for August is illustrated in Fig. 2.4. While it is clear that there is significant cost savings from these DR programs, it is difficult to identify the contribution of various types of DR to microgrid performance. Therefore the following sections explain the impact of TCL, DL, and EL individually.

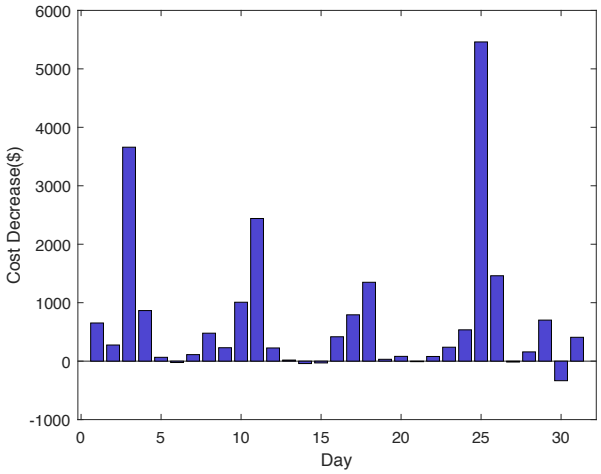

Figure 2.4: Microgrid cost saving from TCL, DL and EL in August

2.5.2 Thermostatically-Controlled Loads (TCL)

TCLs have a wide range of impacts on the operational cost of the microgrid. For example, Fig. 2.5 shows the daily benefits to the microgrid, in terms of cost reduction, over the month of August. The range of benefit is from a minimum approximately 10$/day to a maximum of 300$/day on day 26. The specifics that contribute to these savings are detailed in Fig. 2.6. Fig. 2.6 shows the response of the TCLs relative to baseline TCL load on day 26. Specifically, the TCLs respond to the high price signal in the afternoon hours, to reduce microgrid load, leading to a significant cost reduction. As a counter-point, Fig. 2.7 shows the same details for day 11, which also exhibits high prices. However the temperatures observed on day 11 are sufficiently high that AC units need to maintain fairly continuous operations to maintain comfort constraints. As a result, significant TCL load reduction is not possible, even during the peak pricing hours of the day and very little costs savings are observed.

It is hard to generalize the relationship between the TCL cost reduction and the RTP variability and TCL adjustment flexibility separately. Because RTP variability is more impactful only when there is the ability to adjust TCLs, generally associated with moderate ambient temperatures, as previously described. To illustrate this interactive effect, we create a new variable that incorporates interactions by taking the product of the daily RTP variance and the TCL adjustment(ie: $\sum_{t=1}^{24} |(P_{t,s}^{c} - P_{t,s}^{cb}(\mathcal{T}))|$). As shown in Fig. 2.8, this interactive variable has a significant influence on cost savings in the microgrid.

The legend notes correlations for each season type, indicating that spring and summer months may provide better DR opportunities from TCLs, but in order for cost savings to occur, both an increase in RTP and available TCL adjustment are necessary conditions. Note that the relatively small correlation (0.66) for August is due to a single outlier at the top of the figure, without which the correlation increases to 0.73.

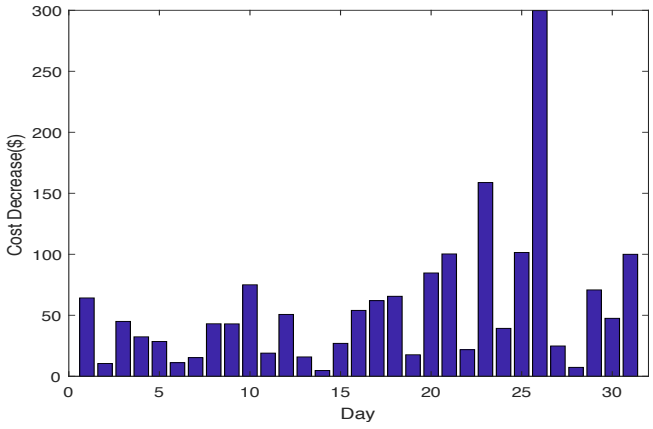

Figure 2.5: Microgrid cost saving from TCL in August

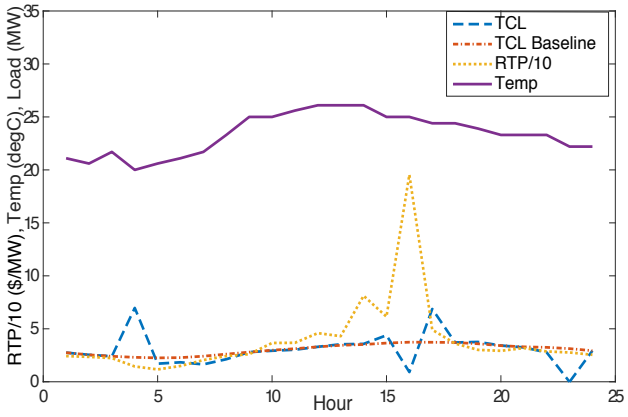

Figure 2.6: Microgrid operation details for day 26 with high cost reduction from TCL

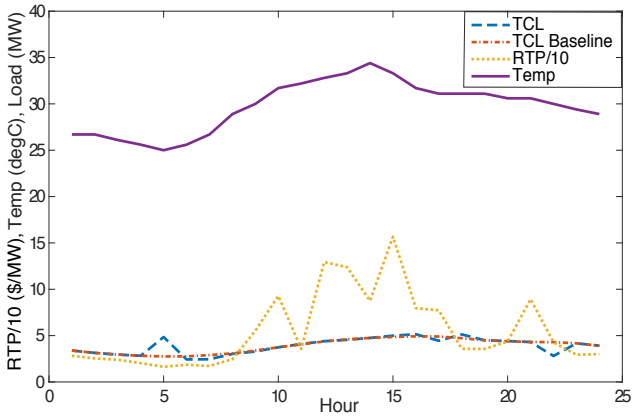

Figure 2.7: Microgrid operation details for day 11 with low cost reduction from TCL

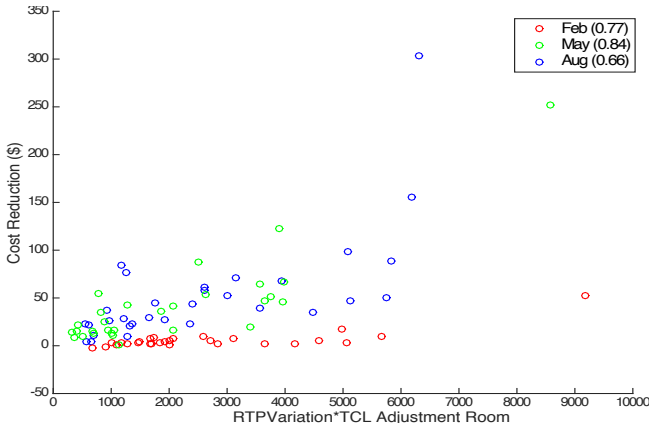

Figure 2.8: TCL Cost Reduction VS RTP Variation × TCL Adjustment Magnitude. In order for cost savings to occur, the variation in RTP and available TCL adjustment are needed at the same time.

2.5.3 Deferrable Loads (DL)

For DL, periods with very high energy import cost are set to be eligible for load reduction incentives. The deferrable load program in this case study is structured such that loads will be considered for deferral during daytime hours (6am to 9pm) when the system price exceeds a specific threshold. Deferred loads must be served before 9 pm on the same day. In the results presented here, a price threshold is set at 55$/MWh, to represent a fairly high daytime price. Day-ahead prices are based on the forecast of the real-time load, renewable and other system conditions. Therefore day-head prices are used as forecasts for the real-time prices. From Fig. 2.9, it can be seen that this type of DR does not always reduce operational cost. For example, the operation details for day 9 are displayed in Fig. 2.10, showing a cost increase due to the inaccurate day-ahead price forecast. Specifically, the day-ahead price forecast induces a shift in DL to later in the day, when prices are expected to decline. However, in reality, the DLs were shifted to the latest possible hour, which also coincides with a price spike. This phenomenon is also observed on days 10 and 30 in this case study. As a counter-example, Fig. 2.11 presents the case with considerable DL cost reduction, which is due to appropriate deferral of DL from price peak hours in the afternoon to the low price hour 19. Hence, avoiding price peaks and high quality price forecasts significantly contribute to the operational cost reduction from DL.

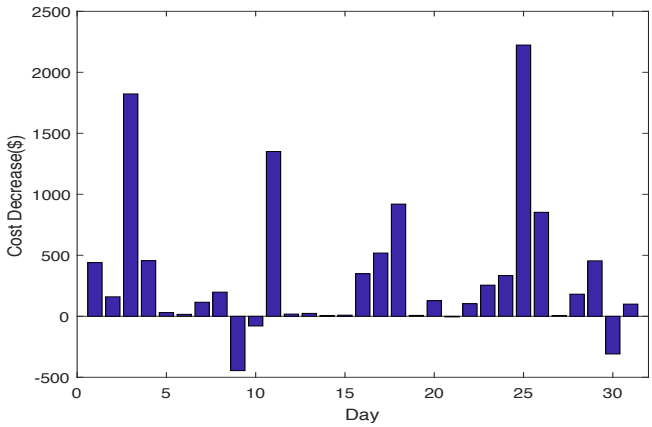

Figure 2.9: Microgrid cost saving from DL in August

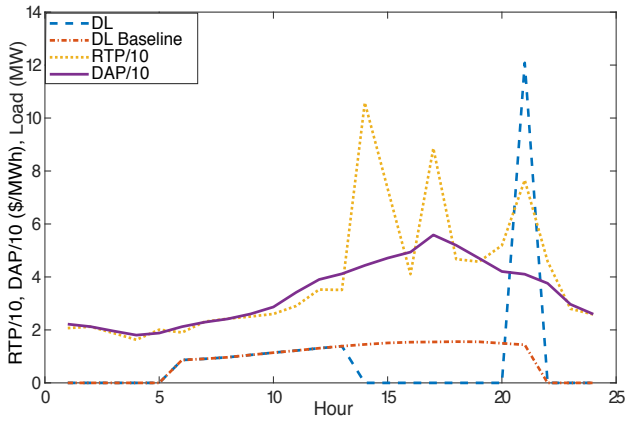

Figure 2.10: Microgrid operation details for day 9 with increased cost from DL

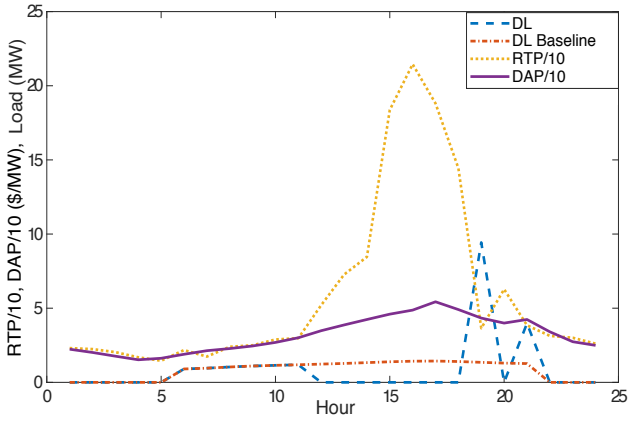

Figure 2.11: Microgrid operation details for day 26 with high cost reduction from DL

Fig.2.12, illustrates a positive correlation between the max daily RTP and the cost reduction from DL, which corroborates the assertion that avoiding the price peaks has a major contribution to the high DL cost reduction.

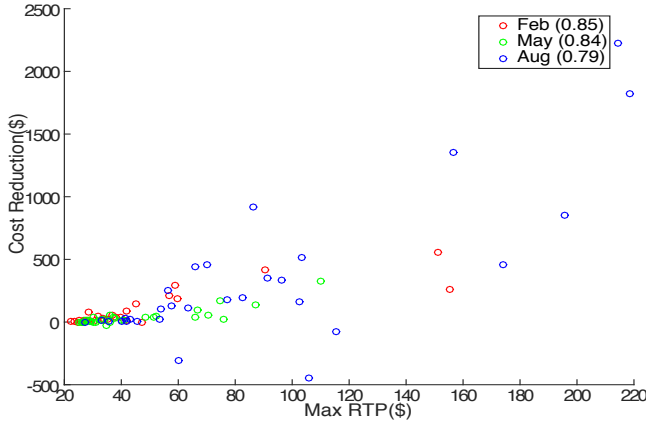

Figure 2.12: DL Cost Reduction VS Max RTP

2.5.4 Elastic Load (EL)

It is assumed that ELs are only in effect between 6am and 9pm as people will not manipulate load consumption during nighttime hours. The residential electricity elasticity is -0.24 at the national level [37], and in this case, a value of -0.2 is assumed to provide conservative results. The reference price is 30.8 $/MWh, which is the average annual RTP, and the base load profile is with respect to this fixed price. Similar to DL, EL does not always produce cost savings, due to the fact that the total daily EL consumption is not fixed. As shown in Fig. 2.13, the EL consumption could be either higher or lower than the baseline consumption. Specifically, the total daily EL consumption does not need to be the same as the total daily EL baseline consumption, as these loads are reduced if the RTP is higher than the reference price and vice versa, not deferred to later. Note that

there is a net negative bias in Fig. 2.13, due to the timing of elastic load use, and the dynamic prices over the course of the day. Specifically, it is assumed elastic loads are only in effect between 6am and 9pm, as people will be far less likely to manipulate load consumption during nighttime hours. Since the periods when elastic load is available, tends to have higher prices than the reference prices, the price elasticity leads to a net negative bias in the energy consumption. The daily microgrid operation cost with EL DR is given in Fig. 2.14. Comparison of Fig. 2.13 and Fig. 2.14 illustrates that the operation costs increase for most of the days, which have higher consumption compared to the baseline. Nevertheless, more EL consumption does not result in cost reduction for day 5 and day 20. That is because EL DR encourages consumption during low price hours and results in a lower average electricity price, with a net effect of reduced cost for more consumption. Fig. 2.15 illustrates the cause behind significant cost saving for day 25, due to the reduced EL consumption during the high price hours 14-18. The minimal real EL consumption deviation from the EL baseline accounts for the small cost saving on day 6 as shown in Fig. 2.16. The deviation is small as the real-time price is not significantly different from the reference price on day 9.

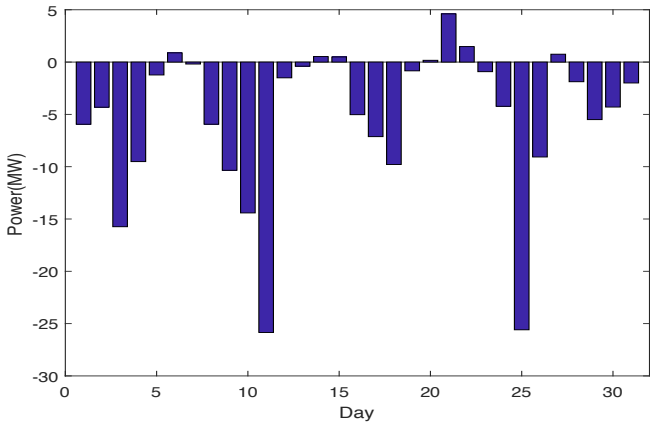

Figure 2.13: Microgrid EL consumption - EL consumption baseline

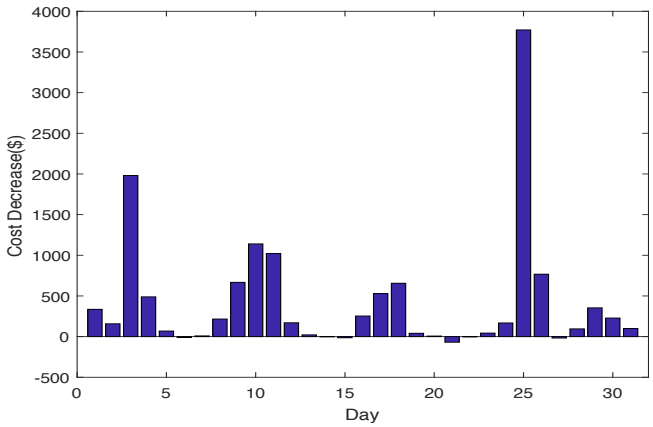

Figure 2.14: Microgrid cost saving from EL in August

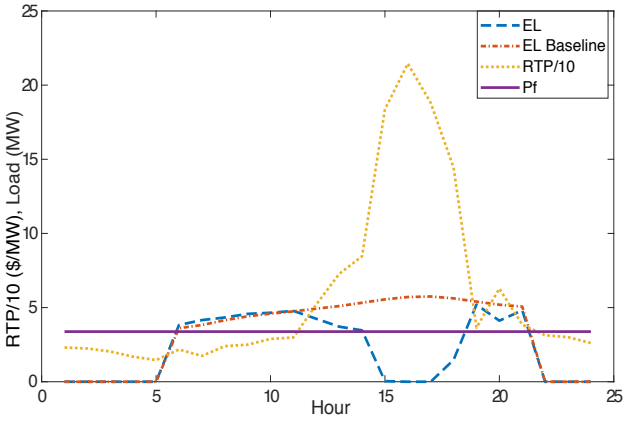

Figure 2.15: Microgrid operation details for day 25 with high cost reduction from DL

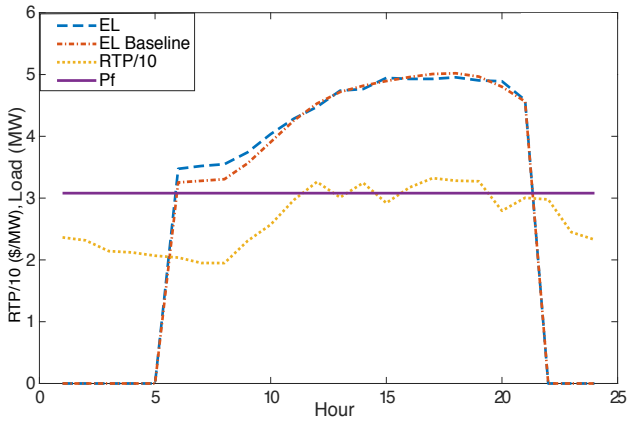

Figure 2.16: Microgrid operation details for day 7 with little cost saving from DL

In Fig. 2.17, the scatter plot illustrates the positive correlation between the maximum daily RTP and the cost reduction from EL to varying degrees across all seasons. It advocates the idea that high price is the main driver for the cost reduction from EL, as high price leads to load response.

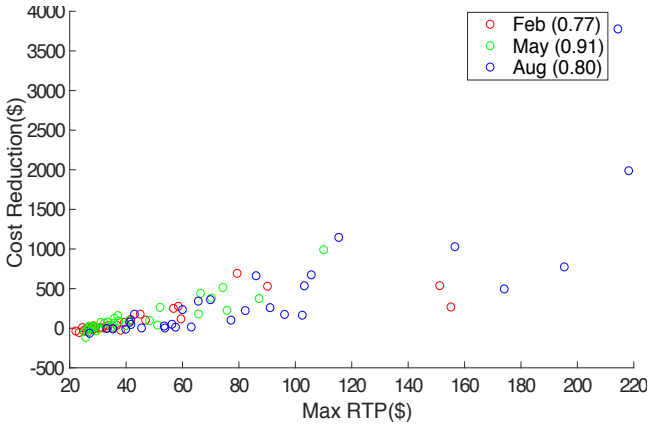

Figure 2.17: EL Cost Reduction VS Max RTP

2.5.5 Demand Response Benefit Comparison: Microgrids and Distribution Systems

Here we differentiate between a grid-connected microgrid and a traditional distribution system which we define as one which does not have any independent types of power generation. If the microgrid generators and renewables are removed, the microgrid essentially becomes a distribution system, to which the DR models described here also apply. However, the contribution of the DR in a microgrid is more significant than that in a distribution system primarily due to the additional flexibility offered by the microgrid generators that could be utilized by the DR in the microgrid. Table. 2.3 displays TCL and DL saving in a microgrid and a distribution network. TCL and DL have more cost benefit in

a microgrid than in a distribution system. Specifically, the generation from the microgrid is sometimes less expensive than the generation from the main grid, which enables the microgrid to arbitrage by using less expensive generation to meet its needs. Since EL is only affected by the energy import price, which is the same in the microgrid and the distribution system, the behavior of EL DR is consistent for both cases.

	TCL	DL
Microgrid	1%	6%
Distribution Network	0.63%	4%

Table 2.3: DR saving in a microgrid and a distribution system

2.6 Concluding Remarks

This paper presents an analysis of a grid-connected microgrid with DR and distributed generation. A stochastic rolling horizon model is used to simulate the decision process of a microgrid energy management system to manage loads, generation, and purchases from the main grid. The rolling horizon scheme allows exploitation of the forecast updates for the prices and renewables in the real-time market. Therefore this load categorization and the corresponding DR designs enable the best utilization of the DR potential. Insights from the analysis of different DR provides microgrid operators and designers with the knowledge to incorporate the various types of DR that are suitable for the given system conditions. In general, TCL achieves fine performance based on provision of load reduction during peak price periods. Accurate deferral of loads to off-peak periods, in conjunction with good price forecasts is the basis for cost savings from DL. In contrast, EL accomplishes energy saving primarily from energy conser-

vation under high price periods. However, lower operational cost is possible for an increased consumption as a result of the reduced average energy price. Lastly, it is shown that DR in a microgrid has the potential to provide more cost savings than in a distribution network, since a microgrid provides more flexibility for DR to arbitrage.

An important future direction is to model the microgrid interconnection with the transmission network and explore how DR in the microgrid benefits the main system. Such a study will likely reveal new benefits of the microgrid DR programs. One crucial area is to investigate the DR's ability to shape the load profile at the connecting bus, which could impact the congestion likelihood in the main system, assist in the management of variability, and reduce locational marginal prices. In addition, incorporating more detailed physical constraints such as voltage magnitude and power losses is also a promising direction.

2.7 Acknowledgments

This material is based upon work supported by the US Department of Energy under Award Number DE-OE0000843. Disclaimer: This report was prepared as an account of work sponsored by an agency of the United States Government. Neither the United States Government nor any agency thereof, nor any of their employees, makes any warranty, express or implied, or assumes any legal liability or responsibility for the accuracy, completeness, or usefulness of any information, apparatus, product, or process disclosed, or represents that its use would not infringe privately owned rights. Reference herein to any specific commercial product, process, or service by trade name, trademark, manufacturer, or otherwise does not necessarily constitute or imply its endorsement, recommendation, or favoring by the United States Government or any agency thereof. The views and opinions of the authors expressed herein do not necessarily state or reflect those of the United States Government or any agency thereof.

CHAPTER 3

BI-LEVEL OPTIMIZATION OF MICROGRID AND TRANSMISSION SYSTEMS FOR CO-OPERATION AND RENEWABLE INTEGRATION

The growth in distributed energy resources (DER), both generation and consumption, challenges the traditional centralized control framework of electric power systems. Microgrids (MG) are one emerging framework for coordinating DER and distribution system operations, both within the distribution system itself and for interactions with the bulk power system. This growing influence of DER on bulk power system operations could evolve to the point that the low- and high- voltage systems play equal roles in maintaining system stability and reliability, as well as in market operations. Such evolution will require co-operative system operations. The co-operation of the N-1 security constrained integrated systems is analyzed in a bi-level optimization framework developed in this chapter. This chapter first describes the formulation and solution methodology to this bi-level problem, and then compares performance on the basis of system economics and renewable integration under different system configurations. The results with the bi-level framework show that integrated microgrids could provide improvement to system cost and feasible wind penetration. The framework which independently optimizes the systems without interaction, is shown to be inadequate to fully reveal the benefits that are demonstrated by the bi-level co-optimization framework. The analysis in this paper provides insights for future integrated co-operation to enable a more sustainable power system and boost the system operation efficiency.

Nomenclature

Paremeters	
T	length of the planning horizon
G	total number of generators in the transmission system
$\overline{R}_g / \underline{R}_g$	upper/lower ramp rate limit of transmission system generator g
$\overline{P}_g / \underline{P}_g$	generation upper/lower bound of transmission system generator g
$\overline{L}$	transmission system line limit
C_g^1 / C_g^2	linear/quadratic cost coefficient (\$/MW) of transmission system generator
C_g^c	commitment cost coefficient (\$/MW) of transmission system generator g
C_g^r	reserve cost coefficient (\$/MW) of transmission system generator g
GSF	generation shift factor matrix for transmission system
GSF_i^{con}	generation shift factor matrix when transmission line l trips
W_t^f	transmission forecasted wind power in period t
W_t^{up} / W_t^{dn}	upward/downward deviation from the forecast wind power in period t in the transmission system
N_b	number of buses in the transmission system
L_t	transmission system load power vector in period t
$\underline{L}_t^d / \overline{L}_t^d$	lower/upper bound for microgrid aggregated dispatchable load in period t
$\underline{L}_t^i$	microgrid inelastic load in period t
$\overline{B} / \underline{B}$	max/min level of microgrid storage energy state
C^b	microgrid storage energy maintenance cost coefficient (\$/MW)
C^{m1} / C^{m2}	microgrid generation linear/quadratic cost coefficient (\$/MW)
C^d	microgrid utility for consuming dispatchable load
C^{dr1} / C^{dr2}	microgrid linear/quadratic demand response cost coefficient
$\overline{P}^m / \underline{P}^m$	upper/lower bound on microgrid generation
$\underline{P}^b / \overline{P}^b$	microgrid storage discharging/charging limit
$R_{g,t}^{con}$	contingency reserve requirement for transmission system generator g in period t
Variables	
$r_{g,t}^{up} / r_{g,t}^{dn}$	upward/downward reserve of transmission system generator g in period t
p_t^{dr}	microgrid demand response price in period t (\$/MW)
$p_{g,t}$	generation of transmission system generator g in period t
p_t^m	microgrid generation in period t
b_t	microgrid storage energy state at the beginning of period t
p_t^{ex} / p_t^{im}	microgrid exported/imported power in period t
c_t^{ex} / c_t^{im}	price of microgrid exported/imported power in period t
p_t^b	microgrid storage power (charging/discharging) output in period t
l_t^d	microgrid aggregated dispatchable load in period t
dr_t^{up} / dr_t^{dn}	upward/downward demand response of microgrid dispatchable load in period t
$pinj_t$	transmission bus power injection vector in period t
$w_{g,t}$	transmission system generator commitment variable for generator g in period t
$r_{g,t}^{con}$	contingency reserve for transmission system generator g in period t

3.1 Introduction

Future power systems are envisioned to move toward a green and decentralized system with high penetration of renewable energy and distributed generation [56]. Microgrids will play a critical role in this evolution, as they feature protocols that allow grid coordination and islanded operation, and facilitate increased flexibility and resilience for the evolving power systems. With the possibility of many microgrids connected to and exchanging power with the main grid, the power system operation will also need to evolve. Each microgrid could become an independent entity with its own operation objective, which could conflict with that of the transmission system's. Strategies to co-optimize the two levels within the power systems will become crucial for the efficient operation of the integrated system.

The co-optimization of the transmission system and microgrid operation is a relatively new area. In [57], a framework in which microgrids embedded in a distribution network could transact with the transmission network and maximize each system's benefit is proposed. The process of information exchange between the systems is discussed. The work in [58] models the interaction between a central production unit and an energy service provider consisting of several microgrids in a bi-level framework. The benefit of this operation is compared with operation under central control of both parties. The optimal scheduling of microgrid operation with demand response is discussed in [59]. The author of [60] presents a control scheme with microgrid demand response and energy storage to provide tie-line smoothing service with the transmission system. A microgrid expansion problem is formulated as a two-stage stochastic co-optimization problem that considers the influence of the generation and

transmission companies in [61]. It is shown that integration of traditional energy resources could boost the system reliability and reduce the operation cost. A method for generation and transmission expansion planning based on microgrid co-optimization is explored in [62]. The effectiveness of the proposed method is demonstrated and compared to the traditional generation and transmission upgrade approach. The transmission system in [57, 58, 59, 60] is modeled as a single node which connects to the microgrid and exchanges energy at fixed prices. Neglecting the transmission system characteristics reduces model realism, as nodal energy exchange and price information rely upon the network characteristics of transmission and can change over time. Consequently, optimization of a microgrid in those models becomes less realistic and the effect of the microgrid on the transmission system is not adequately represented. This is particularly important as the aggregate capacity of microgrids increases. The microgrids in [61, 62] are modeled at a very high level (i.e., distributed generation with aggregated load). However, microgrids increasingly include energy storage units and provide demand response, which benefit from a separate energy management system for the microgrid. Neglecting to model both a variety of DER technologies in the microgrid and networked transmission lines at the high voltage level fails to capture the true impact of microgrids on the transmission system.

The upper- and lower- level hierarchy of bi-level optimization is suitable for the study of various aspects of the power systems including the interaction of the transmission and microgrid interaction. For example, in [63], a bi-level framework is applied in a microgrid to minimize the system operation cost in the upper level problem and power fluctuations induced by renewable forecast errors in the lower level problem. The planning of and investment in power

system elements such as energy storage units and distributed generation using a bi-level optimization framework is investigated in [64, 65]. In [66, 67], the bidding strategies of generation companys (GENCO) are studied. Specifically, the GENCO's payoff optimization is formulated as the upper-level problem and the independent system operator (ISO)'s dispatch problem is formulated as the lower-level problem. Bi-level optimization is applied in [68, 69, 70] to examine power system vulnerability issues and minimize the system loss under terrorist attacks on transmission lines or generators.

As renewable resources are of increasing importance in modern power systems, there has been extensive study of different ways to manage increased renewable penetration in the transmission system. In addition to the common method of using reserves to accommodate transmission level renewables [71, 72, 73], demand response is an effective resource for support of renewable integration [74, 75]. The role of energy storage in promoting renewable penetration in the transmission system is investigated in [76, 77]. Moreover, electric vehicles could also support the penetration of renewables [78, 79].

What this study adds to the literature is an analysis of the impact of flexible microgrid operations on the transmission system operation through co-optimization with a decoupled DC power flow model for both systems. This allows the analysis of the technologies inside the transmission and microgrid systems on the operation of each other in the future power systems. With a bi-level framework for the transmission system and microgrid, the factors that affect the transmission system renewable penetration level and the system operation cost are analyzed. The highlights of this work are summarized below:

(1) Co-optimization of the N-1 security constrained transmission system with a responsive microgrid is implemented in a bi-level framework, allowing modeling of each system with sufficient detail.

(2) A concise single-level reformulation scheme is developed, which enables more efficient solution of the bi-level optimization problem.

(3) Factors that affect the system wind penetration level and operation cost are identified and analyzed.

(4) The impact on system cost is examined with an increasing number of microgrids.

(5) Demand response is located and modeled at the low-voltage level where the micro-grid resides, to realistically reflect the anticipated expansion of DR at this level.

The paper is structured as follows: The problem under analysis is described in Section 3.2. Section 3.3 delineates the bi-level optimization formulation, with a reformulation of the bi-level problem to an easily solvable format in Section 4.3. Numerical results are reported in Section 4.4. Concluding remarks follow in Section 4.5.

3.2 Problem Description

The transmission system model solves a unit commitment problem. The microgrid model implements an optimal power dispatch problem. Those two problems and the co-operation of the systems are the focus of this study and are described below.

3.2.1 Transmission System Day-Ahead Unit Commitment Problem

The transmission system is modeled as a network of transmission lines and buses. Traditional and renewable generation units, loads, and microgrids are connected to buses in the network. The transmission system solves a day-ahead unit commitment problem, which involves the energy and ancillary services markets. The objective of this problem is to find cost-effective operation schedules for the energy resources to meet the load considering renewable generation uncertainty. Specifically, for the energy market, the transmission system aims to minimize the cost of meeting the system demand with its own generation or energy imported from microgrids. For the ancillary services market, the goal is to minimize the cost of providing reserves to account for the renewable forecast uncertainty. The reserve resource is procured from a combination of the transmission system generators' reserve and the microgrid's DR. The energy and ancillary services market decisions are determined together. The interested reader is referred to [80] for a detailed treatment of the unit commitment problem.

3.2.2 Microgrid Optimal Dispatch Problem

The size of a microgrid could vary from a few kW to hundreds of MW [81]. The microgrid may be part of the distribution system or the entire distribution system and so directly connects to the transmission system through the substation. The case of direct connection to the transmission system is considered in this work. The microgrid has an aggregated dispatchable load and a non-dispatchable load, an energy storage unit, and a distributed generator. This

model provides sufficient detail to capture microgrid interaction with the bulk transmission system. In the day-ahead market, the microgrid solves an optimal dispatch problem. The dispatchable load is scheduled at a level between its upper and lower bounds. The difference between the upper/lower bound and its preset load level could be used to provide upward/downward DR. The objective of the microgrid is to minimize the cost of meeting its demand either via its distributed generation or energy import from the transmission system, and to maximize the revenue from providing DR and optional energy export. For a detailed description of the microgrid optimal dispatch problem, see [82].

3.2.3 Transmission System and Microgrid Operation Modes

The integrated system, including the transmission system and the microgrid, may operate in two modes. The first one of these is the standalone mode, in which the systems are disconnected and can neither exchange energy, nor allow the microgrid to provide DR to the transmission system. In the second (co-operative) mode, the two systems have the capability to transact. Specifically, the transmission system determines the price of microgrid energy import and export as well as the price for the microgrid DR purchases, and the microgrid responds to the prices by determining the amount of energy exchange and provision of DR to the transmission system.

3.3 Bi-level Optimization Model

Bi-level optimization is a common game-theoretic approach to analyze the interactive behavior between market entities [83]. It has a two-level problem structure, as shown in the following general formulation:

$$\begin{aligned}
&\text{Upper-Level Problem: } {}_{x\in X}F(x,y)\\
&\qquad\text{s.t.: } G_i(x,y)\le 0,\ i\in\{1,2,...,I\}\\
&\qquad\quad H_k(x,y)=0,\ k\in\{1,2,...,K\}\\
&\text{Lower-Level Problem: } {}_{y\in Y}f(x,y)\\
&\qquad\text{s.t.: } g_j(x,y)\le 0,\ j\in\{1,2,...,J\}\\
&\qquad\quad h_m(x,y)=0,\ m\in\{1,2,...,M\}
\end{aligned} \tag{3.1}$$

In (4.1), the variable set of the upper/lower-level problem is X/y, $F(x,y)/f(x,y)$ is the objective function, and $(G_i, H_k)/(g_j, h_m)$ are the constraints. In this work, bi-level optimization is a natural approach to co-optimize the transmission system and microgrid in the power markets. The co-operative behavior between the two systems, described in Section 2.3, is illustrated in a bi-level optimization structure in Fig. 4.2.

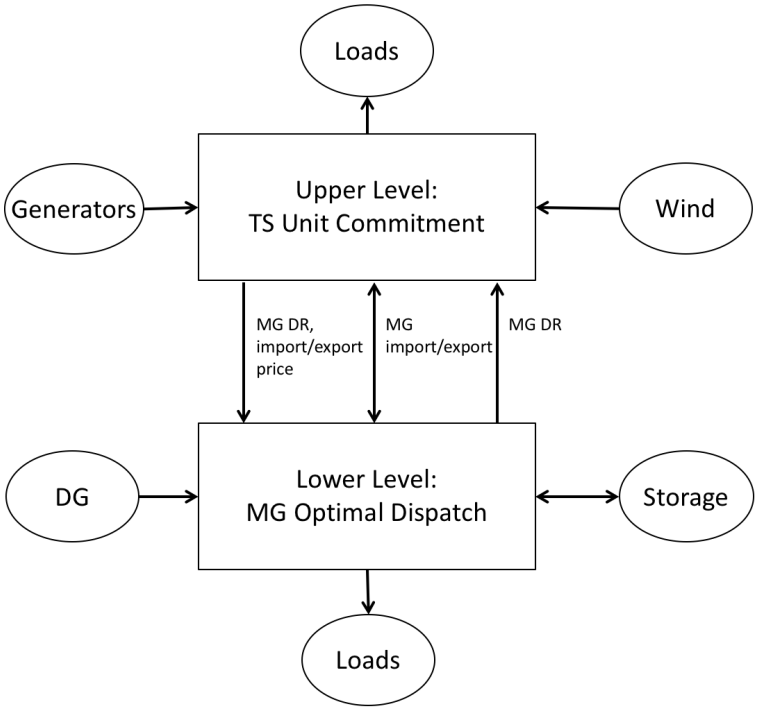

Figure 3.1: Illustration of a bi-level optimization framework. The upper-level transmission system decides the energy and demand response price signals, and the lower-level microgrid problem responds by deciding the quantity of energy exchanged and the demand response.

The specifics of the bi-level optimization model in this study are given below.

3.3.1 Upper-Level Problem: Transmission System Day-Ahead Unit Commitment Problem

The upper-level day-ahead unit commitment problem seeks operation schedule that minimizes the cost of operation of the transmission system i.e., the generator commitment status $w_{g,t}$, generation output $p_{g,t}$, the generator's upward and downward reserve $r^{up}_{g,t}$, $r^{dn}_{g,t}$, the microgrid DR price p^{dr}_t, and the prices of the microgrid's imported and exported energy c^{im}_t, c^{ex}_t. The optimization variables are

denoted by the vector x_t:

$$x_t = [w_{g,t}, p_{g,t}, r^{up}_{g,t}, r^{dn}_{g,t}, p^{dr}_t, c^{im}_t, c^{ex}_t]$$

The objective of the upper-level optimization problem is to minimize the transmission system operation cost including transmission generation, the reserve, energy exchange with the microgrid, and microgrid DR cost. The objective function is

$$\begin{aligned} F(\{x_t\}_{t=1}^T) &= \sum_{t=1}^T \sum_{g=1}^G (C^c_g w_{g,t} + C^1_g p_{g,t} + C^2_g (p_{g,t})^2 + C^r_g (r^{up}_{g,t} + r^{dn}_{g,t}) \\ &- c^{im}_t p^{im}_t + c^{ex}_t p^{ex}_t + p^{dr}_t (dr^{up}_t + dr^{dn}_t)) \end{aligned} \tag{3.2}$$

and is minimized under the following constraints:

- ***Power Flow:***

$$-\overline{L} \leq GSF \times pinj_t \leq \overline{L}, \qquad t \in \{1, ..., T\} \tag{3.3}$$

$$-\overline{L} \leq GSF \times pinj^*_t \leq \overline{L}, \qquad t \in \{1, ..., T\} \tag{3.4}$$

  where $pinj_t$ is the nodal net power injection vector accounting for traditional generation, wind generation, and demand for all the buses in period t. $pinj^*_t$ incorporates the error in the forecasted wind power, generator reserves and microgrid DR into the base $pinj_t$. Eqs. (3.3) and (4.4) bound the power flows through the transmission lines.

- ***Generation Capacity:***

$$\underline{P}_g \times w_{g,t} \leq p_{g,t} \leq \overline{P}_g \times w_{g,t}, \qquad t \in \{1,\ldots,T\}, g \in \{1,\ldots,G\} \tag{3.5}$$

$$(p_{g,t} + r^{up}_{g,t}) - (p_{g,t-1} - r^{dn}_{g,t-1}) \leq \overline{R}_g, \qquad t \in \{2,\ldots,T\}, g \in \{1,\ldots,G\} \tag{3.6}$$

$$\underline{R}_g \leq (p_{g,t} - r^{dn}_{g,t}) - (p_{g,t-1} + r^{up}_{g,t-1}), \qquad t \in \{2,\ldots,T\}, g \in \{1,\ldots,G\} \tag{3.7}$$

Eq. (4.5) restricts the generators' outputs to lie within their capacities. The generator ramping limits are represented in Eqs. (4.6) and (4.7). The ramp limit is in MW/hour as the the dispatch and wind estimation are carried out in an hourly frequency.

- ***Power Balance:***

$$\sum_{g=1}^{G} p_{g,t} - (\mathbf{1}_{1\cdot N_b} \cdot L_t) + W^f_t = p^{im}_t - p^{ex}_t, \qquad t \in \{2,\ldots,T\}, g \in \{1,\ldots,G\} \tag{3.8}$$

where $\mathbf{1}_{1\times N_b}$ is an N_b -dimentional vector filled of 1's. The dot product $\mathbf{1}_{1\times N_b} \cdot L_t$ gives the total load in the system. Eq. (4.8) balances the system's power supply and demand.

- ***Contingencies:***

$$r^{con}_{g,t} \geq R^{con}_{g,t}, \qquad t \in \{2,\ldots,T\}, g \in \{1,\ldots,G\} \tag{3.9}$$

$$-\overline{L} \leq GSF^{con}_l \times pinj_t \leq \overline{L}, \qquad t \in \{1,...,T\}, l \in \{1,\ldots,L\} \tag{3.10}$$

$$-\overline{L} \leq GSF^{con}_l \times pinj^*_t \leq \overline{L}, \qquad t \in \{1,...,T\}, l \in \{1,\ldots,L\} \tag{3.11}$$

A robust N-1 security criteria is implemented which considers generator and transmission line contingencies based on the method in [84]. Eq. (3.9) ensures that each generator has enough contingency reserves $r^{con}_{g,t}$ for any

generator outage. Please refer to [84] for the calculation of the generator contingency reserve requirement $R^{con}_{g,t}$. Eqs. (3.10) and (3.11) ensure feasibility for any transmission line outage.

- ***Wind Power Forecast Uncertainty:***

  For the wind generation forecast and a set of possible wind generation scenarios, the upward/downward wind power deviation W^{up}_t/W^{dn}_t from the forecast is calculated by taking the difference between the maximum/minimum generation scenario and the forecast for period t. The downward/upward transmission generation reserve $r^{dn}_{g,t}/r^{up}_{g,t}$ and upward/downward microgrid DR dr^{up}_t/dr^{dn}_t are used to offset the upward/downward wind power deviation from the forecast. dr^{up}_t/dr^{dn}_t indicates the amount of increase/decrease in the microgrid dispatchable load consumption relative to its baseline l^d_t. This is essentially a robust approach under the bi-level framework as the reserve allocation is optimized to handle the worst wind scenarios.

$$W^{up}_t \leq dr^{up}_t + \sum_{g=1}^{G} r^{dn}_{g,t}, \qquad t \in \{1, ..., T\} \tag{3.12}$$

$$W^{dn}_t \leq dr^{dn}_t + \sum_{g=1}^{G} r^{up}_{g,t}, \qquad t \in \{1, ..., T\} \tag{3.13}$$

Eqs. (4.9) and (3.13) ensure that there is enough generator reserve and microgrid DR to compensate for wind forecast deviation. Finally, the transmission system unit commitment problem can be expressed as follows:

$$\min_{\{x_t\}_{t=1}^T} F\left(\{x_t\}_{t=1}^T\right)$$

$$\text{s.t. } (3.3) - (3.13)$$

3.3.2 Lower-Level Problem: Microgrid Operation Optimization

The microgrid modeled in this work is designed to exchange power with the main grid, and consists of distributed generation (DG) with traditional resources, an energy storage unit, an aggregated dispatchable load, and a non-dispatchable load.

The objective of the microgrid dispatch problem is to determine the generation schedule p_t^m, the energy storage power output p_t^b (i.e., the energy storage charging and discharging decision), the microgrid energy import schedule p_t^{im} and export schedule p_t^{ex}, the dispatchable load profile l_t^d, the upward/downward demand response dr_t^{up}/dr_t^{dn} provided by the dispatchable load, and the energy storage energy state b_t. The lower-level optimization variables are collected in the vector y_t:

$$y_t = [p_t^m, p_t^b, p_t^{im}, p_t^{ex}, dr_t^{up}, dr_t^{dn}, l_t^d, b_t]$$

In this problem, the cost of operation of the microgrid, consisting of generation, energy storage, energy exchange with the transmission system, and DR, is minimized. The dispatchable load consumption utility, energy export, and DR revenue, which are negative costs, are maximized. The objective function to be minimized is given by:

$$\begin{aligned} f(\{y_t\}_{t=1}^T) &= \textstyle\sum_{t=1}^T (C^{m1} p_t^m + C^{m2}(p_t^m)^2 + C^b b_t + c_t^{im} p_t^{im} - c_t^{ex} p_t^{ex} \\ &+ C^{dr1}(dr_{g,t}^{up} + dr_{g,t}^{dn}) + C^{dr2}((dr_t^{up})^2 + (dr_t^{dn})^2) \\ &- C^d l_t^d - p_t^{dr}(dr_t^{up} + dr_t^{dn})) \end{aligned} \tag{3.15}$$

Similar to the transmission system problem, the microgrid problem is subject to constraints, as described below. For clarity, the dual variables corresponding to the inequality constraints are denoted by λ and those for the equality constraints are denoted by μ.

- ***Generation Limits:***

$$\underline{P}^m \leq p_t^m \leq \overline{P}^m, \qquad \lambda_{1,t},\ \ \lambda_{2,t},\ t \in \{1, ..., T\} \tag{3.16}$$

Eq. (3.16) limits the microgrid's generation to lie between the upper and lower bounds.

- ***Dispatchable Load Capacity:***

$$\underline{L}_t^d \leq l_t^d \leq \overline{L}_t^d, \qquad \lambda_{3,t},\ \ \lambda_{4,t},\ t \in \{1, ..., T\} \tag{3.17}$$

The dispatchable loads are constrained within predefined bounds shown in Eq. (4.15).

- ***Demand Response:***

$$l_t^d + dr_t^{up} \leq \overline{L}_t^d, \qquad \lambda_{5,t},\ \ t \in \{1, ..., T\} \tag{3.18}$$

$$l_t^d - dr_t^{dn} \geq \underline{L}_t^d, \qquad \lambda_{6,t},\ \ t \in \{1, ..., T\} \tag{3.19}$$

$$0 \leq dr_t^{up} \leq W_t^{up}, \qquad \lambda_{7,t}\ \ \lambda_{8,t},\ \ t \in \{1, ..., T\} \tag{3.20}$$

$$0 \leq dr_t^{dn} \leq W_t^{dn}, \qquad \lambda_{9,t}\ \ \lambda_{10,t},\ \ t \in \{1, ..., T\} \tag{3.21}$$

Eqs. (3.18) and (3.19) limit the DR of the dispatchable load to lie between the upper and lower bounds on the dispatchable load. Additionally, the

DR cannot exceed the wind power deviation from the forecast, as specified in Eqs. (4.16) and (4.17).

- ***Energy Storage Dynamics:***

$$\underline{P}^b \leq p_t^b \leq \overline{P}^b, \qquad \lambda_{11,t},\ \lambda_{12,t},\ t \in \{1, ..., T\} \tag{3.22}$$

$$\underline{B} \leq b_t \leq \overline{B}, \qquad \lambda_{13,t},\ \lambda_{14,t},\ t \in \{1, ..., T\} \tag{3.23}$$

$$b_t = b_{t-1} + p_{t-1}^b, \qquad \mu_{1,t},\ t \in \{1, ..., T\} \tag{3.24}$$

Eqs. (3.22) and (3.23) update the energy storage's output power and the energy state and limit them within their admissible bounds. The energy storage state transition dynamics is described in Eq. (3.24). A positive/negative p_{t-1}^b value corresponds to charging/discharging of the energy storage.

- ***Import and Export Limits:***

$$0 \leq p_t^{im}, \qquad \lambda_{15,t},\ t \in \{1, ..., T\} \tag{3.25}$$

$$0 \leq p_t^{ex}, \qquad \lambda_{16,t},\ t \in \{1, ..., T\} \tag{3.26}$$

Inequalities (3.25) and (3.26) are non-negativity constraints for microgrid import and export power respectively.

- ***Power Balance:***

$$p_t^m - p_t^b - L_t^i - l_t^d = p_t^{ex} - p_t^{im}, \qquad \mu_{2,t},\ t \in \{1, ..., T\} \tag{3.27}$$

Eq. (3.27) ensures that the power is balanced within the microgrid system.

Thus the microgrid dispatch problem can be formulated as follows:

$$\begin{aligned} &\min_{\{y_t\}_{t=1}^T} f\left(\{y_t\}_{t=1}^T\right) \\ &\quad \text{s.t. } (3.16) - (3.27) \end{aligned}$$

As a result, the bi-level optimization of the transmission system and microgrid reads:

$$\begin{aligned} &\min_{\{x_t\}_{t=1}^T} F\left(\{x_t\}_{t=1}^T\right) \\ &\quad \text{s.t. } (3.3) - (3.13) \\ &\min_{\{y_t\}_{t=1}^T} f\left(\{y_t\}_{t=1}^T\right) \\ &\quad \text{s.t. } (3.16) - (3.27) \end{aligned}$$

3.4 Single-Level Reformulation of the Bi-level Problem

Two types of strategies are usually used to tackle bi-level optimization problems. The first employs classical methods, including single-level reduction [85], descent method [86], penalty functions [87], and trust-region methods [88]. Those methods generally exploit mathematical properties of the problems such as convexity, continuous differentiability, and lower semi-continuity. The second category employs evolutionary techniques such as genetic algorithms [89], particle swarm optimization [90], differential evolution [91], and meta-modeling based methods [92]; those methods entail considerable computational effort and are not guaranteed to converge to a global solution [83]. For further accounts of various bi-level optimization techniques, see [83, 93].

Single-level reduction is commonly applied when the lower-level problem is convex and satisfies Slater's constraints qualifications [94]. The reformulation replaces the lower-level problem with its corresponding Karush-Kuhn-Tucker (KKT) conditions. Therefore, though easier to solve, the resulting single-level problem is equivalent to the original one. As the lower-level problem in this study meets the above requirements, its associated KKT conditions, i.e., stationarity, dual feasibility and complementary slackness, are used to reformulate the transmission system and microgrid co-operation problem into a single-level optimization problem, as follow:

- ***Stationarity***

  The Lagrangian function associated with the microgrid problem is:

$$
\begin{aligned}
L(x,y,\lambda,\mu) &= f(x,y) + \lambda_{1,t}(\underline{P}^m - p_t^m) + \lambda_{2,t}(p_t^m - \overline{P}^m) + \lambda_{3,t}(l_t^d - \overline{L}_t^d) \\
&+ \lambda_{4,t}(\underline{L}_t^d - l_t^d) + \lambda_{5,t}(dr_t^{up} + l_t^d - \overline{L}_t^d) + \lambda_{6,t}(dr_t^{dn} - l_t^d + \underline{L}_t^d) \\
&+ \lambda_{7,t}(-dr_t^{up}) + \lambda_{8,t}(dr_t^{up} - W_t^{up}) + \lambda_{9,t}(-dr_t^{dn}) + \lambda_{10,t}(dr_t^{dn} - W_t^{dn}) \\
&+ \lambda_{11,t}(p_t^b - \overline{P}^b) + \lambda_{12,t}(\underline{P}_t^b - p^b) + \lambda_{13,t}(b_t - \overline{B}) \\
&+ \lambda_{14,t}(\underline{B} - b_t) + \lambda_{15,t}(-p_t^{im}) + \lambda_{16,t}(-p_t^{ex}) + \mu_{1,t}(b_t - b_{t-1} - p_{t-1}^b) \\
&+ \mu_{2,t}(p_t^m - p_t^b - L_t^i - l_t^d - p_t^{ex} + p_t^{im})
\end{aligned}
$$

  Stationarity describes a set of first-order optimality conditions, i.e., the first derivative of the Lagrangian function with respect to each decision variable is 0. Thus, the following conditions associated with the decision

variables ($p_t^m, l_t^d, b_t, p_t^{im}, p_t^{ex}, p_t^b, dr_t^{up}, dr_t^{dn}$) are enforced:

$$C^{m1} + 2C^{m2}p_t^m + \lambda_{2,t} - \lambda_{1,t} + \mu_{2,t} = 0, \qquad t \in \{1, ..., T\} \tag{3.30}$$

$$-C_t^d - \lambda_{4,t} + \lambda_{3,t} - \lambda_{6,t} + \lambda_{5,t} - \mu_{2,t} = 0, \qquad t \in \{1, ..., T\} \tag{3.31}$$

$$C^b + \lambda_{13,t} - \lambda_{14,t} + \mu_{1,t} = 0, \qquad t \in \{1, ..., T\} \tag{3.32}$$

$$c_t^{im} - \lambda_{15,t} + \mu_{2,t} = 0, \qquad t \in \{1, ..., T\} \tag{3.33}$$

$$-c_t^{ex} - \lambda_{16,t} - \mu_{2,t} = 0, \qquad t \in \{1, ..., T\} \tag{3.34}$$

$$\lambda_{11,t} - \lambda_{12,t} - \mu_{1,t+1} - \mu_{2,t} = 0, \qquad t \in \{1, ..., T-1\} \tag{3.35}$$

$$-p_t^{dr} + \lambda_{8,t} - \lambda_{7,t} + \lambda_{5,t} = 0, \qquad t \in \{1, ..., T\} \tag{3.36}$$

$$-p_t^{dr} + \lambda_{10,t} - \lambda_{9,t} + \lambda_{6,t} = 0, \qquad t \in \{1, ..., T\} \tag{3.37}$$

- ***Dual feasibility***:

  Non-negativity constraints are imposed on the dual variables associated with the inequality constraints:

$$\lambda_{i,t} \geq 0, \qquad i \in \{1, ..., 16\}, t \in \{1, ..., T\} \tag{3.38}$$

- ***Complementary slackness***:

  The complementary slackness conditions require the product of each inequality and the corresponding variable to be 0. Indeed, it is known from linear programming theory that a dual price is 0 if the corresponding inequality is not saturated, and non-zero otherwise. Therefore, the complementary slackness conditions associated with the constraints (3.16)-(3.23),

(3.25) and (3.26) are:

$$\lambda_{1,t}(\underline{P}^m - p_t^m) = 0, \qquad t \in \{1, ..., T\}$$

$$\lambda_{2,t}(p_t^m - \overline{P}^m) = 0, \qquad t \in \{1, ..., T\}$$

$$\lambda_{3,t}(l_t^d - \overline{L}_t^d) = 0, \qquad t \in \{1, ..., T\}$$

$$\lambda_{4,t}(\underline{L}_t^d - l_t^d) = 0, \qquad t \in \{1, ..., T\}$$

$$\lambda_{5,t}(dr_t^{up} + l_t^d - \overline{L}_t^d) = 0, \qquad t \in \{1, ..., T\}$$

$$\lambda_{6,t}(dr_t^{dn} - l_t^d + \underline{L}_t^d) = 0, \qquad t \in \{1, ..., T\}$$

$$\lambda_{7,t}(-dr_t^{up}) = 0, \qquad t \in \{1, ..., T\}$$

$$\lambda_{8,t}(dr_t^{up} - W_t^{up}) = 0, \qquad t \in \{1, ..., T\}$$

$$\lambda_{9,t}(-dr_t^{dn}) = 0, \qquad t \in \{1, ..., T\}$$

$$\lambda_{10,t}(dr_t^{dn} - W_t^{dn}) = 0, \qquad t \in \{1, ..., T\}$$

$$\lambda_{11,t}(p_t^b - \overline{P}^b) = 0, \qquad t \in \{1, ..., T\}$$

$$\lambda_{12,t}(\underline{P}^b - p_t^b) = 0, \qquad t \in \{1, ..., T\}$$

$$\lambda_{13,t}(b_t - \overline{B}) = 0, \qquad t \in \{1, ..., T\}$$

$$\lambda_{14,t}(\underline{B} - b_t) = 0, \qquad t \in \{1, ..., T\}$$

$$\lambda_{15,t}(-p_t^{im}) = 0, \qquad t \in \{1, ..., T\}$$

$$\lambda_{16,t}(-p_t^{ex}) = 0, \qquad t \in \{1, ..., T\}$$

Observe that the complementary slackness conditions involve bilinear terms. Using the fact that either the dual variable or the primal constraint has to be 0 for their product to be 0, each complementary slackness constraint can be linearized by introducing sufficiently large constants M_i and binary variables ϕ_i. This technique is commonly referred as the big-M method. The interested reader is referred to [95] for details. For each pe-

riod t, the complementary conditions can be replaced by the following equivalent constraints:

$$p_t^m - \underline{P}^m \leq (1 - \phi_1) \times M_1, \qquad t \in \{1, ..., T\} \tag{3.39}$$

$$\overline{P}^m - p_t^m \leq (1 - \phi_2) \times M_2, \qquad t \in \{1, ..., T\} \tag{3.40}$$

$$- l_t^d + \overline{L}_t^d \leq (1 - \phi_3) \times M_3, \qquad t \in \{1, ..., T\} \tag{3.41}$$

$$l_t^d - \underline{L}_t^d \leq (1 - \phi_4) \times M_4, \qquad t \in \{1, ..., T\} \tag{3.42}$$

$$- dr_t^{up} - l_t^d + \overline{L}_t^d \leq (1 - \phi_5) \times M_5, \qquad t \in \{1, ..., T\} \tag{3.43}$$

$$- dr_t^{dn} + l_t^d - \underline{L}_t^d \leq (1 - \phi_6) \times M_6, \qquad t \in \{1, ..., T\} \tag{3.44}$$

$$dr_t^{up} \leq (1 - \phi_7) \times M_7, \qquad t \in \{1, ..., T\} \tag{3.45}$$

$$- dr_t^{up} + W_t^{up} \leq (1 - \phi_8) \times M_8, \qquad t \in \{1, ..., T\} \tag{3.46}$$

$$dr_t^{dn} \leq (1 - \phi_9) \times M_9, \qquad t \in \{1, ..., T\} \tag{3.47}$$

$$- dr_t^{dn} + W_t^{dn} \leq (1 - \phi_{10}) \times M_{10}, \qquad t \in \{1, ..., T\} \tag{3.48}$$

$$- p_t^b + \overline{P}^b \leq (1 - \phi_{11}) \times M_{11}, \qquad t \in \{1, ..., T\} \tag{3.49}$$

$$p_t^b - \underline{P}^b \leq (1 - \phi_{12}) \times M_{12}, \qquad t \in \{1, ..., T\} \tag{3.50}$$

$$- b_t + \overline{B} \leq (1 - \phi_{13}) \times M_{13}, \qquad t \in \{1, ..., T\} \tag{3.51}$$

$$b_t - \underline{B} \leq (1 - \phi_{14}) \times M_{14}, \qquad t \in \{1, ..., T\} \tag{3.52}$$

$$p_t^{im} \leq (1 - \phi_{15}) \times M_{15}, \qquad t \in \{1, ..., T\} \tag{3.53}$$

$$p_t^{ex} \leq (1 - \phi_{16}) \times M_{16}, \qquad t \in \{1, ..., T\} \tag{3.54}$$

$$\lambda_{i,t} \leq \phi_i \times M_i, \qquad i \in \{1, ..., 16\}, t \in \{1, ..., T\} \tag{3.55}$$

In addition, due to the bilinear terms $-c_t^{im} p_t^{im} + c_t^{ex} p_t^{ex} + p_t^{dr}(dr_t^{up} + dr_t^{dn})$ in the upper-level objective function (Eq. (3.2)), the resulting problem still remains non-linear. This can be circumvented by observing that the same bilinear terms also appear

in the lower-level objective function (Eq. (3.15)). The objective function of the dual of the lower-level problem is

$$\begin{aligned} D(\{\lambda_t, \mu_t\}_{t=1}^T) &= \textstyle\sum_{t=1}^T (-C^{dr2}(dr_t^{dn})^2 - C^{dr2}(dr_t^{up})^2 - C^{m2}(p_t^m)^2 \\ &- \mu_{2,t} L_t^i + \lambda_{1,t}\underline{P}^m - \lambda_{2,t}\overline{P}^m - \lambda_{3,t}\overline{L}_t^d + \lambda_{4,t}\underline{L}_t^d - \lambda_{5,t}\overline{L}_t^d + \lambda_{6,t}\underline{L}_t^d \\ &- \lambda_{8,t} W_t^{up} - \lambda_{10,t} W_t^{dn} - \lambda_{11,t}\overline{P}^b + \lambda_{12,t}\underline{P}^b - \lambda_{13,t}\overline{B} + \lambda_{14,t}\underline{B}) \end{aligned} \tag{3.56}$$

Interested readers are referred to [96] for the derivation of the dual problem associated with a primal quadratic program. By strong duality, (3.15) and (3.56) have the same value. Hence, the expression $-p_t^{im}c_t^{im} + p_t^{ex}c_t^{ex} + p_t^{dr}(dr_t^{up} + dr_t^{dn})$ in the upper-level objective function in Eq. (3.2) is equal to the following expression which, after cancellation of pairs of terms that are of equal magnitude and opposite sign, is linear:

$$\begin{aligned} \sum_{t=1}^{T} &(C^{m1}p_t^m + C^{m2}(p_t^m)^2 + C^b b_t + C^{dr1}(dr_t^{up} + dr_t^{dn}) + \\ &+ C^{dr2}((dr_t^{up})^2 + (dr_t^{dn})^2) - C_t^d l_t^d - D(\{\lambda_t, \mu_t\}_{t=1}^T) \end{aligned}$$

As a result, the upper-level objective function Eq. (3.2) can be reformulated as

$$\begin{aligned} F'\left(\{x_t, y_t, \lambda_t, \mu_t\}_{t=1}^T\right) &= \textstyle\sum_{t=1}^T \sum_{g=1}^G (C_g^c w_{g,t} + C_g^1 p_{g,t} + C_g^2 (p_{g,t})^2 + C_g^r (r_{g,t}^{up} + r_{g,t}^{dn})) \\ &+ \textstyle\sum_{t=1}^T (C^{m1}p_t^m + C^{m2}(p_t^m)^2 + C^b b_t + C^{dr1}(dr_t^{up} + dr_t^{dn}) + \\ &+ C^{dr2}((dr_t^{up})^2 + (dr_t^{dn})^2) - C_t^d l_t^d - D(\{\lambda_t, \mu_t\}_{t=1}^T) \end{aligned}$$

The reformulated single-level problem can then be expressed as follows:

$$\begin{aligned} &\min_{\{x_t, y_t, \lambda_t, \mu_t\}_{t=1}^T} F'\left(\{x_t, y_t, \lambda_t, \mu_t\}_{t=1}^T\right) \\ &\qquad \text{st: } (3.3) - (3.13), (3.16) - (3.27), (4.3) - (3.55) \end{aligned}$$

After removing the nonlinearity in the complementary slackness and upper-level objective function, the bi-level problem now becomes a single-level mixed-integer linear problem which can be solved with a wide range of commercial solvers such as CPLEX.

3.5 Numerical Experiments

In this section, the performance of system operation is analyzed under the bi-level optimization mode and standalone mode. Specifically, the impact of wind penetration in the transmission system is analyzed, considering a range of microgrid sizes, locations, and dispatchable load levels. The second metric under consideration is the system cost, including the impact of co-operative decision making on the costs of both the transmission and microgrid systems, under increasing wind penetration levels, different microgrid sizes, dispatchable load levels and multiple microgrids.

The transmission model described in Section 3.3 is applied to the IEEE 30-bus system shown in Fig. 4.4(a). The total generation capacity of the system is 335 MW. For consistency with realistic market conditions, it is assumed that the energy buy-back price in the wholesale market is slightly lower than the energy sale price. As a result, the microgrid export cost c_t^{ex} is defined as $0.9 \times c_t^{im}$. A 25 MW microgrid, with parameters provided in Table 4.2, is used to demonstrate system operations under the bi-level framework. The intention of this case study is to analyze this approach under a possible future configuration of the energy system, including relatively high penetrations of microgrids within a transmission system. The microgrid comprises a generator, a storage unit, an

aggregated dispatchable load, and non-dispatchable load, and is able to operate in islanded and grid-connected modes.

Parameters	$\underline{L}_t^d$	$\overline{L}_t^d$	L_t^i	$\overline{B}$	$\underline{B}$	C^b	C_t^{m1}	C_t^{m2}
Values	6.6 MW	12 MW	12 MW	10 MW	0 MW	\$0.1/MW	\$4/MW	\$0.07/MW

Parameters	C^{dr1}	C^{dr2}	C_t^d	$\overline{P}_t^d$	$\overline{P}^m$	$\underline{P}^m$	$\underline{P}^b$	$\overline{P}^b$
Values	\$0.4/MW	\$0.3/MW	\$6/MW	\$1/MW	25 MW	0 MW	-5 MW	5 MW

Table 3.1: MG parameter values

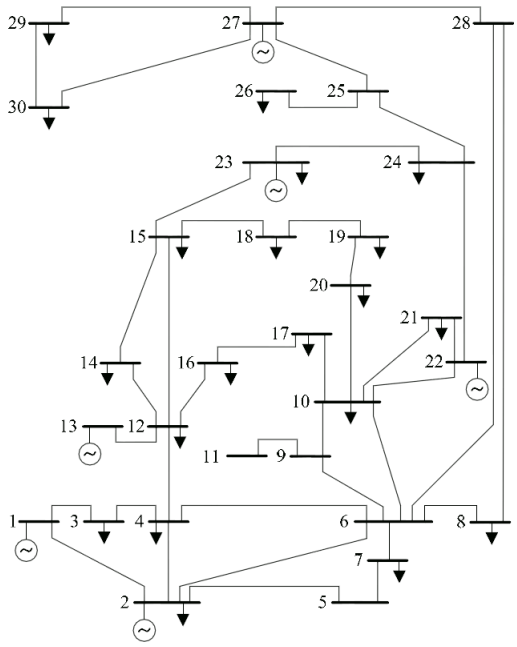

Figure 3.2: IEEE 30-bus system. The interested reader is referred to [2] for details of the parameters of this transmission system.

The renewable generation in this study is wind generation from wind farms at different transmission system buses. The wind data are selected from the NREL-Eastern Wind Integration Study dataset [97]. Using three years of data, 24-hour trajectories are grouped to identify a set of 54 trajectories with a common initial condition. The set of trajectories is used to represent the realizations

that could arise from a similar forecast. The central trajectory of the group is selected as the wind power forecast, and the remaining trajectories are used to estimate the distribution of forecast errors. Based on the forecast error distribution, 10000 scenarios are generated to represent an uncertainty set of wind realizations, each of which would introduce error with respect to the base case wind forecast. Those error scenarios are then added to the forecast to create wind generation scenarios. See [98] for details of this scenario generation method.

In the figures in this section, SA stands for standalone mode, COOP for co-optimization mode, MG for microgrid, and TS for transmission system.

3.5.1 Impact of Co-optimization on Wind Penetration

This work uses the European Wind Energy Association's definition of wind penetration, i.e., the ratio of the installed wind capacity to the peak system load [96]. The objective of this section is to consider the impact of co-optimization on the use of wind resources in a future system with microgrids and renewables.

Location of Wind Resources

For benchmarking purposes, the maximum wind penetration is recorded with wind farms positioned at different buses in the transmission system with no microgrid. Results for some representative buses, and the reasons why no further wind power could be incorporated are given in Table 3.2.

Wind Bus	Max Wind Penetration	Limitation
5	38%	Generator reserve
8	21%	Transmission capacity
15	35%	Transmission capacity
30	17%	Transmission capacity
8 and 30	38%	Generator reserve

Table 3.2: Wind penetration at different buses

Buses have different capacities for renewable injection due to different transmission line capacities connected to them. Table 3.2 shows that bus 8, 15 and 30 permit a lower level of wind penetration compared to bus 5, as buses 8, 15 and 30 connect to transmission lines with a smaller capacity. For bus 5, the connected line capacity is large enough to absorb all the generator reserve and reach a maximal level of wind penetration. When there are wind farms at buses 8 and 30, all the generator reserve could be used to account for the wind power deviation from the forecast, as the combined line capacity at those two buses is sufficiently large to accommodate the power flow of the reserve resource. The results suggest that wind farms should be placed at locations with generous transmission capacity and possibly at multiple locations to achieve maximum wind penetration.

Impact of a Microgrid

To illustrate the effects of a microgrid on wind penetration, a 25 MW microgrid with 50% dispatchable load is connected to the wind buses in the previous section, and system operation is simulated with the bi-level optimization framework presented above. A high percentage of dispachable load is chosen to explore the effect of high levels of dispachable load in the future and ensure system reliability as flexible load increases. Here the dispatchable load fraction

is defined as the ratio of the dispatchable load to the sum of the dispatchable and non-dispatchable loads. The results for feasible wind penetration at different buses with and without the microgrid is shown in Fig. 3.3.

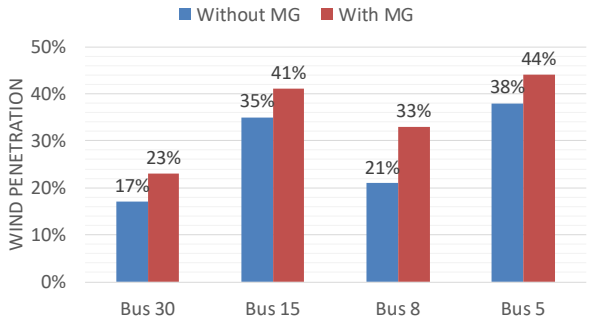

Figure 3.3: Wind penetration at different buses with and without the microgrid

Fig. 3.3 illustrates that feasible wind penetration increases with the addition of the microgrid since the DR provided by the microgrid can act as reserve and locally offset the error in the forecasted wind power at the wind bus. The increase in wind penetration for bus 8 is more than that of bus 5, 15 and 30 as the microgrid and transmission system energy exchange at bus 8 frees some line capacity for the generator reserves. This case shows that the microgrid could alleviate transmission congestion under the current energy exchange pricing scheme.

The microgrid and wind farm are located at the same bus in the previous analysis. Table 3.3 shows the maximum wind penetration when the microgrid is placed at a bus other than the wind farm bus. Comparison of Table 3.3 and Fig. 3.3 shows that the wind penetration level when the wind farm and microgrid are at different buses is upper bounded by the penetration level when they are at the same bus, as the transmission constraints could be bypassed and the errors in the forecasted wind power could be locally offset in the latter case.

Wind Bus	Microgrid Bus	Max Wind Penetration
5	8	44%
5	15	44%
5	30	44%
8	5	21%
8	15	21%
8	30	21%

Table 3.3: Wind penetration with the wind farm and microgrid at different buses

Increasing Microgrid Size and Dispatchable Load Level

As the amount of reserve is proportional to the size of the microgrid and the amount of dispatchable load in the microgrid, the effects of these two factors on wind are analyzed here. The microgrid is scaled by a constant factor to simulate varying sizes. The wind farm and microgrid are both located at bus 5 to guarantee enough line capacity and thus eliminate the effects of line constraints. Fig. 3.4 shows the wind penetration for different sizes of a microgrid with 50% dispatchable loads, and Fig. 3.5 the wind penetration for a 25 MW microgrid with different dispatchable load levels. It can be seen from the two figures that the wind penetration is linearly proportional to the microgrid size and dispatchable load level, as a larger microgrid and more dispatchable load provide more DR resources to offset forecasted wind power error.

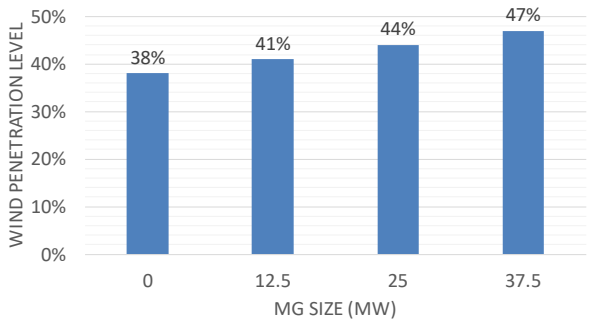

Figure 3.4: Wind penetration for different microgrid sizes

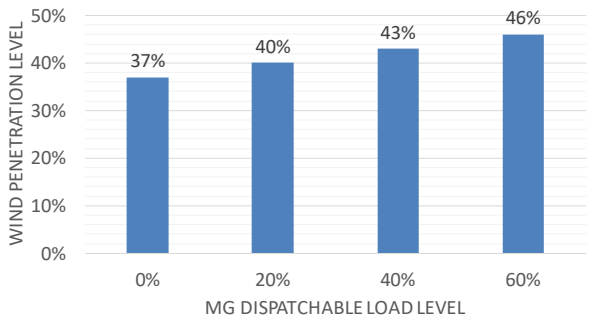

Figure 3.5: Wind penetration for different dispatchable load levels

3.5.2 System Cost Impact

In addition to increasing flexibility to improve integration of renewables, the cost impact of co-optimization is of significant interest. In this section, the cost implications of the two systems are explored in the COOP mode and in the SA mode. In addition, the impact of multiple MGs on the system cost is examined. It is expected that the COOP mode will provide additional flexibility to operations, as the microgrid is able to exchange energy with the transmission system and provide DR as reserve to mitigate the effects of wind power uncertainty. In the SA mode, the microgrid is separated from the transmission system and thus cannot exchange energy with it, nor can the microgrid provide any DR.

Cost Impact of Wind Penetration

As wind penetration is a key concern for the grid of the future, and also a focus of this study, the wind penetration is varied to appraise the impact on transmission system and microgrid costs. A wind farm and a 25 MW microgrid with a 50% dispatchable load are connected to bus 5 for the case study. Results are

summarized in Fig. 3.6(a).

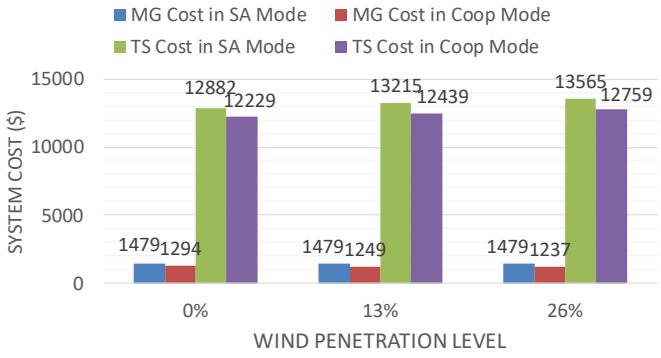

(a) System costs

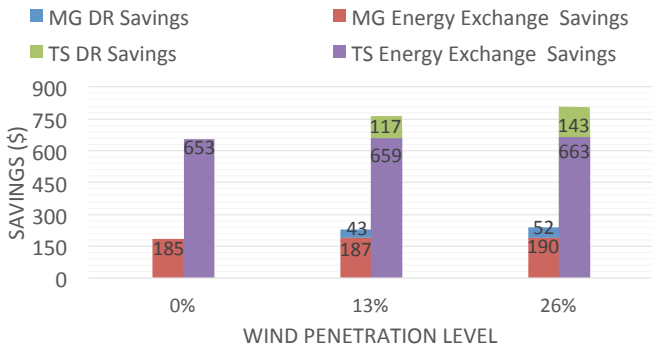

(b) Savings breakdown

Figure 3.6: Transmission system and microgrid costs and savings breakdown for different wind penetration levels

As shown in Fig. 3.6(a), the operation costs of the two systems are smaller in the COOP mode because of the mutual benefits from the energy exchange and DR. In the SA mode, the microgrid cost is not affected by wind penetration levels, as the microgrid configuration stays the same. Fig. 3.6(b) shows the breakdown of the microgrid and transmission system savings in terms of DR and energy exchange. When there is no wind power, the difference in the operation cost for the two modes of operation originates from the energy exchange benefits. As wind penetration increases, DR savings for the microgrid and transmission system increase, because more low cost DR from the micro-

grid is engaged in the ancillary market. The energy exchange savings for the two systems are almost the same across wind penetration levels because the energy exchange price and quantity do not differ significantly. With higher wind penetration, the total savings in the COOP mode with a higher wind penetration is greater for both systems, as a higher wind penetration provides more opportunity for the DR to reduce costs.

Impact of Microgrid Size on Cost

The transmission system is optimized with microgrids of different capacity connected to bus 5. In all cases, the dispatchable load level in the microgrid is 50%. The wind farm is connected to bus 5, and a fixed 10% wind penetration is used. The operation cost for the two systems are shown in Fig. 3.7(a).

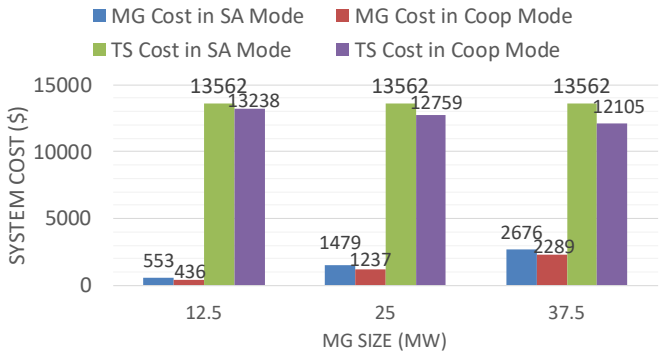

(a) System costs

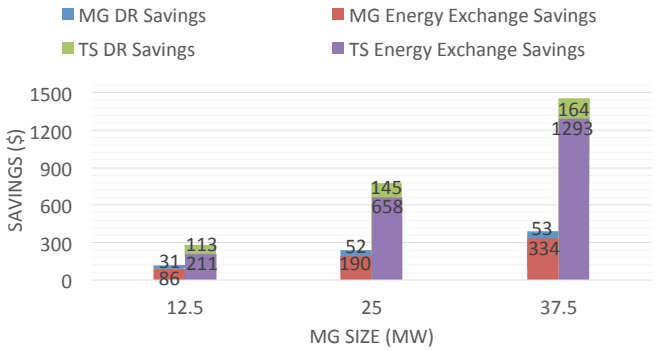

(b) Savings breakdown

Figure 3.7: Transmission system and microgrid cost and savings breakdown for different microgrid sizes

Fig. 3.7(a) shows that the cost of the transmission system in the COOP mode decreases with the increasing microgrid size. Cost savings are due to increasing availability of the DR and energy exchange with a larger microgrid. In addition, the individual systems' costs are always lower in the COOP mode than in the SA mode as the COOP mode provides both systems opportunities for arbitrage in the energy exchange transactions in addition to the benefits from the reserve provision. In the SA mode, the transmission system cost is the same for all three microgrid sizes, as the transmission system configuration does not change. Fig. 3.7(b) shows the breakdown of the microgrid and transmission system savings in terms of DR and energy exchange. As the microgrid size increases, the ben-

efits from the energy exchange increases for both systems since the energy exchange volume increases with a larger microgrid. The DR benefits also increase for both systems as a larger microgrid can provide more DR service. This case study shows that the total savings in the COOP mode with a larger microgrid are greater for both systems.

Cost Impact of Dispatchable Load Level

For the setting of a 25 MW microgrid and 10% wind penetration at bus 5, the transmission system and microgrid operation costs at different levels of dispatchable load in the microgrid are shown in Fig. 3.8(a).

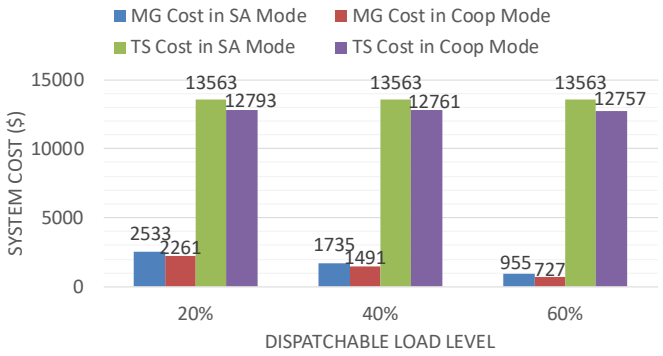

(a) System costs

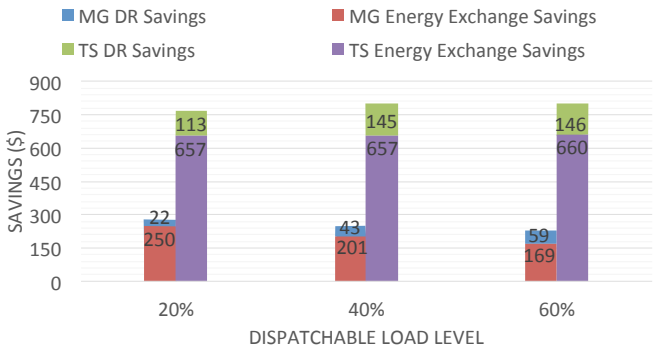

(b) Savings breakdown

Figure 3.8: Transmission system and microgrid cost and savings breakdown for different microgrid dispatchable load levels

It is shown in Fig. 3.8(a) that the transmission system cost declines with increased dispatchable load level, as more wind forecast error is handled by the lower cost DR from the microgrid dispatchable load. The microgrid cost also decreases with an increasing dispatchable load level, as the microgrid has more DR to sell and more load flexibility. Once again, the COOP framework enables mutual benefits from the reserve service and energy exchange and thus reduces the costs of both systems. The savings breakdown in Fig. 3.8(b) gives further insight into the optimal co-operation. For the transmission system, the energy exchange savings is virtually the same for different dispatchable load levels, as the magnitude of the net energy exchange are nearly the same in those cases. Although the energy exchange savings for the microgrid decrease with an increasing dispatchable load level, the percentage cost savings increases. The DR savings for both systems increase with an increasing dispatchable load level, as a higher dispatchable load level provides more DR resources. However, the DR savings for the transmission system do not increase significantly when the dispatchable load level is increased from 40% to 60% because the marginal cost benefit for that additional DR is very small. This case study shows that more load flexibility enables lower operation costs for both systems especially for the MG in the COOP mode.

Cost Impact of Multiple Microgrids

As MG integration increases in the power systems, it is crucial to examine the cost effects of multiple MGs. In this section, three MGs with parameters as given in Table 4.2 are positioned at buses 5, 8, and 15. The wind farm is connected to bus 5, and a fixed 10% wind penetration is used. The three MGs have the

same cost when connected to the transmission system due to the same topology and parameters. In Table 3.4, the cost comparison of three cases is illustrated. Each of the cases adds one more microgrid to the system; case 1 has a single microgrid at bus 5, case 2 adds an additional MG at bus 8, and are 3 adds a third to bus 15. It can be seen that the average MG cost increases while transmission system cost decreases with additional MGs in the system because more MGs in the system increases DR supply, which lowers DR price. Conversely, more MGs increase the demand for energy import, which raises the energy import price. The results here show that multiple MGs in the power systems under the bi-level framework clearly follow the market economic rules, and the addition of more MGs could increase operation efficiency of the transmission system.

	Average MG Cost ($)	TS Cost ($)	Import Price ($/MWh)	DR Price ($/MWh)
Case 1	1237	12759	5.61	3.10
Case 2	1302	12108	5.66	2.84
Case 3	1330	11505	5.72	2.68

Table 3.4: Case 1 has one MG at bus 5, case 2 has same MGs at bus 5 and 8, case 3 has same MGs at bus 5, 8 and 15. The average MG cost increases while the transmission system cost decreases with more MGs in the system.

3.6 Concluding Remarks

This paper presents a bi-level co-optimization framework to model the interaction of a transmission system and a microgrid. Both the energy and ancillary markets are optimized under this framework. By comparing the co-optimization and standalone operation modes of the systems, it is shown that co-optimization could reduce their operation cost for both systems because of the additional flexibility and arbitrage opportunities. The transmission system operation cost decreases with addition of more microgrids connected to

it. Moreover, the microgrid could increase the wind penetration in the transmission system, and the wind integration is most conveniently facilitated when the microgrid and wind farm are at the same bus. The system analysis under the bi-level framework in this paper will provide insight for future inter-system co-operation and microgrid development, to enable a more sustainable power system and boost operation efficiency. Those results also promote and support massive future deployment of microgrids in power systems.

3.7 Acknowledgments

This material is based upon work supported by the US Department of Energy under Award Number DE-OE0000843. Disclaimer: This report was prepared as an account of work sponsored by an agency of the United States Government. Neither the United States Government nor any agency thereof, nor any of their employees, makes any warranty, express or implied, or assumes any legal liability or responsibility for the accuracy, completeness, or usefulness of any information, apparatus, product, or process disclosed, or represents that its use would not infringe privately owned rights. Reference herein to any specific commercial product, process, or service by trade name, trademark, manufacturer, or otherwise does not necessarily constitute or imply its endorsement, recommendation, or favoring by the United States Government or any agency thereof. The views and opinions of the authors expressed herein do not necessarily state or reflect those of the United States Government or any agency thereof.

CHAPTER 4

A CO-OPTIMIZATION FRAMEWORK FOR TRANSMISSION AND DISTRIBUTION OPERATIONS UNDER UNCERTAINTY FROM RENEWABLE GENERATION

With rapid growth of distributed energy resources (DER) in electric power systems, the distribution system (DS) is becoming more similar to the bulk system in terms of the functionality, which results in a growing need for updated optimization framework and market simulator with more detailed representation of distribution operations for decision making in power systems. The uncertainties added by the increasing penetration of renewable energy further complicate power scheduling and operations. The traditional co-optimization framework with a high level representation of distribution systems may not be sufficient for the systems of the future. This chapter proposes an alternative system optimization hierarchy, based on bi-level optimization, to co-optimize the transmission system (TS) and distribution system in a way that caters the needs of the evolving transmission and distribution systems, and takes advantage of demand response (DR) to address the stochasticity of renewable energy sources. The proposed bi-level framework is compared to a representative traditional centralized optimization approach based on system cost, renewable resource utilization, system expansion, and environmental impact. Computational studies show that bi-level optimization allocates the system costs in a more economically intuitive way, puts more emphasis on the decentralized optimization of the distribution system, and yields certain economic and environmental benefits. This bi-level approach is also shown to effectively incorporate future distribution characteristics such as distributed generation (DG) and energy export, which is not supported by the traditional approach. As an early work in

power system optimal operation through bi-level optimization, the analysis in this study offers a new point of view for future system co-optimization, and provides a basis for more research on the decentralized system control frameworks.

Nomenclature

Sets and Indexes	
T	length of the planning horizon
G	total number of generators in the transmission system
N_b^d	total number of buses in the distribution system
$t \in \{1, ..., T\}$	a time interval from the beginning through the end of a period
$g \in \{1, ..., G\}$	a transmission system network generator
$i \in \{1, ..., N_b^d\}$	a distribution system network bus
Parameters	
N_b	total number of buses in the transmission system
$\overline{R}_g / \underline{R}_g$	upper/lower ramp rate limit of transmission system generator g
$\overline{P}_g / \underline{P}_g$	generation upper/lower bound of transmission system generator g
$\overline{L}$	transmission system line limit
C_g^1 / C_g^2	linear/quadratic cost coefficient of transmission system generator g
C_g^c	commitment cost coefficient of transmission system generator g
C_g^r	reserve cost coefficient of transmission system generator g
M^{GSF}	transmission system generation shift factor matrix
M^{GSFd}	distribution system generation shift factor matrix
W_t^f	forecasted wind power in hour t
W_t^{up} / W_t^{dn}	upward/downward deviation from the forecast wind power in hour t
L_t	transmission system load vector in hour t
$\overline{L}_i^d / \underline{L}_i^d$	upper/lower bound of distribution system dispatchable load at bus i
$\underline{L}_i^{ie}$	distribution system inelastic load at bus i
$\overline{P}_i / \underline{P}_i$	upper/lower bound of distribution system power flow to bus i
C_i^{d1} / C_i^{d2}	linear/quadratic cost coefficient of distribution system DG at bus i
C^d	distribution system utility for consuming dispatchable load
C^{dr1} / C^{dr2}	linear/quadratic cost coefficient of distribution system demand response
$\overline{P}_i^d / \underline{P}_i^d$	upper/lower bound of distribution system DG generation at bus i
S^{dr}	DR scaling factor
Variables	
$r_{g,t}^{up} / r_{g,t}^{dn}$	upward/downward reserve of transmission system generator g in hour t
p_t^{dr}	distribution system demand response price in hour t
$p_{g,t}$	generation of transmission system generator g in hour t
p_t^{im}	distribution system imported power in hour t
$l_{i,t}^d$	distribution system dispatchable load in hour t at bus i
$p_{i,t}^d$	distribution system DG power in hour t at bus i
$p_{i,t}$	distribution system power flow to bus i in hour t
$dr_{i,t}^{up} / dr_{i,t}^{dn}$	upward/downward DR of distribution system in hour t at bus i
c_t^{im}	distribution system energy import price in hour t
$w_{g,t}$	transmission system generator commitment variable in hour t for generator g
p_t^{inj}	transmission bus power injection vector in hour t
p_t^{injd}	distribution bus power injection vector in hour t

4.1 Introduction

With advances in smart grid technologies, the electricity market has been transforming from a centralized structure to one that includes many decentralized resources at the distribution level such as energy storage units, demand response and distributed generation [99]. As distribution systems become more participatory in the overall system operation, advanced market simulators and decision frameworks will be required. The traditional optimization mechanisms that treat a distribution system as a simple node with demand bid will not be capable of leveraging the capabilities of future system structure. It is necessary to adopt optimization models that better characterize the interactions between transmission and distribution systems. If we consider distribution systems as participants in the wholesale energy market, the power system problem faced by the independent system operator (ISO) can be approached from a game-theory perspective. Specifically, bi-level optimization originating from a Stackelberg game is one suitable approach, and is explored in this work to capture the interaction between the transmission and distribution systems.

Figure. 4.1 summarizes past power system bi-level studies in four categories. The long-term expansion planning problem of power systems is explored using a bi-level optimization framework in [100, 101, 102, 64, 65]. The bidding strategies of generation companys (GENCO), with the GENCO's revenue optimization as the upper-level problem and the ISO's dispatch problem as the lower-level problem is described in [103, 104, 105, 66, 67]. The bi-level optimization approach is used to examine power system vulnerability and minimize loss under terrorist attacks on transmission lines or generators in [106, 70, 107, 108, 109]. The bi-level optimization work with a focus on the interaction between trans-

mission and distribution systems appears in [110, 111, 112]. It is worth noting that in all of these previous references, the distribution system optimal dispatch is the upper level problem, while the transmission system optimization is the lower level problem. In [110], the author implements bi-level optimization for the operational decision making of a distribution system in a competitive market with multiple distribution systems, and a bi-level multi-period energy acquisition model is proposed for a distribution system with DG and interruptible load in [111]. The effect of DG and interruptible load on congestion alleviation is also analyzed under that framework. Trading strategies of distribution systems with DG are examined in the day-ahead market and real time market in [112]. It is worth noting that the previous work models the distribution system problem as the upper level problem to help with the decision making for distribution systems. It is unrealistic, however, to assume the upper level distribution system problem has access to the information on the lower level TS problem. Formulating the problem with the ISO's problem as the upper level problem and the distribution system as the lower level problem may be more suitable as the ISO receives information from the distribution systems at the top level in the power system hierarchy.

Figure 4.1: Summary of past studies on power system bi-level optimization.

In this work, the transmission system day-ahead unit commitment of the ISO is modeled as the upper level problem, and the distribution system optimal dispatch is formulated as the lower level problem. Under this structure, the upper level problem determines the energy and DR prices of the distribution systems, while the lower level problem responds to those price signals by deciding the quantity of DR and energy import. The highlights of this work are summarized as follows:

1. A bi-level optimization framework is presented for the transmission and distribution system co-optimization with a logical system hierarchy.

2. A single-level optimization scheme is formulated from bi-level framework, which enables more efficient solution of the bi-level optimization problem.

3. The bi-level optimization approach is compared with the traditional approach based on system cost for different renewable penetration and loading scenarios, and environmental impact in terms of carbon emissions.

4. The bi-level optimization scheme is tested for a future distribution system configuration with DG, meshed network and power export capability.

The structure of the paper is as follows: Section 4.2 delineates the bi-level optimization formulation, with a reformulation of the bi-level problem to a tractable model in Section 4.3. Numerical results are reported in Section 4.4. Concluding remarks and recommendations for future work follow in Section 4.5.

4.2 Bi-level Optimization Model

The interactive behavior between market entities is commonly analyzed under a game-theoretic approach known as bi-level optimization [83]. The following general formulation illustrates the two-level problem structure under the bi-level framework:

$$\begin{aligned}
&\text{Upper-Level Problem: } {}_{x\in X}F\,(x,y)\\
&\qquad\qquad\text{s.t.: } G_i\,(x,y)\le 0,\ i\in\{1,2,...,I\}\\
&\qquad\qquad\quad H_k\,(x,y)=0,\ k\in\{1,2,...,K\}\\
&\text{Lower-Level Problem: } {}_{y\in Y}f(x,y)\\
&\qquad\qquad\text{s.t.: } g_j(x,y)\le 0,\ j\in\{1,2,...,J\},\\
&\qquad\qquad\quad h_m(x,y)=0,\ m\in\{1,2,...,M\}
\end{aligned} \tag{4.1}$$

The set of decision variables, objective function, and constraints of the upper/lower problem are denoted by X/y, $F(x,y)/f(x,y)$, and $(G_i,H_k)/(g_j,h_m)$ respectively in (4.1). The co-optimization of the transmission system and distribution system in the power market is naturally modeled under the bi-level framework in this study. Specifically, as shown in Fig. 4.2, the energy and demand response price signals are determined by the upper-level transmission system, and the quantity of energy import and the demand response are decided by the lower-level distribution system problem in response to the upper level price signals.

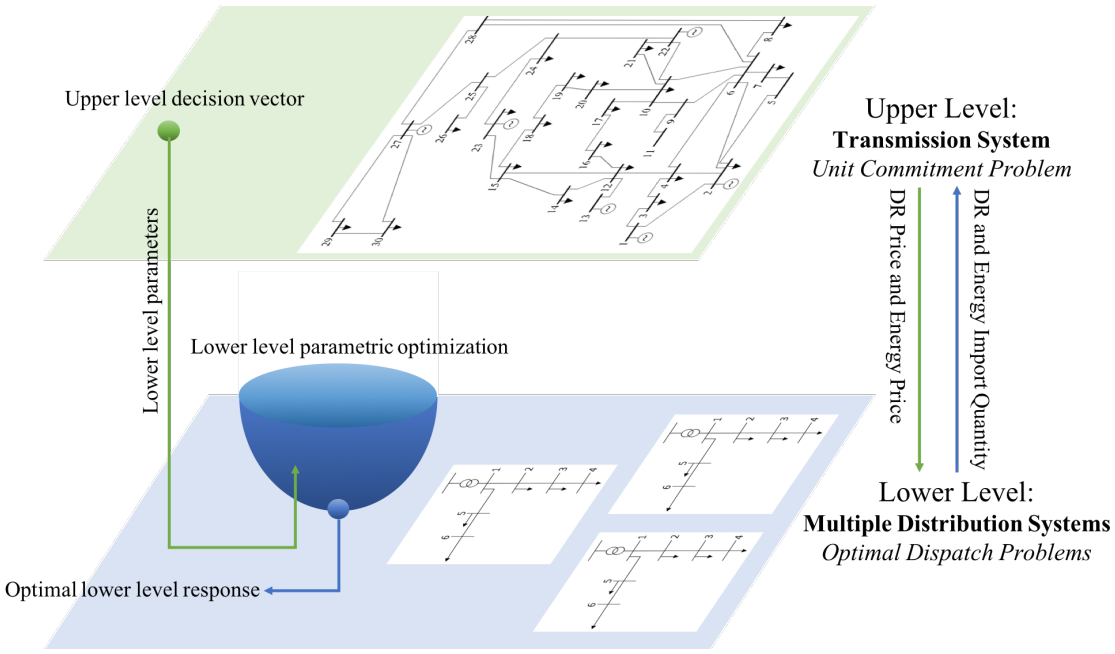

Figure 4.2: The upper-level transmission system determines the energy and demand response price signals, and the lower-level distribution system problem responds by deciding the quantity of energy import and the demand response.

The specifics of the bi-level optimization model in this study are given below.

4.2.1 Upper-Level Problem: Transmission System Day-Ahead Unit Commitment Problem

A transmission system consists of a network of transmission lines and buses, which connect generation units, loads, and distribution systems. The optimal operation schedules in the transmission system are solved from day-ahead unit commitment problems for the energy and ancillary services markets. The energy market minimizes generation cost of meeting the system demand, while the ancillary services market minimizes the cost of providing reserves to com-

pensate short-term variability from renewables. The reserve resource is obtained from a mix of the transmission system generators' reserve and the distribution system's demand response.

As the upper-level problem, the day-ahead unit commitment problem minimizes the operational cost of the transmission system by making scheduling decisions x_t, including the generator commitment status $w_{g,t}$, generation output $p_{g,t}$, the generator's upward and downward reserve $r^{up}_{g,t}$, $r^{dn}_{g,t}$, the distribution system's demand response price p^{dr}_t, and the prices of the distribution system's imported energy c^{im}_t:

$$x_t = [w_{g,t}, p_{g,t}, r^{up}_{g,t}, r^{dn}_{g,t}, p^{dr}_t, c^{im}_t].$$

The goal of the upper-level unit commitment problem is to minimize the operational cost of the transmission system including the generation cost ($C^c_g w_{g,t} + C^1_g p_{g,t} + C^2_g(p_{g,t})$), the reserve cost ($C^r_g(r^{up}_{g,t} + r^{dn}_{g,t})$), the revenue from energy export to the distribution system ($c^{im}_t p^{im}_t$), and the distribution system's demand response cost ($p^{dr}_t(dr^{up}_t + dr^{dn}_t)$). The objective function is given in (4.2), with relevant constraints in (4.3) - (4.10):

$$\begin{aligned} F(\{x_t\}_{t=1}^T) &= \sum_{t=1}^T \sum_{g=1}^G (C^c_g w_{g,t} + C^1_g p_{g,t} + C^2_g (p_{g,t})^2 + C^r_g (r^{up}_{g,t} + r^{dn}_{g,t}) \\ &- c^{im}_t p^{im}_t + p^{dr}_t (dr^{up}_t + dr^{dn}_t)) \end{aligned} \tag{4.2}$$

- ***Power flow capacity:***

$$-\overline{L} \leq M^{GSF} p^{inj}_t \leq \overline{L}, \qquad t \in \{1, ..., T\} \tag{4.3}$$

$$-\overline{L} \leq M^{GSF} p^{inj*}_t \leq \overline{L}, \qquad t \in \{1, ..., T\} \tag{4.4}$$

The nodal net power injection vector p_t^{inj} accounts for the traditional generation, wind generation, and demand for all the buses in period t. The error in the forecasted wind power, generator reserves and distribution system's demand response is incorporated into the base p_t^{inj} to give p_t^{inj*}.

- ***Generation capacity:***

$$\underline{P}_g w_{g,t} \leq p_{g,t} \leq \overline{P}_g w_{g,t}, \qquad t \in \{1,\ldots,T\}, g \in \{1,\ldots,G\} \tag{4.5}$$

$$(p_{g,t} + r_{g,t}^{up}) - (p_{g,t-1} - r_{g,t-1}^{dn}) \leq \overline{R}_g, \qquad t \in \{2,\ldots,T\}, g \in \{1,\ldots,G\} \tag{4.6}$$

$$\underline{R}_g \leq (p_{g,t} - r_{g,t}^{dn}) - (p_{g,t-1} + r_{g,t-1}^{up}), \qquad t \in \{2,\ldots,T\}, g \in \{1,\ldots,G\} \tag{4.7}$$

The generation outputs and hourly ramping are restricted within their limits according to Eqs. (4.6) and (4.7).

- ***Power balance:***

$$\sum_{g=1}^{G} p_{g,t} - (\mathbf{1}_{1\times N_b} \cdot L_t) + W_t^f = p_t^{im}, \qquad t \in \{2,\ldots,T\}, g \in \{1,\ldots,G\} \tag{4.8}$$

where $\mathbf{1}_{1\times N_b}$ is an N_b -dimentional vector filled of 1's. The dot product $\mathbf{1}_{1\times N_b} \cdot L_t$ gives the total load in the system.

- ***Wind forecast uncertainty:***

Along with the environmental benefits, the increasing penetration of wind power also brings the challenges of uncertainties to the system operational decisions. Here, the generation reserve at the transmission level, and the distribution system's demand response are used to offset the wind power deviation from the forecast. Given the wind forecast as well as a set of possible wind power realizations, the upward/downward wind output deviation, W_t^{up}/W_t^{dn}, is calculated as the deviation between the wind forecast and the maximum/minimum wind realization in period t. The upward/downward wind output deviation is compensated

by the downward/upward transmission generation reserve $r^{dn}_{g,t}/r^{up}_{g,t}$ and upward/downward distribution system's demand response $dr^{up}_{i,t}/dr^{dn}_{i,t}$ respectively.

$$W^{up}_t \leq \sum_{i=1}^{N^d_b} dr^{up}_{i,t} + \sum_{g=1}^{G} r^{dn}_{g,t}, \qquad t \in \{1, ..., T\} \tag{4.9}$$

$$W^{dn}_t \leq \sum_{i=1}^{N^d_b} dr^{dn}_{i,t} + \sum_{g=1}^{G} r^{up}_{g,t}, \qquad t \in \{1, ..., T\} \tag{4.10}$$

Compiling these constraints, the upper level day-ahead unit commitment problem of the transmission system is summarized as follows:

$$\min_{\{x_t\}^T_{t=1}} F\left(\{x_t\}^T_{t=1}\right)$$
$$\text{s.t. } (4.3) - (4.10)$$

4.2.2 Lower Level Problem: Optimizing Distribution System Operation Optimization

In this framework, optimal dispatch of the distribution systems is modeled as the lower level optimization problem. The distribution system may have either a radial or meshed network with the potential to provide demand response as dispatchable load at each bus. The dispatchable load is scheduled between its upper and lower limits. In the lower level problem, the optimal distribution decisions y_t include the energy import schedule p^{im}_t, nodal load consumption p_i, and the upward/downward demand response dr^{up}_t, dr^{dn}_t provided by the dispachable load:

$$y_t = [p_{i,t}, p_t^{im}, l_{i,t}^d, dr_{i,t}^{up}, dr_{i,t}^{dn}]$$

The goal of distribution system optimization is to seek the minimum distribution system operational cost including its energy import cost ($p_t^{im} c_t^{im}$) and demand response cost ($C^{dr1}(dr_{i,t}^{up}+dr_{i,t}^{dn})+C^{dr2}((dr_{i,t}^{up})^2+(dr_{i,t}^{dn})^2)$), while maximizing the dispatchable load utility ($C^d l_{i,t}^d$) and demand response revenue ($p_t^{dr}(dr_{i,t}^{up} + dr_{i,t}^{dn})$), with its objective function expressed as follows:

$$\begin{aligned} f(\{y_t\}_{t=1}^T) = \sum_{t=1}^{T} \sum_{i=1}^{N_b^d} (p_t^{im} c_t^{im} + C^{dr1}(dr_{i,t}^{up} + dr_{i,t}^{dn}) + C^{dr2}((dr_{i,t}^{up})^2 + (dr_{i,t}^{dn})^2) \\ -C^d l_{i,t}^d - p_t^{dr}(dr_{i,t}^{up} + dr_{i,t}^{dn})) \end{aligned} \tag{4.12}$$

The constraints for the distribution system are formulated as shown below. For clarity, the dual variables corresponding to the inequality constraints are denoted by λ and those of the equality constraints are denoted by μ.

- ***Power flow:***

  The majority of existing distribution systems are radial [113, 114], as illustrated in Fig. 4.3. There are n buses in the network indexed by $i = 1, ..., n$. Bus 1 is the coupling bus with the transmission system. A simplified version of power flow that only considers active power based on the formulation in [115] is used in this work. The power flow equation at node i could be expressed as:

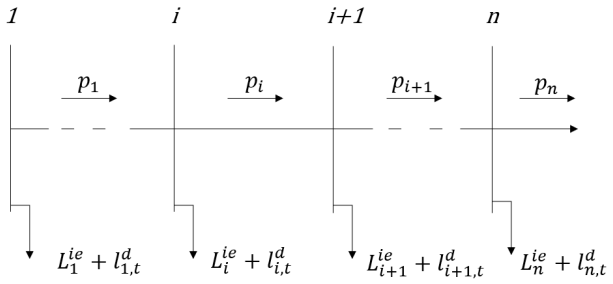

Figure 4.3: Diagram of a radial distribution network

$$p_{i+1,t} = p_{i,t} - (L_i^{ie} + l_{i,t}^d + dr_{i,t}^{up}), \qquad \mu_{1,i,t}, t \in 1, ..., T, i \in 1, ..., N_b^d - 1 \tag{4.13}$$

$$\underline{P}_i \leq p_{i,t} \leq \overline{P}_i, \qquad \lambda_{1,i,t}, \lambda_{2,i,t}, t \in 1, ..., T, i \in 1, ..., N_b^d \tag{4.14}$$

where $L_{i,t}^{ie} + l_{i,t}^d$ is the net load at bus i made up by the sum of inelastic load L_i^{ie} and dispatchable load l_i^d at bus i. Eq. (4.13) regulates the power flow between the nodes in the distribution system. $dr_{i,t}^{up}$ is added to the net load in Eq. (4.13) to ensure that the power flow accomodates the maximum possible load. The power flow within the lines in the distribution system are bounded in Eq. (4.14). Note that $p_{1,t}$ is the same as the distribution system energy import p_t^{im}.

- ***Dispatchable load and demand response limit:***

  The dispatchable loads are restricted within predefined bounds shown in Eq. (4.15). The available demand response is set to be within a certain percentage of the dispatchable load defined by the demand response scaling factor S^{dr} in Eq. (4.16) and (4.17).

$$\underline{L}_i^d \leq l_{i,t}^d \leq \overline{L}_i^d, \qquad \lambda_{3,i,t}, \lambda_{4,i,t}, t \in 1, ..., T, i \in 1, ..., N_b^d \tag{4.15}$$

$$0 \leq dr^{up}_{i,t} \leq S^{dr} l^{d}_{i,t}, \qquad \lambda_{5,i,t}, \lambda_{6,i,t}, t \in 1, ..., T, i \in 1, ..., N^{d}_{b} \tag{4.16}$$

$$0 \leq dr^{dn}_{i,t} \leq S^{dr} l^{d}_{i,t}, \qquad \lambda_{7,i,t}, \lambda_{8,i,t}, t \in 1, ..., T, i \in 1, ..., N^{d}_{b} \tag{4.17}$$

Overall, the lower level optimal dispatch problem of distribution system is formulated as:

$$\min_{\{y_t\}_{t=1,i=1}^{T,N^{d}_{b}}} f\left(\{y_t\}_{t=1}^{T}\right)$$

$$\text{s.t. } (4.10) - (4.17)$$

4.3 Single Level Reformulation of the Bi-level Problem

Bi-level optimization problems are commonly solved by one of two general strategies. The first strategy applies classical methods such as single-level reduction [94, 85], descent methods [86, 116], penalty function [117, 87], and trust-region methods [88, 118], which exploit the mathematical properties of optimization problems such as convexity and regularity. The second strategy takes advantage of some evolutionary methods such as particle swarm optimization [90], genetic algorithms [89], metamodeling-based methods [92], and differential evolution [91]. The interested reader is referred to [83, 93] for a more detailed survey of bi-level optimization techniques.

Using the first strategy, the bi-level optimization problem can be reformulated as a single-level problem if the lower-level problem is convex, and the Slater's constraints qualifications are met, as described in [94]. In the single-

level reformulation, the lower-level problem is substituted by its KKT conditions which are combined with the upper-level problem. Here, the lower-level optimal dispatch problem in the distribution system is convex and the Slater's constraints qualifications are satisfied. Thus, the lower-level problem is replaced by its KKT conditions, i.e. stationarity, dual feasibility and complementary slackness in the single-level reformulation of the system co-optimization problem. Those KKT conditions are given below:

- ***Stationarity***

  The Lagrangian function associated with the distribution system problem is:

$$\begin{aligned} L(x,y,\lambda,\mu) &= f(x,y) + \lambda_{1,i,t}(\underline{P}_i - p_{i,t}) + \lambda_{2,i,t}(p_{i,t} - \overline{P}_i) + \lambda_{3,i,t}(\underline{L}^d_{i,t} - l^d_{i,t}) \\ &+ \lambda_{4,i,t}(l^d_{i,t} - \overline{L}^d_{i,t}) - \lambda_{5,i,t} dr^{up}_{i,t} + \lambda_{6,i,t}(dr^{up}_{i,t} - S^{dr} l^d_{i,t}) \\ &- \lambda_{7,i,t} dr^{dn}_{i,t} + \lambda_{8,i,t}(dr^{dn}_{i,t} - S^{dr} l^d_{i,t}) + \mu_{1,i,t}(p_{i+1,t} - p_{i,t} + L^{ie}_{i,t} + l^d_{i,t} + dr^{up}_{i,t}) \end{aligned}$$

  Stationarity represents a set of first-order optimality conditions, such that the first derivative of the Lagrangian function with respect to each decision variable is zero. Accordingly, the stationarity conditions of the lower-level problem can be formulated as follows:

$$\mu_{1,i-1,t} - \mu_{1,i,t} + \lambda_{2,i,t} - \lambda_{1,i,t} = 0, \qquad t \in 1, ..., T, i \in 2, ..., N_b^d \tag{4.18}$$

$$c_t^{im} - \mu_{1,1,t} + \lambda_{2,1,t} - \lambda_{1,1,t} = 0, \qquad t \in 1, ..., T \tag{4.19}$$

$$2C^d l_{1,t}^d - 2C^d \overline{L}_{i,t}^d + \lambda_{4,1,t} - \lambda_{3,1,t} - S^{dr}\lambda_{6,1,t} - S^{dr}\lambda_{8,1,t} + \mu_{1,i,t} = 0, \qquad t \in 1, ..., T \tag{4.20}$$

$$2C_i^{dr2} dr_{i,t}^{up} + C_i^{dr1} - p_t^{dr} + \lambda_{6,i,t} - \lambda_{5,i,t} + \mu_{1,i,t} = 0, \qquad t \in 1, ..., T, i \in 1, ..., N_b^d \tag{4.21}$$

$$2C_i^{dr2} dr_{i,t}^{dn} + C_i^{dr1} - p_t^{dr} + \lambda_{8,i,t} - \lambda_{7,i,t} = 0, \qquad t \in 1, ..., T, i \in 1, ..., N_b^d \tag{4.22}$$

- ***Dual feasibility***:

  The condition of dual feasibility requires that all the dual variables associated with the inequality constraints must be non-negative.

$$\lambda_{j,i,t} \geq 0, i \in 1, ..., N_b^d, t \in 1, ..., T, j \in 1, ..., 8 \tag{4.23}$$

- ***Complementary slackness***:

  The complementary slackness conditions enforce the product of each inequality constraint and its corresponding dual variable to be zero. Hence, the complementary slackness conditions of the lower-level problem for Eqs. (4.14)-(4.17) are:

$$\lambda_{1,i,t}(\underline{P}_i - p_{i,t}) = 0, \qquad t \in 1, ..., T, i \in 1, ..., N_b^d$$

$$\lambda_{2,i,t}(p_{i,t} - \overline{P}_i) = 0, \qquad t \in 1, ..., T, i \in 1, ..., N_b^d$$

$$\lambda_{3,i,t}(\underline{L}_t^d - l_{i,t}^d) = 0, \qquad t \in 1, ..., T, i \in 1, ..., N_b^d$$

$$\lambda_{4,i,t}(l_{i,t}^d - \overline{L}_t^d) = 0, \qquad t \in 1, ..., T, i \in 1, ..., N_b^d$$

$$\lambda_{5,i,t}(-dr_{i,t}^{up}) = 0, \qquad t \in 1, ..., T, i \in 1, ..., N_b^d$$

$$\lambda_{6,i,t}(dr_{i,t}^{up} - S^{dr} l_{i,t}^d) = 0, \qquad t \in 1, ..., T, i \in 1, ..., N_b^d$$

$$\lambda_{7,i,t}(-dr_{i,t}^{dn}) = 0, \qquad t \in 1, ..., T, i \in 1, ..., N_b^d$$

$$\lambda_{8,i,t}(dr_{i,t}^{dn} - S^{dr} l_{i,t}^d) = 0, \qquad t \in 1, ..., T, i \in 1, ..., N_b^d$$

However, the products of variables in the complementary slackness constraints resulted in nonlinearities in the formulation. The big-M method is employed to linearize the complimentary slackness constraints by introducing a sufficiently large constant M as well as binary variables ϕ_i, with details regarding the big-M method in [95]. Using this approach, the complementary slackness constraints are linearized and reformulated as follows.

$$p_{i,t} - \underline{P}_i \leq (1-\phi_1)M, \qquad t \in 1,...,T, i \in 1,...,N_b^d \tag{4.24}$$

$$\overline{P}_i - p_{i,t} \leq (1-\phi_2)M, \qquad t \in 1,...,T, i \in 1,...,N_b^d \tag{4.25}$$

$$l_{i,t}^d - \underline{L}_t^d \leq (1-\phi_3)M, \qquad t \in 1,...,T, i \in 1,...,N_b^d \tag{4.26}$$

$$\overline{L}_t^d - l_{i,t}^d \leq (1-\phi_4)M, \qquad t \in 1,...,T, i \in 1,...,N_b^d \tag{4.27}$$

$$dr_{i,t}^{up} \leq (1-\phi_5)M, \qquad t \in 1,...,T, i \in 1,...,N_b^d \tag{4.28}$$

$$-dr_t^{up} + S^{dr} l_{i,t}^d \leq (1-\phi_6)M, \qquad t \in 1,...,T, i \in 1,...,N_b^d \tag{4.29}$$

$$dr_{i,t}^{dn} \leq (1-\phi_7)M, \qquad t \in 1,...,T, i \in 1,...,N_b^d \tag{4.30}$$

$$-dr_t^{dn} + S^{dr} l_{i,t}^d \leq (1-\phi_8)M, \qquad t \in 1,...,T, i \in 1,...,N_b^d \tag{4.31}$$

$$\lambda_{j,i,t} \leq \phi_i M \qquad i \in 1,...,10, t \in 1,...,T, i \in 1,...,N_b^d \tag{4.32}$$

An additional challenge results from the bilinear terms $-c_t^{im} p_t^{im} + p_t^{dr}(dr_t^{up} + dr_t^{dn})$ in the upper-level objective function Eq. (4.2). Since these bilinear terms also exist in the lower-level objective function Eq. (4.12), this issue can be addressed by applying the strong duality theorem to the lower level problem. The strong duality theorem states that the optimal value of the objective function of the primal problem is equal to that of the corresponding dual problem. The objective function of the dual of the lower-level problem is:

$$\begin{aligned} D(\{\lambda_{i,t}, \mu_{i,t}\}_{t=1,i=1}^{T,N_b^d}) &= \textstyle\sum_{t=1}^{T} \sum_{i=1}^{N_b^d} (-C^d (l_{i,t}^d)^2 - C^{dr2}((dr_{i,t}^{up})^2 + (dr_{i,t}^{dn})^2) \\ &+ L_{i,t}^{ie} \mu_{1,i,t} + \lambda_{1,i,t} \underline{P}_{i,t} - \lambda_{2,i,t} \overline{P}_{i,t} + \lambda_{3,i,t} \underline{L}_{i,t}^d - \lambda_{4,i,t} \overline{L}_{i,t}^d) \end{aligned} \tag{4.33}$$

For the formulation of the dual problem associated with a quadratic primal program, interested readers are referred to [119]. By equating the objective functions in Eqs. (4.12) and Eq. (4.33), the following equations are obtained.

$$
\begin{aligned}
-p_t^{im}c_t^{im} + p_t^{dr}(dr_t^{up} + dr_t^{dn}) &= \sum_{t=1}^{T}\sum_{i=1}^{N_b^d}(C^{dr1}(dr_{i,t}^{up} + dr_{i,t}^{dn}) + C^{dr2}((dr_{i,t}^{up})^2 + (dr_{i,t}^{dn})^2) \\
&- C^d l_{i,t}^d - D(\{\lambda_{i,t}, \mu_{i,t}\}_{t=1,i=1}^{T,N_b^d})
\end{aligned}
$$

Based on the above representation, the upper-level objective function Eq. (4.2) can be rewritten as

$$
\begin{aligned}
F'\left(\{x_t, y_t, \lambda_{t,i}, \mu_{t,i}\}_{t=1,i=1}^{T,N_b^d}\right) &= \sum_{t=1}^{T}\sum_{g=1}^{G}(C_{g,t}^c w_{g,t} + C_{g,t}p_{g,t} + C_{g,t}^2 p_{g,t}p_{g,t} \\
&+ C_g^r(r_{g,t}^{up} + r_{g,t}^{dn}) - D(\{\lambda_{i,t}, \mu_{i,t}\}_{t=1,i=1}^{T,N_b^d})
\end{aligned}
$$

As a result, the bi-level optimization problem is reformulated as the following single-level mixed integer problem which can be solved with a wide range of commercial solvers such as CPLEX and Gurobi.

$$
\begin{aligned}
&\min_{\{x_t, y_t, \lambda_{i,t}, \mu_{i,t}\}_{t=1,i=1}^{T,N_b^d}} F'\left(\{x_t, y_t, \lambda_{i,t}, \mu_{i,t}\}_{t=1,i=1}^{T,N_b^d}\right) \\
&\qquad \text{st: } (4.3) - (4.10), (4.13) - (4.17), (4.18) - (4.32)
\end{aligned}
$$

4.4 Numerical Results

This work first compares the operational performance of the coordinated system under the bi-level co-optimization framework with a framework representing the traditional practice. Subsequently, the bi-level framework is explored for an envisioned future distribution system with more complexity and autonomy. Two versions of the traditional optimization approach are used in this comparison; one with and one without network constraints in the distribution system.

While the DS network constraints are not currently included in transmission-level operation, it is likely necessary to take them into consideration for increasing distributed resources in future. Both versions of traditional optimization framework solves a single-level optimization problem to maximize the overall social welfare, ie; with an objective of minimizing the total cost and maximizing utility functions of all market participants. The mathematical formulation of the traditional framework is provided in Appendix 4.7.1. Throughout this paper, "Bi-level", "Traditional with network" and "Traditional w/o network" are used to denote the three frameworks in tables and figures. In practice, many ISOs use the locational marginal price resulting from this solution for the energy and DR prices under the traditional framework [120]. For a reasonable comparison, the DR price and energy price are set to the same variable under the bi-level optimization framework.

The transmission model described in Section 4.2.1 is applied to the IEEE 30-bus system, shown in Fig. 4.4(a). Interested readers are referred to [2] for detailed parameters of the transmission system. Three 6-bus distribution systems named as DS1, DS2 and DS3 are connected to bus 5, 15 and 25 in the transmission system respectively, each with the structure illustrated in Fig. 4.4(b). The parameters of the three distribution systems are provided in Appendix 4.7.2.

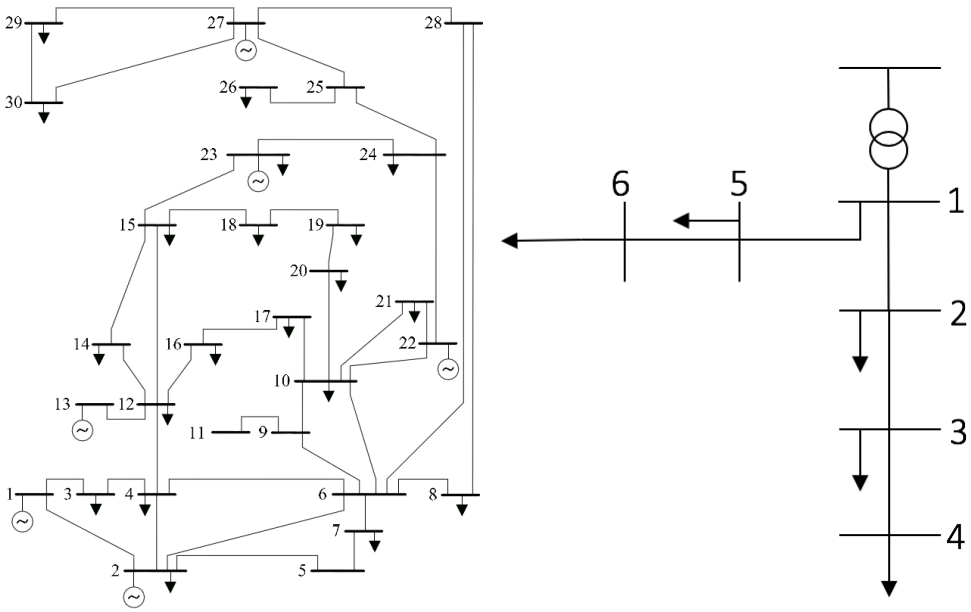

(a) IEEE 30 Bus System (b) 6-bus Distribution System

Figure 4.4: Transmission and Distribution System Schematics.

A wind farm is hosted at bus 8 of the transmission system which represents 25% of installed generation capacity. The generation data for the wind farm are obtained from the NREL-Eastern Wind Integration Study dataset [97], and a set of ten thousand diurnal wind scenarios are generated to represent a diverse set of possible realizations from a single forecast. The interested reader is referred to [98] for details of this scenario generation method.

4.4.1 Base Case: Cost Comparison

For benchmarking purposes, the costs of each of the transmission system, three distribution systems (denoted as DS1, DS2 and DS3), and the total system are compared among the three optimization frameworks. In the bi-level framework, the transmission and distribution costs are the objective function values

of the upper and lower level problem respectively, and the total system cost is the sum of the transmission and distribution costs. In the traditional frameworks, the total system cost is the objective function given by Eq. (4.42), which can be partitioned among transmission and distribution costs based on the decision variables. In this comparison, the transmission and distribution cost terms in the traditional objective function are the same as the upper and lower level objective functions in the bi-level optimization respectively.

The system cost and per unit energy cost information for the three optimization frameworks is shown in Fig. 4.5. The bi-level framework yields the lowest distribution system cost, as this is directly optimized in the lower level of the bi-level framework. In the traditional framework, the operation costs of the distribution systems are not optimized individually, and are thus higher. Including the distribution network constraints in the traditional framework results in the highest distribution system costs, as the feasible region under this framework is reduced by the network constraints. Conversely, the total system cost is the highest under the bi-level framework, as it is not directly optimized under this framework. Since the transmission system cost is calculated as the difference between the total system cost and distribution system cost, the observations for the transmission cost are the same as those for the total cost.

In Fig. 4.5(b) energy costs are normalized by the total load and compared on the cost per unit of load served, which further highlights the savings available to the distribution system under the bi-level structure.

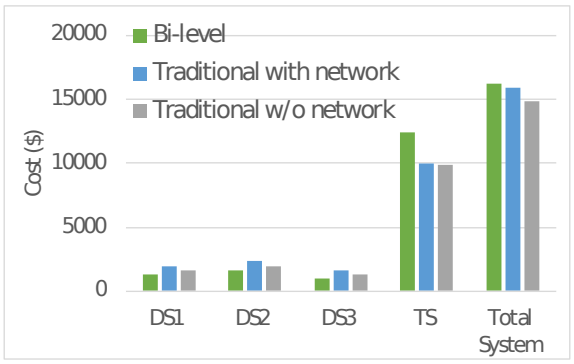

(a) System Cost

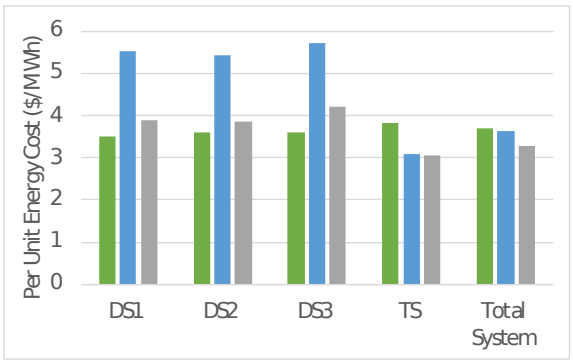

(b) Per Unit Energy Cost

Figure 4.5: Cost comparison between bi-level, single-level and single-level with network shows that bi-level framework results in the lowest costs for distribution systems, while the traditional framework favors transmission system savings.

4.4.2 Distribution System Cost Analysis

The realized costs for different wind scenarios may vary significantly, making it worthwhile to analyze the scenario-specific system costs, including transmission, distribution and the total cost for all the possible wind scenario realizations. To facilitate the analysis, for each wind scenario $s \in S$, the day-ahead energy market decisions are fixed, and the reserve and DR quantities are recalculated according to each scenario. Specifically, the realized generator reserve $r^{dn}_{g,t,s}$ and $r^{up}_{g,t,s}$ and demand response $dr^{up}_{t,s}$ and $dr^{dn}_{t,s}$ for each scenario $s \in S$

can be computed based on equations (4.35)-(4.40), and is an estimate of the additional resources required for system adequacy under each approach. To approximate the distribution of real-time operation cost, it is assumed that the real time error of each wind scenario is allocated to the reserve and DR resources according to their proportions in the day-ahead solution calculated in Equations (4.37)-(4.40).

Scenario-wise reserve and DR calculation:

$$W^{up}_{t,s} = dr^{up}_{t,s} + \sum_{g=1}^{G} r^{dn}_{g,t,s}, t \in 1, ..., T, s \in 1, ..., S \tag{4.35}$$

$$W^{dn}_{t,s} = dr^{dn}_{t,s} + \sum_{g=1}^{G} r^{up}_{g,t,s}, t \in 1, ..., T, s \in 1, ..., S \tag{4.36}$$

$$dr^{up}_{t,s}/W^{up}_{t,s} = dr^{up}_{t}/W^{up}_{t}, t \in 1, ..., T, s \in 1, ..., S \tag{4.37}$$

$$dr^{dn}_{t,s}/W^{dn}_{t,s} = dr^{dn}_{t}/W^{dn}_{t}, t \in 1, ..., T, s \in 1, ..., S \tag{4.38}$$

$$r^{dn}_{g,t,s}/W^{up}_{t,s} = r^{dn}_{g,t}/W^{up}_{t}, g \in 1, ..., G, t \in 1, ..., T, s \in 1, ..., S \tag{4.39}$$

$$r^{up}_{g,t,s}/W^{dn}_{t,s} = r^{up}_{g,t}/W^{dn}_{t}, g \in 1, ..., G, t \in 1, ..., T, s \in 1, ..., S \tag{4.40}$$

With the realized generator reserve and demand response, the actual scenario-wise transmission cost $F_s(\{x_{t,s}\}^T_{t=1})$ and distribution cost $f_s(\{y_{t,s}\}^T_{t=1})$ are obtained for each scenario $s \in S$ with the following equations:

$$\begin{aligned}
F_s(\{x_{t,s}\}^T_{t=1}) &= \textstyle\sum_{t=1}^{T}\sum_{g=1}^{G}(C^c_{g,t}w_{g,t} + C^1_g p_{g,t} + C^2_g p_{g,t}p_{g,t} \\
&+ C^r_g(r^{up}_{g,t,s} + r^{dn}_{g,t,s}) - p^{im}_t c^{im}_t + p^{dr}_t(dr^{up}_{t,s} + dr^{dn}_{t,s})) \\
f_s(\{y_{t,s}\}^T_{t=1}) &= \textstyle\sum_{t=1}^{T}\sum_{i=1}^{N^d_b}(p^{im}_t c^{im}_t \\
&+ C^{dr1}(dr^{up}_{i,t,s} + dr^{dn}_{i,t,s}) + C^{dr2}(dr^{up}_{i,t,s}dr^{up}_{i,t,s} + dr^{dn}_{i,t,s}dr^{dn}_{i,t,s}) \\
&- C^d l^d_{i,t} - p^{dr}_t(dr^{up}_{i,t,s} + dr^{dn}_{i,t,s}))
\end{aligned}$$

The result, shown in Fig. 4.6(a)-4.6(c), is a histogram of the DS costs for all scenarios for the three frameworks under wind uncertainty. The bi-level framework leads to much lower costs for all the DSs, as shown earlier. This analysis shows that the bi-level framework also yields the narrowest distribution among the three frameworks, which is due to lowest consumption of DR resources.

The percentage of DR and generator reserve to compensate the wind forecast errors are displayed in Fig. 4.7, suggesting that the traditional frameworks mostly depend on DR for the task, whereas the bi-level framework leverages more reserves. The heavier use of DR under the traditional framework is due to its lack of consideration for the DR payment in its optimization process, which makes the DR appear to be a more economic ancillary service option compared to the reserve. The higher consumption and variability of DR used by traditional frameworks leads to more uncertainty in DS costs, whereas lower consumption of DR under the bi-level framework yields a more concentrated distribution of operation cost, as a result, the bi-level optimization is shown to be a more risk-averse optimization framework from the perspective of the DS. A comparison of histograms of transmission and total system costs shows similar distributions among the three frameworks, and are excluded for brevity.

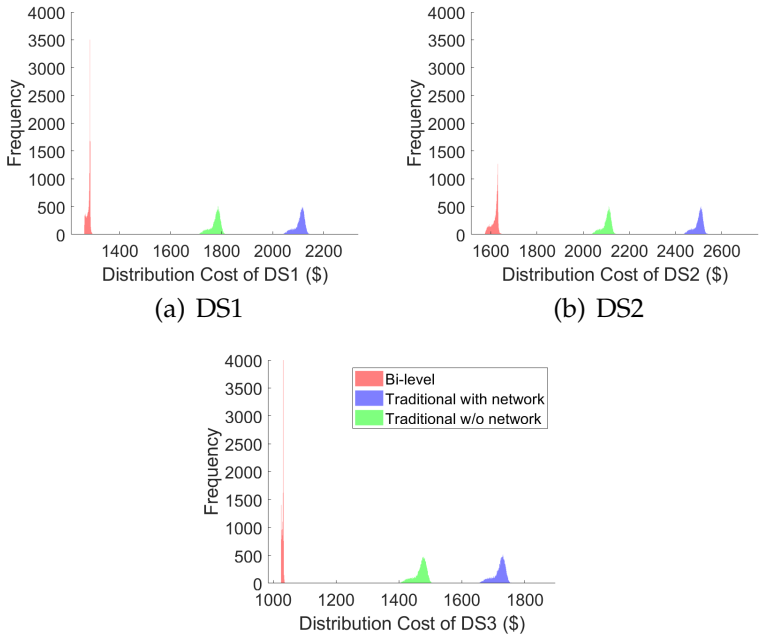

(a) DS1 (b) DS2

(c) DS3

Figure 4.6: Histograms of Distribution Costs of DSs show that the bi-level framework yields the narrowest distribution, implying that this approach is more risk-averse.

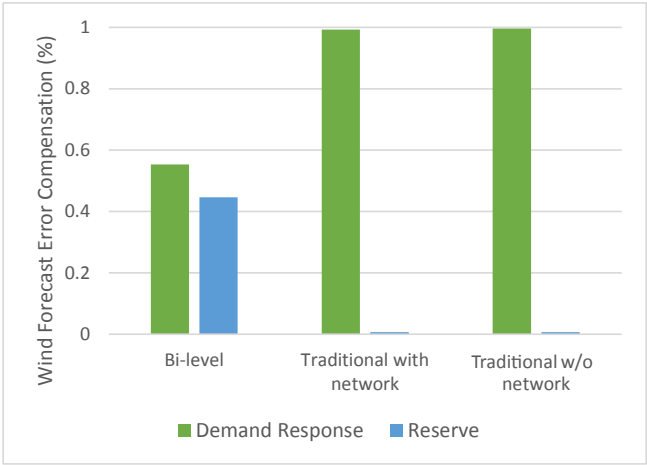

Figure 4.7: Proportion of DR and reserves used to compensate wind forecast error, shows that the bi-level framework uses a more balanced portfolio of DR and reserves to manage uncertainty.

4.4.3 Environmental Impact

As environmental benefits are an important consideration in the future energy system, the impact on CO_2 emissions is also examined here. The environmental impact, as tons of CO_2 emitted, is approximated based on the national average emissions rate across generation sources [121]. The only major difference in environmental impact between the bi-level and traditional frameworks lies in the strategies of dealing with upward wind error W_{up} when the wind energy is under-forecasted, with no perceivable difference when the wind power is over-forecasted. The differences in DR and reserve provision among the frameworks are due to the different DR payment characterizations as explained in the previous section. Recall that W_{up} is compensated either by downward reserve r^{dn} or upward demand response dr^{up}, and the use of r^{dn} leads to reduction of CO_2 emissions due to reduced generation. Table 4.1 shows the amount of dr^{up} and r^{dn} used to mitigate W_{up}, and the CO_2 reduction from r^{dn} for the three frameworks for the same wind forecast errors. It can be seen that the reduction of CO_2 emissions is more significant under the bi-level framework as much more r^{dn} is used under the bi-level framework than the traditional framework, leading to the observation that the bi-level framework can be considered more environmentally friendly.

	Bi-level	Traditional	
		Network	No Network
DR (MW)	68	192	194
Reserves (MW)	130	6	4
CO_2 Reduction (Tons)	13	0.6	0.4

Table 4.1: Comparison of CO_2 emission for balancing wind forecast errors. Note that more CO_2 emissions are reduced under the bi-level approach.

4.4.4 Implications for Increasing Wind Penetration

To analyze the performance of increasing wind utilization in the system, a scenario is considered in which installed wind capacity is scaled up by 50%. The significant wind utilization could increase the requirement for balancing resources including reserves and DR. Fig. 4.8 compares the unit energy cost of the three frameworks between the base case previously discussed, and the case with more wind. Under this scenario, the costs to both the TS and DSs increase under bi-level framework in Fig. 4.8 due to an increasing need for balancing resources. Conversely, the traditional approaches, both with and without DS network constraints, show a cost decrease for the DSs and a cost increase for the TS. When the production cost increases in a buyer-seller market, that cost increase is shared by both the buyer and seller according to fundamental economic principles [122]. The bi-level framework reflects a more equitable sharing of increased production costs between market participants since this framework better represents market interactions.

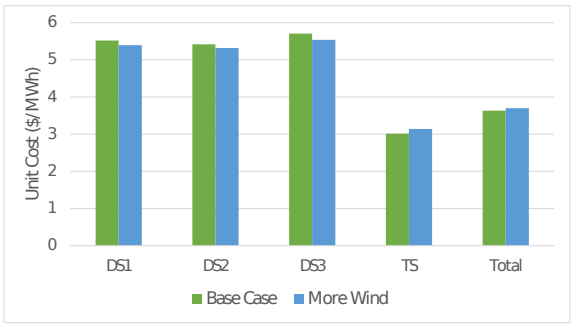

(a) Traditional with network

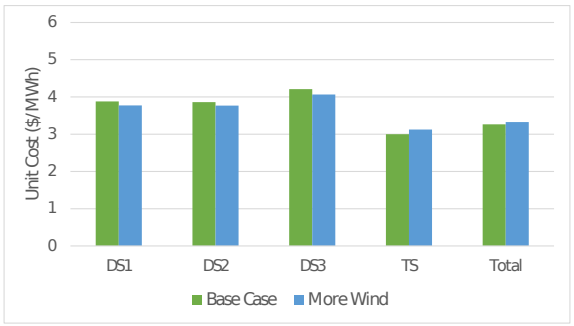

(b) Traditional w/o network

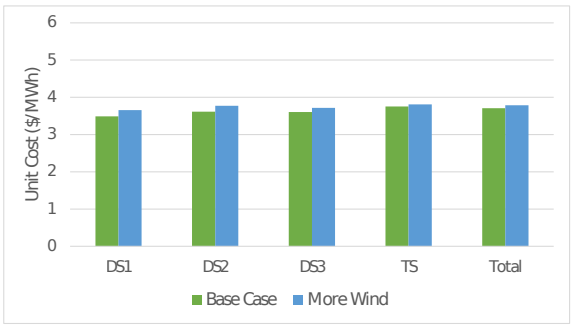

(c) Bi-level

Figure 4.8: Unit cost comparison associated with increased wind penetration shows that an increase in system operational cost is shared between the DSs and TS under the bi-level framework, whereas under the traditional frameworks the increase in system operational cost is borne solely by the TS.

4.4.5 Benefits to a Future Distribution System

As distribution systems evolve in the future, it is hoped that participation and flexibility of loads will increase. To replicate that effect, the upper bounds on

dispatchable load in the three DSs are scaled up by 20%. This increased flexibility is equivalent to increasing the feasible region of the DS optimization problem, which means the DS per unit energy cost will tend to decrease. Fig. 4.9 compares the impact of increased dispatchable load on unit costs of the distribution, transmission, and the total system. The total system unit cost under each of the three frameworks decreases with the increased flexibility in system loads, though the unit cost decrease in the total system cost is attributed differently among the distribution and transmission systems for the alternative frameworks. Under the bi-level approach, there is a higher relative reduction in the DS costs with marginally increase in transmission cost. The increased dispatchable load has less impact on both DS and TS in the traditional framework as shown in Fig. 4.9(a), 4.9(b), because the DSs is not explicitly optimized in traditional framework and the increasing feasible regions do not necessarily result in its objective improvement to the same level as the bi-level framework.

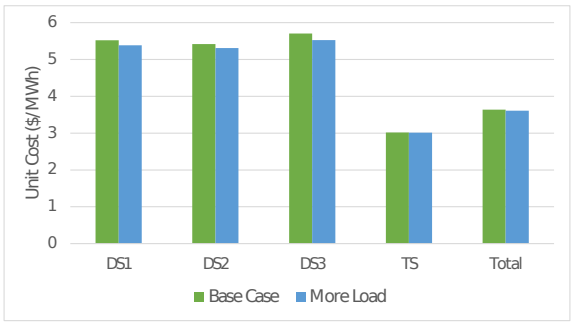

(a) Traditional with network

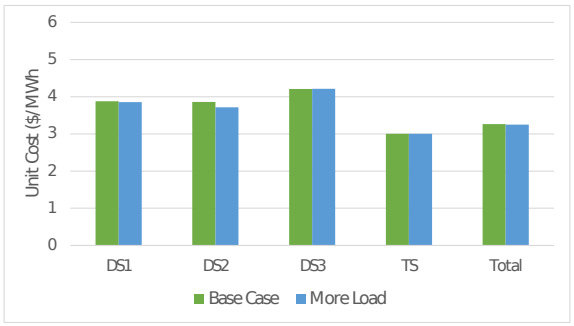

(b) Traditional w/o network

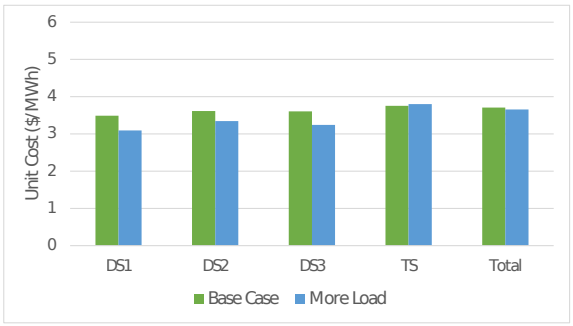

(c) Bi-level

Figure 4.9: Unit cost comparison under increased dispatchable load shows that the DSs experience a higher relative reduction in the energy cost under the bi-level framework, whereas the distribution unit cost does not necessarily decrease under the traditional frameworks.

4.4.6 Incorporating Generation in the Distribution System

A high level of distributed generation (DG) penetration may feature in the future energy system in order to enhance system sustainability, reliability and re-

silience. Effective use of DG will require the power flow in the DS to change from the current structure, which is commonly radial to bi-directional architecture, enabling the DS to sell excess power to the TS under potential changes in FERC policy and technology upgrades. Under this scenario, the DS will become more autonomous, and require more sophisticated consideration in terms of the modeling and optimization frameworks. The bi-level optimization framework is a promising approach to accommodates such needs.

In this case study, each of the three DSs is equipped with DG, bi-directional power flow and energy export capabilities. The DG is positioned at bus 2 of each distribution network, and parameters of the DG are provided in Appendix 4.7.2, with additional and modified constraints related to the DG in Appendix 4.7.3. Fig. 4.10 compares the unit cost of the three DSs with and without DG. The unit costs with DG for the distribution, transmission, and the total system are consistently cheaper than those without DG, since the DG provides an alternative supply to meet demand, and is used whenever it is cheaper than the energy import from the TS. The results here not only demonstrate the capability of the bi-level framework for modeling the future distribution system, but also shows system operation benefits of the future DS with DG under the bi-level framework. Since such future DS cannot be effectively modeled under the traditional frameworks, a comparison with this approach is not available here.

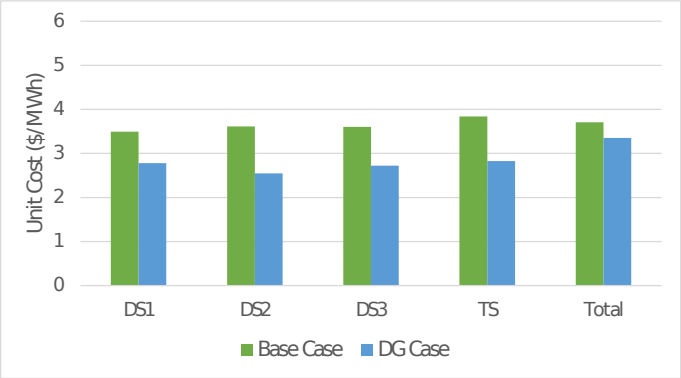

Figure 4.10: Unit cost comparison with addition of DG under bi-level optimization shows that all the market players experience a unit cost decrease.

4.5 Concluding Remarks

This paper presents a bi-level co-optimization framework for a transmission system with multiple distribution systems. Both the energy and ancillary markets are optimized under this framework. The bi-level framework models the transmission and distribution systems as separate optimization problems with possibly conflicting objective functions, which is in contrast to the traditional approach which models both systems as a single optimization problem neglecting details of the distribution system. Results show that the proposed framework provides a powerful and suitable way to represent future distribution system decisions along with the transmission system. As distribution systems become more active and responsive with DER, DG and bi-directional power flow, such a framework will be important for effective energy system integration. In addition, the bi-level approach can yield more environmentally friendly solutions in terms of ancillary resource provision, and make effective use of increasing renewable penetration and flexible loads, which are likely components

of future power system scenarios. In this future, DS and TS operators will require market simulators that incorporate their own decision making with that of the other parties, and this approach is a natural framework to appropriately incorporate multi-stakeholder and multi-level systems.

In the future, it will be worthwhile to analyze the impact of incorporating distributed storage devices and renewable generation in the distribution system as they are becoming increasingly common in the distribution system. The impact of the bi-level approach in terms of handling transmission system congestion is another promising direction.

4.6 Acknowledgments

This material is based upon work supported by the US Department of Energy under Award Number DE-OE0000843. Disclaimer: This report was prepared as an account of work sponsored by an agency of the United States Government. Neither the United States Government nor any agency thereof, nor any of their employees, makes any warranty, express or implied, or assumes any legal liability or responsibility for the accuracy, completeness, or usefulness of any information, apparatus, product, or process disclosed, or represents that its use would not infringe privately owned rights. Reference herein to any specific commercial product, process, or service by trade name, trademark, manufacturer, or otherwise does not necessarily constitute or imply its endorsement, recommendation, or favoring by the United States Government or any agency thereof. The views and opinions of the authors expressed herein do not necessarily state or reflect those of the United States Government or any agency thereof.

4.7 Appendix

4.7.1 Traditional UC Problem

The formulation of the traditional UC problem adopted by the ISOs is based on the UC formulation in [123]. The optimization variables are given below:

$$x_t = [w_{g,t}, p_{g,t}, r^{up}_{g,t}, r^{dn}_{g,t}, p_{i,t}, p^{im}_t, l^d_{i,t}, dr^{up}_{i,t}, dr^{dn}_{i,t}]$$

The objective function is the sum of the upper level and lower level bi-level optimization objective functions without the DR and energy import payment terms.

Objective function:

$$F(\{x_t\}_{t=1}^T) = \sum_{t=1}^{T}\sum_{g=1}^{G}(C^c_g w_{g,t} + C^1_g p_{g,t} + C^2_g (p_{g,t})^2 + C^r_g (r^{up}_{g,t} + r^{dn}_{g,t})) \tag{4.41}$$

$$+ \sum_{t=1}^{T}\sum_{i=1}^{N^d_b}(C^{dr1}(dr^{up}_{i,t} + dr^{dn}_{i,t}) + C^{dr2}((dr^{up}_{i,t})^2 + (dr^{dn}_{i,t})^2) - C^d l^d_{i,t}) \tag{4.42}$$

The constraints of the traditional approach with DS network constraints are the same as the ones used in the upper- and lower- level problems. The formulation is as below:

$$\min_{\{x_t\}_{t=1}^T} F\left(\{x_t\}_{t=1}^T\right)$$

$$\text{s.t.} (4.3) - (4.10), (4.13) - (4.17)$$

If the DS power flow constraints namely Eqs. (4.13) & (4.14) are taken out of the constraint set, the problem becomes the tradition UC without DS network constraints version.

4.7.2 Distribution System Parameters

The parameter values for DS1 are listed in the table below. DS2 and DS3 are derived from DS1 with a 20% increase and 20% decrease in $\overline{L}_i^d$ and $\overline{P}_i$ respectively.

Parameters	Bus 1	Bus 2	Bus 3	Bus 4	Bus 5	Bus 6
$\overline{L}_i^d$(MW)	0	4	5	3	4	2
$\underline{L}_i^d$(MW)	0	0	0	0	0	0
L_i^{ie}(MW)	0	0	0	0	0	0
$\overline{P}_i$(MW)	11.2	6.6	3.6	5.2	3	0
$\underline{P}_i$(MW)	0	0	0	0	0	0
C_i^{d1}(\$/MWh)	0	5	5	5	5	5
C_i^{d2}(\$/MWh)	0	0.02	0.02	0.02	0.02	0.02
$\overline{P}_i^d$(MW)	0	0	0	0	0	10
$\underline{P}_i^d$(MW)	0	0	0	0	0	0

Parameters	Values
C_t^d	\$3/MWh
C_t^{dr1}	\$1/MWh
C_t^{dr2}	\$1/MWh
S_t^{dr}	\$0.5/MWh

Table 4.2: DS parameter values

4.7.3 Additional Constraints with DG

There are three main changes to the distribution system with the proposed addition of DG in Section 4.4.6. The first one is the power flow which changes from radial power flow to meshed power flow in distribution system. Specifically, the power flow equation in 4.13 should be replaced by similar power flow equations as the transmission system's as follow:

$$-\overline{P_i} \leq M^{GSFd} p_t^{injd} \leq \overline{P_i},\ t \in 1, ..., T \tag{4.44}$$

$$-\overline{P_i} \leq M^{GSFd} p_t^{injd*} \leq \overline{P_i},\ t \in 1, ..., T \tag{4.45}$$

where M^{GSFd} is the generation shift factor matrix of the distribution system. p_t^{injd} is the nodal net power injection vector taking distributed generation demand into account. p_t^{injd*} incorporates distribution system DR into the base p_t^{injd}. The second change is the addition of DG in the distribution system. The following constraints capture the behavior of DG:

$$\underline{P}_i^d \leq p_{i,t}^d \leq \overline{P}_i^d, \qquad \lambda_{5,i,t}, \lambda_{6,i,t}, t \in 1, ..., T, i \in 1, ..., N_b^d \tag{4.46}$$

Eqn. (4.46) limits the DG output with its upper and lower generation bounds. In addition, a power balance equation is needed for the distribution system as shown in Eq. 4.47:

$$\sum_{i=1}^{N_b^d} (L_{i,t}^{ie} + l_{i,t}^d) = p_t^{im} + p_{i,t}^d, \qquad t \in 1, ..., T \tag{4.47}$$

The thrid change is incorporating power export capability into the distribution system. The p_t^{im} in Eq. 4.47 could now be a negative number which represent power export.

The KKT conditions associated with those additional equations are not given for simplicity. Readers could refer to [124] and follows the same rules as explained in 4.3 to derive them.

CHAPTER 5

CONCLUSION

This dissertation seeks to develop a new framework to support renewable resource integration and distributed resources. To this end, three projects are presented, each of which considers different aspects of the optimization of the future power system. The first project explored three types of demand response programs (i.e., TCL, DL, and EL) in a microgrid based on the categorization and characteristics of real load. A stochastic rolling horizon approach is leveraged to optimize the microgrid's operational decisions. The second project coordinates a microgrid with demand response, with the main grid under a bi-level optimization framework, which enables appropriately detailed system modeling for each. Results show that the cooperative framework reduces system costs and supports higher levels of renewable resources utilization. The final project presented generalizes the bi-level co-optimization framework from a microgrid to current distribution system structures. The bi-level framework is compared with the traditional optimization framework in terms of the system operation cost, environmental impact, risk-averseness of the solutions, and capabilities to handle possible system expansion with renewable generation uncertainty. Results indicate that bi-level co-optimization provides benefits under current distribution system configurations, and provides potential for more significant benefits under future architectures that include distributed generation and bi-directional energy exchange capabilities with the main grid.

The results of these studies show that for the operation of a MG, a stochastic rolling horizon optimization framework could effectively manage various DR programs, reduce MG operation cost, and support renewable integration.

For transmission and distribution level co-optimization, the bi-level framework is shown to facilitate system renewable penetration, and generate cost savings on top of the standalone mode. The comparison with the traditional framework further highlights the benefits of the bi-level framework including more equitable sharing of cost among the systems, better environmental impacts and support for the DS evolution.

Overall, this dissertation centers around renewable energy integration in the power systems and provide an inter-system and intra-system optimization framework taking various demand response programs into consideration for the future power system. The frameworks and methods established in this dissertation will support developments toward more renewable generation in the power system, while ensuring a robust and efficient future grid with desired components and functionalities that are not currently supported. As the foundation for a nation, an advanced grid infrastructure will greatly boost the development of the society. It is hoped that the studies presented here serve to accelerate the arrival of a more sustainable grid.

BIBLIOGRAPHY

[1] EPA. Draft inventory of u.s. greenhouse gas emissions and sinks: 1990-2014. Technical report, United States Environmental Protection Agency, 2016.

[2] Ray D Zimmerman, Carlos E Murillo-Sánchez, and Robert J Thomas. Matpower's extensible optimal power flow architecture. In *Power & Energy Society General Meeting, 2009. PES'09. IEEE*, pages 1–7. IEEE, 2009.

[3] Ryan Wiser, Christopher Namovicz, Mark Gielecki, and Robert Smith. The experience with renewable portfolio standards in the united states. *The Electricity Journal*, 20(4):8–20, 2007.

[4] Jeff D Makholm. The revolution yields to a more familiar path: New yorks reforming the energy vision (rev). *The Electricity Journal*, 29(9):48–55, 2016.

[5] Benefits of demand response in electricity markets and recommendations for achieving them. Technical report, Department of Energy, February 2006.

[6] C.L. Su and D. Kirschen. Quantifying the effect of demand response on electricity markets. *Power Systems, IEEE Transactions on*, 24(3):1199–1207, 2009.

[7] N. Li, L. Chen, and S.H. Low. Optimal demand response based on utility maximization in power networks. In *Power and Energy Society General Meeting, 2011 IEEE*, pages 1–8, July 2011.

[8] M.H. Albadi and E.F. El-Saadany. A summary of demand response in electricity markets. *Electric Power Systems Research*, 78(11):1989 – 1996, 2008.

[9] N. O'Connell, P. Pinson, H. Madsen, and M. O'Malley. Benefits and challenges of electrical demand response: A critical review. *Renewable and Sustainable Energy Reviews*, 39:686 – 699, 2014.

[10] C Lindsay Anderson and Judith B Cardell. A decision framework for optimal pairing of wind and demand response resources. *IEEE Systems Journal*, 8(4):1104–1111, 2014.

[11] Judith Cardell and Lindsay Anderson. The influence of demand resource

response time in balancing wind and load. In *2013 46th Hawaii International Conference on System Sciences*, pages 2364–2370. IEEE, 2013.

[12] S.H. Madaeni and R. Sioshansi. Measuring the benefits of delayed price-responsive demand in reducing wind-uncertainty costs. *Power Systems, IEEE Transactions on*, 28(4):4118–4126, Nov 2013.

[13] Y. Ikeda, T. Ikegami, K. Kataoka, and K. Ogimoto. A unit commitment model with demand response for the integration of renewable energies. In *Power and Energy Society General Meeting, 2012 IEEE*, pages 1–7, July 2012.

[14] Merrill Smith and Dan Ton. Key connections: The us department of energy's microgrid initiative. *IEEE Power and Energy magazine*, 11(4):22–27, 2013.

[15] Robert H Lasseter. Microgrids and distributed generation. *Journal of Energy Engineering*, 133(3):144–149, 2007.

[16] J. Liu, M.G. Martinez, and C. L. Anderson. Quantifying the impact of microgrid location and behavior on transmission network congestion. *Winter Simulation Conference*, 2016.

[17] Zhonglin Cheng, Guangchao Geng, Quanyuan Jiang, and Josep M Guerrero. Energy management of chp-based microgrid with thermal storage for reducing wind curtailment. *Journal of Energy Engineering*, 144(6):04018066, 2018.

[18] Ming-Che Hu, Yen-Haw Chen, Yen-Hong Chen, and Yung-Ruei Chang. Optimal operating strategies and management for smart microgrid systems. *Journal of Energy Engineering*, 140(1):04013011, 2013.

[19] Ahmad Ghasemi and Mehdi Enayatzare. Optimal energy management of a renewable-based isolated microgrid with pumped-storage unit and demand response. *Renewable Energy*, 123:460–474, 2018.

[20] Vahid Hosseinnezhad, Mansour Rafiee, Mohammad Ahmadian, and Pierluigi Siano. Optimal day-ahead operational planning of microgrids. *Energy Conversion and Management*, 126:142–157, 2016.

[21] Y. Zhang, R. Wang, T. Zhang, Y. Liu, and B. Guo. Model predictive control-based operation management for a residential microgrid with considering

forecast uncertainties and demand response strategies. *IET Generation, Transmission Distribution*, 10(10):2367–2378, 2016.

[22] Farshad Kalavani, Behnam Mohammadi-Ivatloo, and Kazem Zare. Optimal stochastic scheduling of cryogenic energy storage with wind power in the presence of a demand response program. *Renewable Energy*, 2018.

[23] Faran Ahmed Qureshi, Tomasz Tadeusz Gorecki, and Colin Jones. Model predictive control for market-based demand response participation. In *19th World Congress of the International Federation of Automatic Control*, number EPFL-CONF-197950, 2014.

[24] Theodor Borsche, Frauke Oldewurtel, and Göran Andersson. Scenario-based mpc for energy schedule compliance with demand response. *IFAC Proceedings Volumes*, 47(3):10299–10304, 2014.

[25] Rodrigo Palma-Behnke, Carlos Benavides, Fernando Lanas, Bernardo Severino, Lorenzo Reyes, Jacqueline Llanos, and Doris Sáez. A microgrid energy management system based on the rolling horizon strategy. *IEEE Transactions on Smart Grid*, 4(2):996–1006, 2013.

[26] Nima Nikmehr, Sajad Najafi-Ravadanegh, and Amin Khodaei. Probabilistic optimal scheduling of networked microgrids considering time-based demand response programs under uncertainty. *Applied energy*, 198:267–279, 2017.

[27] S. Talari, M. Yazdaninejad, and M. R. Haghifam. Stochastic-based scheduling of the microgrid operation including wind turbines, photovoltaic cells, energy storages and responsive loads. *IET Generation, Transmission Distribution*, 9(12):1498–1509, 2015.

[28] Ali Mehdizadeh, Navid Taghizadegan, and Javad Salehi. Risk-based energy management of renewable-based microgrid using information gap decision theory in the presence of peak load management. *Applied Energy*, 211:617–630, 2018.

[29] Ming Jin, Wei Feng, Chris Marnay, and Costas Spanos. Microgrid to enable optimal distributed energy retail and end-user demand response. *Applied Energy*, 210:1321–1335, 2018.

[30] Alessandra Parisio and Luigi Glielmo. Stochastic model predictive control for economic/environmental operation management of microgrids. In *2013 European Control Conference (ECC)*, pages 2014–2019. IEEE, 2013.

[31] Mohamed H Albadi and Ehab F El-Saadany. Demand response in electricity markets: An overview. In *Power Engineering Society General Meeting, 2007. IEEE*, pages 1–5. IEEE, 2007.

[32] Ming Jin, Wei Feng, Ping Liu, Chris Marnay, and Costas Spanos. Modr: Microgrid optimal dispatch with demand response. *Applied energy*, 187:758–776, 2017.

[33] Simone Baldi, Athanasios Karagevrekis, Iakovos T Michailidis, and Elias B Kosmatopoulos. Joint energy demand and thermal comfort optimization in photovoltaic-equipped interconnected microgrids. *Energy Conversion and Management*, 101:352–363, 2015.

[34] Dan T Ton and Merrill A Smith. The us department of energy's microgrid initiative. *The Electricity Journal*, 25(8):84–94, 2012.

[35] EIA. Annual energy outlook 2017. Technical report, Energy Information Administration, 2017.

[36] J. L. Mathieu, M. Kamgarpour, J. Lygeros, G. Andersson, and D. S. Callaway. Arbitraging intraday wholesale energy market prices with aggregations of thermostatic loads. *IEEE Transactions on Power Systems*, 30(2):763–772, March 2015.

[37] Mark A Bernstein and James M Griffin. *Regional differences in the price-elasticity of demand for energy*. Citeseer, 2006.

[38] DOE. Water heater market profile. Technical report, Department of Energy, 2010.

[39] Jialin Liu, Gabriela Martinez, Bowen Li, Johanna Mathieu, and C. Lindsay Anderson. A comparison of robust and probabilistic reliability for systems with renewables and responsive demand. *To appear in Proceedings of the 49th Hawaii Conference on System Sciences*, pages 1–8, 2016.

[40] M. Vrakopoulou, J. L. Mathieu, and G. Andersson. Stochastic optimal power flow with uncertain reserves from demand response. In *2014 47th Hawaii International Conference on System Sciences*, pages 2353–2362, Jan 2014.

[41] N. Lu. An evaluation of the hvac load potential for providing load balancing service. *IEEE Transactions on Smart Grid*, 3(3):1263–1270, Sept 2012.

[42] M. Roozbehani, D. Materassi, M. I. Ohannessian, and M. A. Dahleh. Robust and optimal consumption policies for deadline-constrained deferrable loads. *IEEE Transactions on Smart Grid*, 5(4):1823–1834, 2014.

[43] Rahul Walawalkar, Stephen Fernands, Netra Thakur, and Konda Reddy Chevva. Evolution and current status of demand response (dr) in electricity markets: Insights from pjm and nyiso. *Energy*, 35(4):1553–1560, 2010.

[44] Rahmat Azami, Amir Hossein Abbasi, Jamal Shakeri, and Amir Faraji Fard. Impact of edrp on composite reliability of restructured power systems. In *PowerTech, 2009 IEEE Bucharest*, pages 1–6. IEEE, 2009.

[45] Lingwen Gan, Adam Wierman, Ufuk Topcu, Niangjun Chen, and Steven H Low. Real-time deferrable load control: handling the uncertainties of renewable generation. In *Proceedings of the fourth international conference on Future energy systems*, pages 113–124. ACM, 2013.

[46] K. McKenna and A. Keane. Residential load modeling of price-based demand response for network impact studies. *IEEE Transactions on Smart Grid*, 7(5), 2016.

[47] D. S. Kirschen, G. Strbac, P. Cumperayot, and D. de Paiva Mendes. Factoring the elasticity of demand in electricity prices. *IEEE Transactions on Power Systems*, 15(2):612–617, 2000.

[48] Suresh Sethi and Gerhard Sorger. A theory of rolling horizon decision making. *Annals of Operations Research*, 29(1):387–415, Dec 1991.

[49] A. Papavasiliou, S. S. Oren, and R. P. O'Neill. Reserve requirements for wind power integration: A scenario-based stochastic programming framework. *IEEE Transactions on Power Systems*, 26(4):2197–2206, Nov 2011.

[50] Anthony Papavasiliou and Shmuel S Oren. Multiarea stochastic unit commitment for high wind penetration in a transmission constrained network. *Operations Research*, 61(3):578–592, 2013.

[51] PJM. Comed historical load data, 2018.

[52] ComED. Comed historical price data, 2018.

[53] NOAA. Chicago ohare international airport wind and temperature data, 2018.

[54] Pavlos Nikolaidis and Andreas Poullikkas. Cost metrics of electrical energy storage technologies in potential power system operations. *Sustainable Energy Technologies and Assessments*, 25:43–59, 2018.

[55] EIA. Average power plant operating expenses for major u.s. investor-owned electric utilities, 2007 through 2017. Technical report, Energy Information Administration, 2010.

[56] Lindsay Anderson, Luckny Zéphyr, and Judy Cardell. A vision for co-optimized t&d system interaction with renewables and demand response. In *Proceedings of the 50th Hawaii International Conference on System Sciences*, 2017.

[57] Amin Kargarian Marvasti, Yong Fu, Saber DorMohammadi, and Masoud Rais-Rohani. Optimal operation of active distribution grids: A system of systems framework. *IEEE Transactions on Smart Grid*, 5(3):1228–1237, 2014.

[58] Georgia E Asimakopoulou, Aris L Dimeas, and Nikos D Hatziargyriou. Leader-follower strategies for energy management of multi-microgrids. *IEEE transactions on smart grid*, 4(4):1909–1916, 2013.

[59] Hamed Hosseinnia and Behrouz Tousi. Optimal operation of dg-based micro grid (mg) by considering demand response program (drp). *Electric Power Systems Research*, 167:252–260, 2019.

[60] D. Wang, S. Ge, H. Jia, C. Wang, Y. Zhou, N. Lu, and X. Kong. A demand response and battery storage coordination algorithm for providing microgrid tie-line smoothing services. *IEEE Transactions on Sustainable Energy*, 5(2):476–486, April 2014.

[61] Aida Khayatian, Masoud Barati, and Gino J Lim. Integrated microgrid expansion planning in electricity market with uncertainty. *IEEE Transactions on Power Systems*, 33(4):3634–3643, 2018.

[62] Amin Khodaei and Mohammad Shahidehpour. Microgrid-based co-optimization of generation and transmission planning in power systems. *IEEE transactions on power systems*, 28(2):1582–1590, 2013.

[63] Chengquan Ju, Peng Wang, Lalit Goel, and Yan Xu. A two-layer energy

management system for microgrids with hybrid energy storage considering degradation costs. *IEEE Transactions on Smart Grid*, 9(6):6047–6057, 2018.

[64] Ying Zhou, Lizhi Wang, and James D McCalley. Designing effective and efficient incentive policies for renewable energy in generation expansion planning. *Applied Energy*, 88(6):2201–2209, 2011.

[65] L Baringo and AJ Conejo. Wind power investment within a market environment. *Applied Energy*, 88(9):3239–3247, 2011.

[66] Guangquan Zhang, Guoli Zhang, Ya Gao, and Jie Lu. Competitive strategic bidding optimization in electricity markets using bilevel programming and swarm technique. *IEEE Transactions on Industrial Electronics*, 58(6):2138–2146, 2011.

[67] Panagiotis Andrianesis, George Kozanidis, Eftychia Kostarelou, and Liberopoulos George. Mixed integer bilevel programming for optimal bidding strategies in day-ahead electricity markets with indivisibilities. *BALCOR 2011*, page 72, 2011.

[68] Nasim Nezamoddini, Seyedamirabbas Mousavian, and Melike Erol-Kantarci. A risk optimization model for enhanced power grid resilience against physical attacks. *Electric Power Systems Research*, 143:329–338, 2017.

[69] Yingmeng Xiang and Lingfeng Wang. A game-theoretic study of load redistribution attack and defense in power systems. *Electric Power Systems Research*, 151:12–25, 2017.

[70] Yingmeng Xiang, Lingfeng Wang, and Nian Liu. Coordinated attacks on electric power systems in a cyber-physical environment. *Electric Power Systems Research*, 149:156–168, 2017.

[71] Yi Ding, Chanan Singh, Lalit Goel, Jacob Østergaard, and Peng Wang. Short-term and medium-term reliability evaluation for power systems with high penetration of wind power. *IEEE Transactions on Sustainable Energy*, 5(3):896–906, 2014.

[72] Alexandre Moreira, Bruno Fanzeres, and Goran Strbac. Energy and reserve scheduling under ambiguity on renewable probability distribution. *Electric Power Systems Research*, 160:205–218, 2018.

[73] Yi Ding, Peng Wang, Lalit Goel, Poh Chiang Loh, and Qiuwei Wu. Long-term reserve expansion of power systems with high wind power penetration using universal generating function methods. *IEEE Transactions on Power Systems*, 26(2):766–774, 2011.

[74] Javad Saebi, Mohammad Hossein Javidi, and Majid Oloomi Buygi. Toward mitigating wind-uncertainty costs in power system operation: A demand response exchange market framework. *Electric Power Systems Research*, 119:157–167, 2015.

[75] D Karl Critz, Sarah Busche, and Stephen Connors. Power systems balancing with high penetration renewables: The potential of demand response in hawaii. *Energy conversion and management*, 76:609–619, 2013.

[76] John P Barton, David G Infield, et al. Energy storage and its use with intermittent renewable energy. *IEEE transactions on energy conversion*, 19(2):441–448, 2004.

[77] Emmanouil A Bakirtzis, Christos K Simoglou, Pandelis N Biskas, and Anastasios G Bakirtzis. Storage management by rolling stochastic unit commitment for high renewable energy penetration. *Electric Power Systems Research*, 158:240–249, 2018.

[78] David B Richardson. Electric vehicles and the electric grid: A review of modeling approaches, impacts, and renewable energy integration. *Renewable and Sustainable Energy Reviews*, 19:247–254, 2013.

[79] Francis Mwasilu, Jackson John Justo, Eun-Kyung Kim, Ton Duc Do, and Jin-Woo Jung. Electric vehicles and smart grid interaction: A review on vehicle to grid and renewable energy sources integration. *Renewable and sustainable energy reviews*, 34:501–516, 2014.

[80] Amit Bhardwaj, Vikram Kumar Kamboj, Vijay Kumar Shukla, Bhupinder Singh, and Preeti Khurana. Unit commitment in electrical power system-a literature review. In *Power Engineering and Optimization Conference (PEDCO) Melaka, Malaysia, 2012 Ieee International*, pages 275–280. IEEE, 2012.

[81] Eklas Hossain, Ersan Kabalci, Ramazan Bayindir, and Ronald Perez. Microgrid testbeds around the world: State of art. *Energy Conversion and Management*, 86:132–153, 2014.

[82] Changsong Chen, Shanxu Duan, Tong Cai, Bangyin Liu, and Gangwei Hu. Smart energy management system for optimal microgrid economic operation. *IET renewable power generation*, 5(3):258–267, 2011.

[83] Ankur Sinha, Pekka Malo, and Kalyanmoy Deb. A review on bilevel optimization: from classical to evolutionary approaches and applications. *IEEE Transactions on Evolutionary Computation*, 2017.

[84] Jose Fernando Prada and Marija D Ilić. Locational allocation and pricing of responsive contingency reserves. In *2015 IEEE Power & Energy Society General Meeting*, pages 1–5. IEEE, 2015.

[85] Jonathan F Bard and James E Falk. An explicit solution to the multilevel programming problem. *Computers & Operations Research*, 9(1):77–100, 1982.

[86] Charles D Kolstad and Leon S Lasdon. Derivative evaluation and computational experience with large bilevel mathematical programs. *Journal of optimization theory and applications*, 65(3):485–499, 1990.

[87] Douglas J White and G Anandalingam. A penalty function approach for solving bi-level linear programs. *Journal of Global Optimization*, 3(4):397–419, 1993.

[88] Benoît Colson, Patrice Marcotte, and Gilles Savard. A trust-region method for nonlinear bilevel programming: algorithm and computational experience. *Computational Optimization and Applications*, 30(3):211–227, 2005.

[89] R Mathieu, L Pittard, and G Anandalingam. Genetic algorithm based approach to bi-level linear programming. *RAIRO-Operations Research*, 28(1):1–21, 1994.

[90] Xiangyong Li, Peng Tian, and Xiaoping Min. A hierarchical particle swarm optimization for solving bilevel programming problems. In *International Conference on Artificial Intelligence and Soft Computing*, pages 1169–1178. Springer, 2006.

[91] Xiaobo Zhu, Qian Yu, and Xianjia Wang. A hybrid differential evolution algorithm for solving nonlinear bilevel programming with linear constraints. In *Cognitive Informatics, 2006. ICCI 2006. 5th IEEE International Conference on*, volume 1, pages 126–131. IEEE, 2006.

[92] G Gary Wang and Songqing Shan. Review of metamodeling techniques in support of engineering design optimization. *Journal of Mechanical design*, 129(4):370–380, 2007.

[93] Ankur Sinha, Pekka Malo, and Kalyanmoy Deb. A review on bilevel optimization: from classical to evolutionary approaches and applications. *IEEE Transactions on Evolutionary Computation*, 22(2):276–295, 2018.

[94] Wayne F Bialas and Mark H Karwan. Two-level linear programming. *Management science*, 30(8):1004–1020, 1984.

[95] Wayne L Winston, Munirpallam Venkataramanan, and Jeffrey B Goldberg. *Introduction to mathematical programming*, volume 1. Thomson/Brooks/Cole Duxbury; Pacific Grove, CA, 2003.

[96] European Wind Energy Association. *Wind energy-the facts: a guide to the technology, economics and future of wind power*. Routledge, 2012.

[97] Great Lakes Regional Wind Energy. Eastern wind integration and transmission study. *Technical Report, National Renewable Energy Laboratory (NREL)*, 2010.

[98] CL Anderson and RD Zimmerman. Wind output forecasts and scenario analysis for stochastic multiperiod optimal power flow. *PSERC Webinar*, pages 1–38, 2011.

[99] Kalpesh Joshi and Naran Pindoriya. Advances in distribution system analysis with distributed resources: survey with a case study. *Sustainable Energy, Grids and Networks*, 15:86–100, 2018.

[100] Pranjal Verma, Krishnendu Sanyal, Dipti Srinivsan, and KS Swarup. Information exchange based clustered differential evolution for constrained generation-transmission expansion planning. *Swarm and Evolutionary Computation*, 2018.

[101] Saeed Zolfaghari and Tohid Akbari. Bilevel transmission expansion planning using second-order cone programming considering wind investment. *Energy*, 154:455–465, 2018.

[102] Hrvoje Pandžić, Yury Dvorkin, and Miguel Carrión. Investments in merchant energy storage: Trading-off between energy and reserve markets. *Applied Energy*, 230:277–286, 2018.

[103] V Vahidinasab and S Jadid. Multiobjective environmental/techno-economic approach for strategic bidding in energy markets. *Applied Energy*, 86(4):496–504, 2009.

[104] S Soleymani, AM Ranjbar, and AR Shirani. New approach to bidding strategies of generating companies in day ahead energy market. *Energy Conversion and Management*, 49(6):1493–1499, 2008.

[105] George Kozanidis, Eftychia Kostarelou, Panagiotis Andrianesis, and George Liberopoulos. Mixed integer parametric bilevel programming for optimal strategic bidding of energy producers in day-ahead electricity markets with indivisibilities. *Optimization*, 62(8):1045–1068, 2013.

[106] Yanling Yuan, Zuyi Li, and Kui Ren. Modeling load redistribution attacks in power systems. *IEEE Transactions on Smart Grid*, 2(2):382–390, 2011.

[107] Joes M Arroyo and Federico J Fernández. A genetic algorithm approach for the analysis of electric grid interdiction with line switching. In *Intelligent System Applications to Power Systems, 2009. ISAP'09. 15th International Conference on*, pages 1–6. IEEE, 2009.

[108] Ali Pinar, Juan Meza, Vaibhav Donde, and Bernard Lesieutre. Optimization strategies for the vulnerability analysis of the electric power grid. *SIAM Journal on Optimization*, 20(4):1786–1810, 2010.

[109] José Manuel Arroyo. Bilevel programming applied to power system vulnerability analysis under multiple contingencies. *IET generation, transmission & distribution*, 4(2):178–190, 2010.

[110] Hossein Haghighat and Scott W Kennedy. A bilevel approach to operational decision making of a distribution company in competitive environments. *IEEE Transactions on Power Systems*, 27(4):1797–1807, 2012.

[111] Haiying Li, Yuzeng Li, and Zuyi Li. A multiperiod energy acquisition model for a distribution company with distributed generation and interruptible load. *IEEE Transactions on Power Systems*, 22(2):588–596, 2007.

[112] Chunyu Zhang, Qi Wang, Jianhui Wang, Magnus Korps, Pierre Pinson, Jacob Østergaard, and Mohammad E Khodayar. Trading strategies for distribution company with stochastic distributed energy resources. *Applied energy*, 177:625–635, 2016.

[113] P Balakrishna, K Rajagopal, and KS Swarup. Application benefits of distribution automation and ami systems convergence methodology for distribution power restoration analysis. *Sustainable Energy, Grids and Networks*, 2:15–22, 2015.

[114] Marco Pau, Edoardo Patti, Luca Barbierato, Abouzar Estebsari, Enrico Pons, Ferdinanda Ponci, and Antonello Monti. A cloud-based smart metering infrastructure for distribution grid services and automation. *Sustainable Energy, Grids and Networks*, 15:14–25, 2018.

[115] Mesut E Baran and Felix F Wu. Network reconfiguration in distribution systems for loss reduction and load balancing. *IEEE Transactions on Power delivery*, 4(2):1401–1407, 1989.

[116] Gilles Savard and Jacques Gauvin. The steepest descent direction for the nonlinear bilevel programming problem. *Operations Research Letters*, 15(5):265–272, 1994.

[117] Yibing Lv, Tiesong Hu, Guangmin Wang, and Zhongping Wan. A penalty function method based on kuhn–tucker condition for solving linear bilevel programming. *Applied Mathematics and Computation*, 188(1):808–813, 2007.

[118] Patrice Marcotte, Gilles Savard, and DL Zhu. A trust region algorithm for nonlinear bilevel programming. *Operations research letters*, 29(4):171–179, 2001.

[119] William S Dorn. Duality in quadratic programming. *Quarterly of Applied Mathematics*, 18(2):155–162, 1960.

[120] David J Lawrence. 2001 performance of new york iso demand response programs. In *2002 IEEE Power Engineering Society Winter Meeting. Conference Proceedings (Cat. No. 02CH37309)*, volume 2, pages 995–998. IEEE, 2002.

[121] Ralph EH Sims, Hans-Holger Rogner, and Ken Gregory. Carbon emission and mitigation cost comparisons between fossil fuel, nuclear and renewable energy resources for electricity generation. *Energy policy*, 31(13):1315–1326, 2003.

[122] Robert S Pindyck, Daniel L Rubinfeld, et al. Microeconomics, 2013.

[123] Anthony Papavasiliou and Shmuel S Oren. Multiarea stochastic unit commitment for high wind penetration in a transmission constrained network. *Operations Research*, 61(3):578–592, 2013.

[124] Ryan Tibshirani. Karush-kuhn-tucker conditions. 2015.